

UC Berkeley

HVAC Systems

Title

Assessment and Improvements of the CBE Underfloor Air Distribution (UFAD) Cooling Load Design Tool

Permalink

<https://escholarship.org/uc/item/40h5c3nv>

Author

Chen, Bin

Publication Date

2014-10-01

Assessment and Improvements of the CBE Underfloor Air Distribution (UFAD) Cooling Load
Design Tool

By
Bin Chen

A thesis submitted in partial satisfaction of the
Requirements for the degree of
Master of Science
In
Architecture
In the
GRADUATE DIVISION
of the
UNIVERSITY OF CALIFORNIA, BERKELEY

Committee in charge:

Professor Stefano Schiavon, Chair
Professor Luisa Caldas
Professor Dave Auslander
Project Scientist Fred Bauman

Fall 2014

Table of Contents

| | |
|--|------|
| List of Figures | v |
| List of Tables | viii |
| List of Acronyms and Symbols | ix |
| Acknowledgements..... | xii |
| Abstract..... | 1 |
| 1. Background..... | 1 |
| 1.1. Room air distribution | 2 |
| 1.1.1. Mixed air distribution systems..... | 2 |
| 1.1.2. Displacement ventilation (DV) systems | 3 |
| 1.1.3. UFAD systems | 5 |
| 1.1.3.1. Air distribution principle..... | 5 |
| 1.1.3.2. Potential benefits of UFAD system..... | 5 |
| 1.1.3.3. Integrated design approach | 7 |
| 1.1.3.4. UFAD case study | 10 |
| 1.2. Room air stratification..... | 12 |
| 1.3. Underfloor air supply plenums..... | 15 |
| 1.4. EnergyPlus UFAD model | 16 |
| 1.5. Simplified UFAD design tool | 17 |
| 1.5.1. CBE UFAD cooling load design tool | 17 |
| 1.5.2. ASHRAE RP-1522 UFAD design tool..... | 18 |
| 1.6. Statement of the problem | 19 |
| 1.7. Objectives..... | 20 |
| 1.8. Significance..... | 20 |

| | | |
|--------|---|----|
| 2. | The comparison of two UFAD design tools | 21 |
| 2.1. | Feature comparison | 21 |
| 2.1.1. | Design cooling load | 21 |
| 2.1.2. | Thermal stratification profile | 23 |
| 2.1.3. | Air distribution models for predicting thermal stratification | 25 |
| 2.1.4. | Supply plenum cooling load | 29 |
| 2.1.5. | Plenum configurations | 30 |
| 2.1.6. | Diffuser types | 32 |
| 2.1.7. | Air distribution effectiveness | 32 |
| 2.1.8. | Work scheme of the tools | 34 |
| 2.1.9. | User interfaces | 35 |
| 2.2. | Numeric comparison | 36 |
| 2.2.1. | Method | 36 |
| 2.2.2. | Result | 38 |
| 2.3. | Conclusion and discussion | 40 |
| 3. | Updated $\Gamma - \Phi$ model | 41 |
| 3.1. | Combined UFAD database..... | 41 |
| 3.2. | Method | 41 |
| 3.2.1. | Statistical analysis..... | 41 |
| 3.2.2. | Model selection indexes..... | 42 |
| 3.3. | Results | 42 |
| 3.3.1. | $\Gamma - \Phi$ plots..... | 42 |
| 3.3.2. | Regression model selection result..... | 45 |

| | | |
|----------|---|----|
| 3.4. | Comparison between old and updated Γ - Φ equation..... | 48 |
| 3.4.1.1. | Γ - Φ equation comparison..... | 48 |
| 3.4.1.2. | Case comparison..... | 52 |
| 3.5. | Numeric comparison of the accuracy between the old and updated Γ - Φ equations..... | 57 |
| 3.6. | Conclusion..... | 59 |
| 4. | Updated CBE UFAD Cooling Load Design Tool | 60 |
| 4.1. | New features..... | 60 |
| 4.1.1. | Alert function to prevent reverse stratification | 60 |
| 4.1.2. | New diffuser type..... | 62 |
| 4.1.3. | Dual-unit system | 64 |
| 4.1.4. | Air distribution effectiveness..... | 64 |
| 4.1.5. | In-floor cooling unit..... | 65 |
| 4.1.6. | New data visualization..... | 66 |
| 4.2. | The updated CBE UFAD cooling load design tool example | 67 |
| 4.2.1. | Preventing reverse stratification in the perimeter zone..... | 68 |
| 4.2.1.1. | Adding the number of diffuser | 69 |
| 4.2.1.2. | Reducing the cooling load for perimeter zone..... | 70 |
| 4.2.2. | Adjusting the parameters in the interior zone to achieve acceptable stratification and thermal comfort..... | 71 |
| 4.3. | Conclusions | 72 |
| 5. | Conclusions..... | 74 |
| 6. | Reference | 76 |
| 7. | Appendix..... | 82 |
| 7.1. | CBE full-scale experimental database..... | 82 |

| | | |
|--------|---|-----|
| 7.1.1. | Experimental input parameters | 82 |
| 7.1.2. | Experimental results..... | 85 |
| 7.2. | RP-1522 CFD simulation database | 88 |
| 7.2.1. | Experimental input parameters | 88 |
| 7.2.2. | Experimental results..... | 89 |
| 7.3. | Numeric comparison results..... | 91 |
| 7.4. | R package example..... | 95 |
| 7.1. | Code for updated CBE UFAD online design tool..... | 98 |
| 7.1.1. | Gamma Phi equations | 98 |
| 7.1.2. | Interior air distribution effectiveness | 100 |
| 7.1.3. | Infloor unit | 101 |

List of Figures

| | |
|--|----|
| Figure 1 The approach to net zero energy buildings (McGregor et al., 2013)..... | 1 |
| Figure 2 Conventional overhead (mixed) air distribution system (ASHRAE, 2013b)..... | 3 |
| Figure 3 Displacement ventilation room air distribution characteristics (ASHRAE, 2013b) | 4 |
| Figure 4 Underfloor Air Distribution System (ASHRAE, 2013b) | 5 |
| Figure 5 Information flow for (a) linear design approach, and (b) integrated design approach for UFAD system (Montanya et al., 2009)..... | 8 |
| Figure 6 comparison of typical floor-to-floor heights for ceiling-based and UFAD system (Bauman, 2003). | 9 |
| Figure 7 The Seattle Central Library (Source : http://blog.historyofscience.com/2008/07/25-most-modern-libraries-in-world.html) | 10 |
| Figure 8 EPA Region 8 Headquarters, Denver, CO (Webster et al., 2008a)..... | 11 |
| Figure 9 Exterior of the tower portion of the Times Building. Copyright: The Times Company (Webster et al., 2013)..... | 12 |
| Figure 10 Comparison of typical vertical temperature profiles for OH, DV and UFAD system (ASHRAE, 2013b). The figure is revised based on Figure 2.7 in (ASHRAE, 2013b)..... | 13 |
| Figure 11 Effect of room airflow variation at constant heat input, swirl diffusers, interior zone (Webster et al., 2002a)..... | 14 |
| Figure 12 Effect of (a) supply air temperature in the interior zone and (b) blinds in the perimeter zone (Webster et al., 2002b) | 14 |
| Figure 13 (a) Swirl diffuser (b) VAV directional diffuser (c) linear bar grille..... | 18 |
| Figure 14 Cooling load profiles for overhead (mixing) vs. UFAD systems..... | 22 |
| Figure 15 Example room air temperature profile in stratified UFAD room. (Schiavon et al., 2010b) | 24 |
| Figure 16 Computed temperature points in the thermal stratification model. (Jiang et al., 2012) | 25 |

| | |
|--|----|
| Figure 17 Schematic flow diagram of CBE design tool showing transformation from cooling load calculated for an overhead mixing system into a UFAD cooling load and then divided between the supply plenum, zone (room), and return plenum..... | 29 |
| Figure 18 Series plenum configuration..... | 31 |
| Figure 19 Reverse series plenum configuration..... | 31 |
| Figure 20 Independent plenums configuration | 31 |
| Figure 21 Common plenum configuration..... | 31 |
| Figure 22 work scheme of CBE UFAD cooling load design too..... | 34 |
| Figure 23 work scheme of ASHRAE RP-1522 UFAD design tool..... | 35 |
| Figure 24 web based version of CBE tool | 35 |
| Figure 25 screenshot of the ASHRAE RP-1522 tool..... | 36 |
| Figure 26 The comparison of $T_{0.1}$ with cases using swirl for interior zone, VAV directional diffuser for interior and perimeter zone, linear bar grille for perimeter zone. | 38 |
| Figure 27 The comparison of $T_{1.7}$ with cases using swirl for interior zone, VAV directional diffuser for interior and perimeter zone, linear bar grille for perimeter zone. | 39 |
| Figure 28 Γ - Φ plots for swirl and VAV directional diffusers in the interior zone | 43 |
| Figure 29 Γ - Φ plots for VAV directional diffusers and linear bar grille in perimeter zone..... | 44 |
| Figure 30 Comparison of old and updated Γ - Φ equation for swirl and VAV directional diffusers in the interior zone | 50 |
| Figure 31 Comparison of old and updated Γ - Φ equation for VAV directional diffusers and linear bar grille in the perimeter zone | 51 |
| Figure 32 Floor plan for design tool example showing diffusers and underfloor fan coil units... | 53 |
| Figure 33 The comparison of $T_{0.1}$ with cases using swirl and VAV directional for the interior zone, and VAV directional diffusers for the perimeter zone..... | 57 |
| Figure 34 The comparison of $T_{1.7}$ with cases using swirl and VAV directional for the interior zone, and VAV directional diffusers for the perimeter zone..... | 58 |

| | |
|--|----|
| Figure 35 The Γ - Φ equation for linear bar grille in perimeter zone | 60 |
| Figure 36 Screenshot of the alert information when reverse stratification happens | 61 |
| Figure 37 Dropdown menu of diffuser type in old CBE UFAD design tool | 62 |
| Figure 38 Dropdown menu for diffuser selection in updated CBE UFAD cooling load design tool | 62 |
| Figure 39 Γ - Φ plots of linear bar grille from CBE and RP-1522 database | 63 |
| Figure 40 Screenshot of dual unit system of updated CBE UFAD Cooling Load Design Tool .. | 64 |
| Figure 41 Screenshot of results panel showing air distribution effectiveness | 65 |
| Figure 42 Tate in-floor cooling unit..... | 65 |
| Figure 43 Screenshot of input panel of the updated CBE Cooling Load Design Tool..... | 66 |
| Figure 44 Thermal stratification profile visualization from (a) old (b) updated CBE UFAD Cooling Load Design Tool | 67 |
| Figure 45 Inputs of the example | 68 |
| Figure 46 Screenshot of the first case calculation result..... | 69 |
| Figure 47 Temperature Profile with (a) 15 linear bar grille (b) 18 linear bar grille | 70 |
| Figure 48 Screenshot of the thermal profile (a) before and (b) after reducing the cooling load .. | 71 |
| Figure 49 Screenshot of thermal stratification profile with (a) 13 swirl diffusers (b) with 17 swirl diffusers (c) with 20 swirl diffusers | 72 |

List of Tables

| | |
|--|----|
| Table 1 Energy Star ratings of selected UFAD buildings (ASHRAE, 2013b) | 6 |
| Table 2 Γ - Φ relationships at 0.1 and 1.7 m for the diffuser types used in the design tool | 27 |
| Table 3 Summary of coefficients in Equation 10 | 28 |
| Table 4 Summary of coefficients in Equation 11 | 28 |
| Table 5 Comparison of diffuser types in two UFAD design tools..... | 32 |
| Table 6 Case configuration of combined database | 36 |
| Table 7 Statistical summaries of Φ | 45 |
| Table 8 Results of statistical analysis for Γ - $\Phi_{0.1}$ regression model selection | 45 |
| Table 9 Results of statistical analysis for Γ - Φ_{oz} regression model selection..... | 46 |
| Table 10 Results of statistical analysis for Γ - $\Phi_{1.7}$ regression model selection | 47 |
| Table 11 Updated Γ - Φ relationships at 0.1, occupied zone, and 1.7 m. | 47 |
| Table 12 Old Γ - Φ equations for each type of diffusers | 48 |
| Table 13 Design input parameters for the modeled UFAD system (series plenum). | 53 |
| Table 14 Interior swirl diffusers case comparison | 54 |
| Table 15 Interior VAV directional diffusers case comparison | 54 |
| Table 16 Case comparison for VAV directional diffusers and linear bar grille in perimeter zone..... | 55 |
| Table 17 Results of the temperature stratification and calculated airflow rate per diffuser from updated CBE UFAD Cooling Load Design Tool | 71 |

List of Acronyms and Symbols

EIA – Energy Information Administration

EPA – Energy Protection Agency

HVAC – Heating Ventilation and Air Conditioning

UFAD – Underfloor Air Distribution

IAQ – Indoor Air Quality

ASHRAE – American Society of Heating, Refrigerating and Air-Conditioning Engineers

OH – Overhead System

DV – Displacement Ventilation

VAV – Variable Air Volume

CBE – Center for the Built Environment

TDV – Traditional Displacement Ventilation

COP – Coefficient of Performance

LEED – Leadership in Energy and Environment Design

MEP – Mechanical, Electrical and Plumbing

DOE – Department of Energy

UCLR – UFAD Cooling Load Ratio

SPF – Supply Plenum Fraction

SPF^P – Supply Plenum Fraction for the Perimeter Zone

ZF – Zone Fraction

RPF – Return Plenum Fraction

SAT – Supply Air Temperature

CL^{UFAD} – UFAD Cooling Load

CL^{OH} – Overhead System Cooling Load

Γ – Gamma

Φ – Phi

G_r – Grashof Number

Re – Reynolds Number

E_z – air distribution effectiveness

C_e – Contaminant Concentration at the Exhaust

C_s – Contaminant Concentration at the Supply

C_b – Contaminant Concentration at the Breathing Zone.

$\cos \varphi$ – Cosine of Discharge Angle for Diffuser Flow

n – Number of Diffusers

m – Number of Plumes

P_z – Zone Population

n' – Number of Cases

η – Supply Plenum Heat Gain Ratio

T – Room Air Temperature ($^{\circ}\text{C}$ or $^{\circ}\text{F}$)

T_x – Room Design Temperature ($^{\circ}\text{C}$ or $^{\circ}\text{F}$)

T_s – Supply Air Temperature at the Floor ($^{\circ}\text{C}$ or $^{\circ}\text{F}$)

T_R – Return Air Temperature ($^{\circ}\text{C}$ or $^{\circ}\text{F}$)

T_{set} – Temperature Setpoint of Thermostat ($^{\circ}\text{C}$ or $^{\circ}\text{F}$)

$T_{0.1}$ – Air Temperature at the Ankle Level ($^{\circ}\text{C}$ or $^{\circ}\text{F}$)

$T_{1.7}$ – Air Temperature at the Head Level ($^{\circ}\text{C}$ or $^{\circ}\text{F}$)

$T_{oz,avg}$ – Average Occupied Zone Temperature ($^{\circ}\text{C}$ or $^{\circ}\text{F}$)

T_i – Measured Temperature of the Experiment ($^{\circ}\text{C}$ or $^{\circ}\text{F}$)

\hat{T}_i – Predicted Temperature ($^{\circ}\text{C}$ or $^{\circ}\text{F}$)

\bar{T}_i – Averaged Measured Temperature of the Experiment ($^{\circ}\text{C}$ or $^{\circ}\text{F}$)

T_s^P – Temperature of Air Supplied at Diffuser of the Perimeter Zone ($^{\circ}\text{C}$ or $^{\circ}\text{F}$)

T_{plenum}^P – Temperature of Air Entering Supply Plenum of the Perimeter Zone ($^{\circ}\text{C}$ or $^{\circ}\text{F}$)

Q – Room Airflow (m^3/s or cfm)

A_d – Diffuser Effective Area (m^2 or ft^2)

A_f – Zone Floor area (m^2 or ft^2)

W – Zone Cooling Load (supply and return plenum cooling loads are not included plenum) (kW or kBtu/hr).

W_L – Zone Extraction Rate per Unit Length of Zone (kW/m or kBtu/hr·ft²)

W_{tot} – Total Summer Design Cooling Load (kW or kBtu/hr)

Q_d – Diffuser Design Airflow Rate (L/s or cfm)

H – Room Height (m or ft)

A_z – Zone Floor Area: The Net Occupiable Floor Area Of The Ventilation Zone (m^2 or ft^2)

R_p – Outdoor Airflow Rate Required Per Person (L/s·person or cfm·person)

R_a – Outdoor Airflow Rate Required Per Unit Area (L/s·m² or cfm·ft²).

V_f – Minimum Airflow Rate of Fresh Air (L/s or cfm)

V_{bz} – Required Minimum Supply Airflow Rate Required in the Breathing Zone (L/s or cfm)

W^P – Design Cooling Load for UFAD of The Perimeter Zone (kW or kBtu/hr)

W_{unit} – Cooling Capacity of the In-floor Cooling Unit (kW or kBtu/hr)

Q_{room}^T – Total Airflow (Through Diffusers Plus Category II Leakage) (L/s or cfm).

g – Gravitational Constant ($m^3/kg·s^2$)

β – Thermal Expansion Coefficient (1/m·K)

L – Characteristic Length (m)

ν – Kinematic Viscosity ($g/cm·s$)

u – Air Velocity (m/s)

C_p – Specific Heat Capacity Of Air (kJ/kg·K)

Acknowledgements

I would like to express my deepest appreciation to my committee chair Professor Stefano Schiavon and supervisor Fred Bauman for their guidance throughout this project. I am grateful for their insightful instructions on research, their great patience in answering my questions, and their general regard for my wellbeing. In particular, I have benefited greatly from Professor Stefano Schiavon's rigorous academic attitude and thoughtfulness. I would like to thank my committee members, Professor Luisa Caldas and Professor Dave Auslander for their guidance and constructive commentary in the review process.

I would like to thank Tyler Hoyt who helped me with the CBE UFAD design tool updating, Tom Webster who helped with UFAD field study clarification, and David Lehrer who helped with UFAD case studies. I would like to also thank Professor Gail Brager, Hui Zhang, and Professor Edward Arens for their encouragement, suggestions and sincere support.

In addition, a thank you to my colleagues, Margaret Pigman, Kristine Walker, Dove Feng and Anoop Honnekeri, who all helped me with proofreading this thesis.

Finally, I want to thank my parents for their love and support throughout my academic career. This project was made possible through funding from the Center for the Built Environment.

Abstract

The necessity of energy efficient Heating Ventilation and Air Conditioning (HVAC) technologies has been growing with the development of green buildings to reduce the impact of built environment on the US energy consumption. In this context, underfloor air distribution (UFAD) appears as an innovative air distribution method that has the potential benefits of reduced energy use, improved indoor air quality (IAQ) and thermal comfort. Currently, there are two UFAD design tools (CBE and RP-1522 tools) in the ASHRAE UFAD design guide to help HVAC designers predict thermal stratification and calculate air flow rate. The aim of this thesis is to comprehensively compare these two UFAD design tools and update the CBE UFAD Cooling Load Design Tool with new stratification models and extended capabilities. The comparison will provide HVAC designers with a reference when deciding which design tool to use.

The comparison consists of two parts. The first one compares features, including design cooling load, thermal stratification profile, air distribution models, diffuser types, supply plenum heat balance, plenum configurations and air distribution effectiveness. The second part is a numeric comparison to assess the accuracy of thermal stratification predictions of the two tools using a new database that is composed of 79 full-scale experiments and 31 CFD simulations. A new stratification model was then developed for each type of diffuser based on the combined database. The old and updated stratification models were also compared. Major functionality that has been added to the CBE tool includes a new linear bar grille in the perimeter zone, air distribution effectiveness, and the in-floor cooling unit. Design examples are provided to illustrate how users can interact and make design decisions based on the feedback from the design tool.

The results of the comparison show that both tools have practical advantages and limitations. The CBE tool has the key advantage of being able to predict the UFAD cooling load, calculate heat gain in the supply plenum, model different plenum configurations and zone types. It has the limitation of primarily being used in office buildings and not able to calculate air distribution effectiveness. The RP-1522 tool covers more buildings types (classrooms, offices, workshops, restaurants, retail shops, conference rooms and auditoriums), and is able to calculate the air distribution effectiveness. However it requires users to input the zone cooling load, supply plenum factor and the supply airflow rate of each diffuser, which is difficult to get during the design stage for UFAD system. The two design tools are both acceptably accurate prediction models for design purposes, thus validating both air distribution models, which were developed independently. The updated stratification prediction models developed from the combined database do not yield significant differences in stratification prediction compared to the old models, except in the case of VAV directional diffusers in the interior zone. The new model for interior VAV directional diffuser has been implemented in the updated CBE UFAD Cooling Load Design Tool.

1. Background

The built environment has a significant impact on the US energy consumption. According to data from the U.S. Energy Information Administration (EIA), buildings accounted for 38.9 percent of total U.S. energy consumption in 2005 (EIA, 2012). On the other hand, green building, which refers to the design and construction practices that significantly reduce or eliminate the negative impact of buildings on the environment and occupants, plays an important role in maximizing buildings' environmental performance, as well as providing greater occupant satisfaction (EPA, 2012a). In terms of reducing building energy consumption, McGregor et al. (2013) provide a simple approach to reaching low energy buildings. Figure 1 illustrates the approach as a sequence of steps, which are prioritized based on cost-effectiveness to achieve low energy buildings. Reducing both the external loads entering the building, and the loads generated inside the building is essential before any energy systems designs during the architectural design phase. Passive systems, including passive solar, natural ventilation, and daylighting, should then be considered to provide occupant comfort without using mechanical and electrical systems. Once the first two steps have been followed, the most appropriate active systems can then be developed to deal with much-reduced loads (McGregor et al., 2013). A building's heating, ventilation and air conditioning (HVAC) system, as part of the "active systems" approach, is responsible for a great part of buildings' energy consumption. The air distribution principles in a building's HVAC system is strongly associated with the indoor environmental quality for occupants' well-being, as well as the energy costs for space heating and cooling (Thais Aya et al., 2006, Lim et al., 2012).

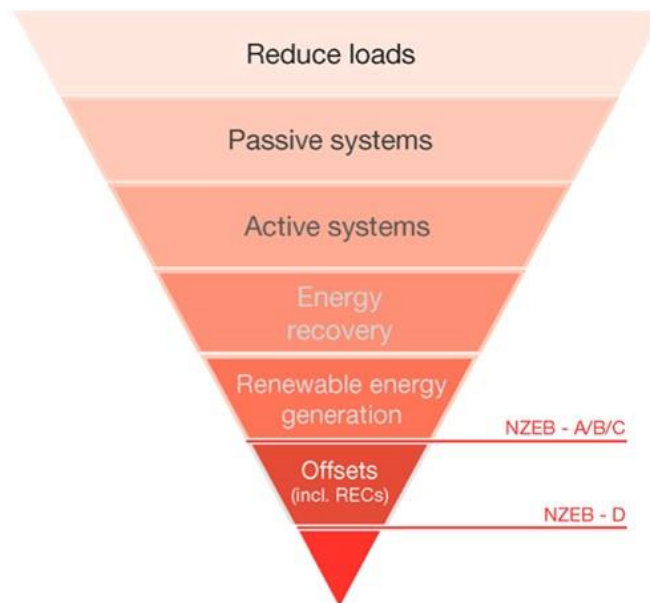


Figure 1 The approach to net zero energy buildings (McGregor et al., 2013).

Underfloor air distribution (UFAD) is an innovative air distribution method of delivering conditioned air to building spaces in order to achieve thermal comfort. Underfloor air distribution

has gained increasing interest due to its potential advantages for improved indoor air quality (IAQ), thermal comfort and energy performance (in suitable climates). Underfloor air distribution derives its name from using the underfloor plenum beneath a raised floor to provide conditioned air through floor diffusers (ASHRAE, 2013b). Since first being introduced into office buildings in West Germany in the 1970s (Sodec and Craig, 1990), UFAD has attracted growing interest and achieved market penetration in new commercial office building construction in North America (Bauman et al., 2007b, Bauman et al., 2010). Other types of air distribution methods include traditional overhead distribution and displacement ventilation (ASHRAE, 2013a). In order to better understand the thermal performance and benefits of UFAD systems, it is important to know the difference between UFAD and other air distribution methods.

1.1. Room air distribution

The purpose of room air distribution systems is to provide required thermal comfort and ventilation for space occupants and processes (ASHRAE, 2013a). Based on the extent of thermal stratification, the 2013 ASHRAE Handbook (Applications) categorized room air distribution methods as follows:

- **Mixed systems** (e.g., overhead (OH) distribution), which have little or no thermal stratification of air within the occupied and/or process space.
- **Full thermal stratification systems** (e.g. displacement ventilation), which have little or no air mixing in the occupied and/or process space.
- **Partially mixed systems** (e.g., most UFAD systems), which provide limited air mixing in the occupied and/or process space.

In next section, the overhead well-mixed system, the displacement ventilation system and the UFAD system will be introduced respectively. The difference between UFAD and the other two air distribution methods will be discussed in terms of thermal comfort, indoor air quality and energy performance.

1.1.1. Mixed air distribution systems

Overhead (OH) systems are often referred to as mixed air distribution systems. Historically, the OH system has been used to both supply and return the air at the ceiling level, and is the most common air distribution method used in North America. Figure 2 illustrates a conventional overhead air distribution system. The velocity of the supply jets from the diffuser outlets is usually higher than the occupants' acceptable level. After mixing with the room air in the unoccupied zone, the supply jet's velocity will decrease to the occupants' acceptable level when entering the occupied zone. Therefore, occupant comfort is maintained by the secondary air motion from mixing in the unoccupied zone. The supply air temperature may be higher, equal to or lower than the room air setpoint, depending on the zone heating or cooling load. Similar to the velocity drop, the supply jet's temperature quickly approaches the entrained room air to maintain the thermal comfort in the occupied zone after the rapid mixing with room air (Rock and Zhu, 2002, ASHRAE, 2013a, ASHRAE, 2013b).

Because overhead systems promote fully mixing the supply air with room air to maintain the same temperature in the occupied space, contaminants are spread evenly in the space as well. The

approach of the OH systems to maintain the indoor air quality (IAQ) in the occupied space is to deliver a specified volume of ventilation to dilute the pollutant concentration. This method is referred to as dilution ventilation. ASHRAE 62.1-2013 specified the minimum outdoor airflow required in the breathing zone of the occupiable space with an OH system. The required airflow rate varies depending on the zone floor area, number of occupant and the occupancy category. Detailed information can be found in Table 6.2.2.1 in the standard mentioned above (ASHRAE, 2013b, ANSI/ASHRAE, 2013b).

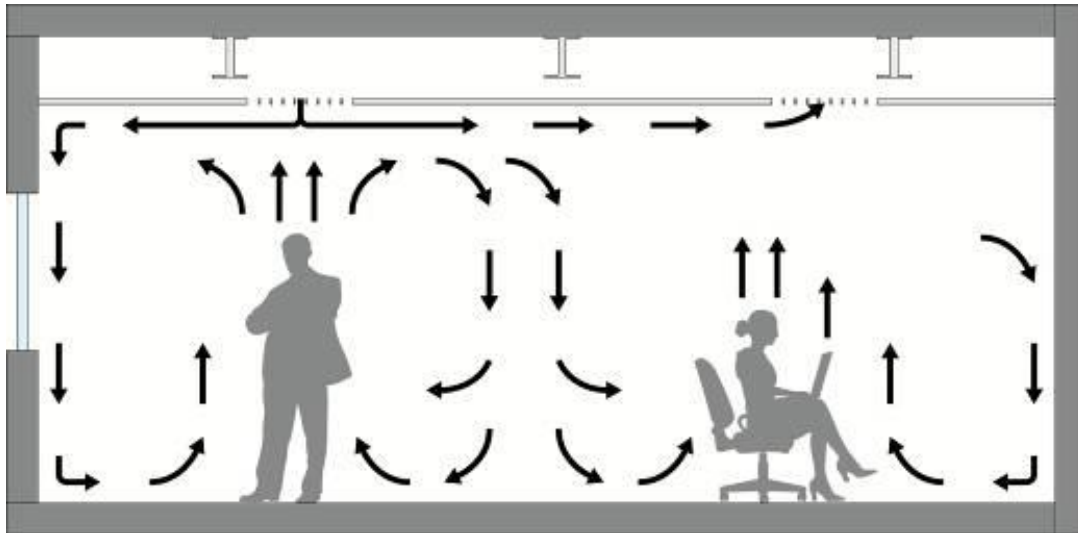


Figure 2 Conventional overhead (mixed) air distribution system (ASHRAE, 2013b)

1.1.2. Displacement ventilation (DV) systems

Displacement ventilation is an air distribution method that delivers conditioned air at the floor level or near the side wall to provide ventilation and space conditioning. It has been used in both industrial and non-industrial premises for many years in Scandinavian countries and Europe, and has been gaining more notoriety in North America recently. Figure 3 shows a classically defined DV system (ASHRAE, 2013b). As displacement ventilation systems provide cool air directly to the occupied zone, the supply air temperature is generally above 16 °C (60.8 °F) to prevent cold feet, except that a lower supply air temperature may be used for some industrial applications, exercise or sports facilities. The supply air discharging velocity of DV systems is much smaller than that of OH systems. DV system has the potential to save energy compared to OH systems by means of only conditioning the occupied zone without unnecessarily delivering cool air to other areas of the space (ASHRAE, 2013a, ASHRAE, 2013b, Skistad et al., 2011).

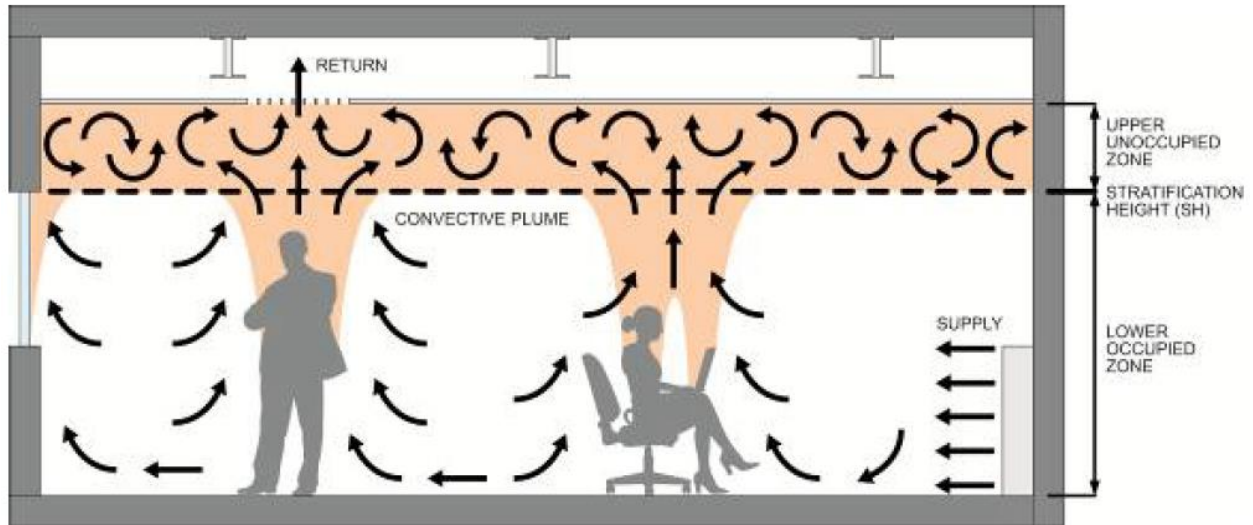


Figure 3 Displacement ventilation room air distribution characteristics (ASHRAE, 2013b)

As the supply air enters the space, there is some degree of mixing with the room air, which makes the supply air a little bit warmer. However, the mixture is still cooler and heavier than the air in the upper level, which creates a negative buoyancy. This in addition to the low velocity of the supply air restricts the air to spread gradually in the lower level. Thermal plumes are a driving force of the floor-to-ceiling movement in DV. As the convective heat transfers between the heat source and the cooler air, the convection currents form a heat plume around and above the heat source, and naturally rise through the space until they hit the ceiling. Because of these thermal plumes, contaminants associated with the heat source are transported to the upper part of the zone and are removed with the return air through the ceiling without spreading over the lower part (ASHRAE, 2013a, ASHRAE, 2013b, Skistad et al., 2011). Therefore, DV systems are able to provide improved indoor air quality when pollutants are associated with heat sources in the space. Besides, DV systems are typically configured to by 100% outside air systems and are primarily aimed at providing a high quality ventilation environment in the occupied zone. (Jung and Zeller, 1994) performed full-scale experiments to study the air change effectiveness and the ventilation efficiency in mechanically ventilated rooms. They found that DV system significantly increased the supply of fresh air within the breathing zone of the occupants and have better indoor air quality than OH system. Lee et al. (2009c) also conducted full-scale experimental measurements and proved that DV systems had better ventilation performance than the mixing ventilation systems. Later on, Xing et al. (2001) and Lin et al. (2005) reached the similar conclusion from CFD simulation studies.

However, DV may not provide better IAQ than OH systems if the contaminant sources are not associated with the heat sources, such as particulate matter, ozone or VOCs from building materials or ground-level contaminants (like those from carpets) (Lin et al., 2005). Through CFD simulations and experimental measurement study, Rim and Novoselac found that the buoyancy-driven convective plume around a body seems to have a significant role in transporting pollutants from floor level to the breathing zone in a stratified environment (Rim and Novoselac, 2009, Rim

and Novoselac, 2010). The contaminants at the ground level will be simply displaced into the breathing zone in DV system, which may have a negative impact on the indoor air quality. In addition, DV generally has a lower cooling capacity than UFAD systems, so is applied only in cases where it can be effective. DV systems are commonly used in spaces with high ceilings, such as theaters, auditoriums, and assembly halls etc. (ASHRAE, 2013a).

1.1.3. UFAD systems

1.1.3.1. Air distribution principle

As mentioned before, UFAD systems deliver conditioned air through diffusers mounted on the raised access floor panel, and return air at the ceiling level. This is the major difference between UFAD systems and traditional OH systems. Figure 4 presents a schematic diagram of a UFAD system for an office building. Besides, UFAD systems are different from DV systems primarily in the way that supply air is delivered to the space. First, the supply air discharging velocity through the small-size outlets are much higher in the UFAD system and there is relatively greater mixing compared to DV systems in the lower zone. Second, the location of the diffuser is more flexible and occupants usually have better control of the local air condition, which allows better thermal comfort than DV systems. Apart from that, the overall airflow patterns between UFAD and DV are similar once the air rises above the influence of the air diffusers (ASHRAE, 2013b).

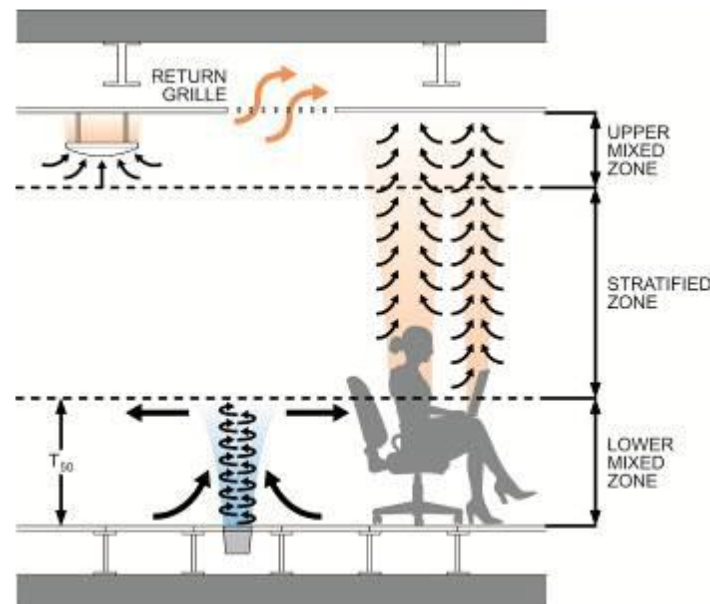


Figure 4 Underfloor Air Distribution System (ASHRAE, 2013b)

1.1.3.2. Potential benefits of UFAD system

UFAD systems have several potential benefits. First, UFAD systems provide better indoor air quality and ventilation efficiency by delivering a fresh supply air at floor level or near the occupant. In ASHRAE research project-1373, Lee et al. (2009c) compared the airflow and contaminant distributions in rooms with DV and UFAD systems. They performed a full-scale experimental study in a test chamber, which can simulate three types of spaces including office, classroom and

workshop using UFAD system. They found that DV and UFAD systems had similar air distribution effectiveness, and were better than the mixing OH system under cooling mode. This topic has also been investigated by both Chou et al. (2004) and Ho et al. (2011) through experimental measurements and CFD simulation studies, and they came to similar conclusions. Shah et al. (2005) also found that the application of UFAD led to acceptable thermal comfort and IAQ in the office space in a field study of an office building in a hot and humid climate using a UFAD system.

Second, UFAD systems provide improved thermal comfort by allowing individual occupants to control their local thermal environment. There are significant variations in individual comfort preferences in today's work environment, because of the differences in clothing, activity level and individual preferences. UFAD systems can accommodate individual's comfort preferences more easily than a centralized control overhead system. Research has shown that people who believe they have greater control over their thermal environment will tend to be more satisfied with their comfort (Bauman et al., 1998). Fisk et al. (2006) measured several aspects of the performance of a UFAD system installed in a medium-size office building in Pennsylvania, including an occupant survey to evaluate perceptions of thermal conditions and air quality. Survey results showed that the level of satisfaction with thermal comfort was at the 85th percentile, and this high satisfaction rating could possibly be due, in all or part, to the use of a UFAD system. Bos and Love (2013) did a field measurements and questionnaires study to assess the thermal comfort in a cold climate office environment with a UFAD system. The findings supported earlier lab (Bauman et al., 1995, Lee et al., 2012a) and numerical simulation studies (Zhou and Haghghat, 2009, Lee et al., 2012a) that found better thermal comfort conditions and occupant responses in UFAD systems.

Third, UFAD systems have potential energy savings in suitable climates by controlled thermal stratification, higher supply air temperatures, and reduced static pressures in the underfloor plenum. According to Bauman and Webster (2001), the energy savings of UFAD systems over OH systems are primarily from: 1) reduced cooling energy by economizer operations; 2) increased chiller coefficient of performance (COP); 3) reduced fan energy consumption. Since climate is the determining factor in how much the economizer can reduce cooling energy, the energy savings of UFAD system is only significant in suitable climates, where it's cool and mild (ASHRAE, 2013b). Table 1 shows a few examples of ENERGY STAR (EPA, 2012b) ratings for UFAD buildings as compared to national averages for office buildings. It can be noticed in Table 1 that all of the six buildings are above the ENERGY STAR-label threshold of 75, which indicates that buildings with UFAD systems have very good energy performance, though it cannot be said that it is due solely to the UFAD system. The energy performance of UFAD systems was a subject of much interest, research and development. Details on how to optimize the energy performance of UFAD systems can be found in chapter 8 of 2013 ASHRAE UFAD design guide (ASHRAE, 2013b). This topic will also be further discussed in paragraph 1.4.

Table 1 Energy Star ratings of selected UFAD buildings (ASHRAE, 2013b)

| | AVERAGE | ENERGY STAR | CASE 1 | CASE 2 | CASE 3 | CASE 4 | CASE 5 | CASE 6 |
|--------------------|----------------|--------------------|---------------|---------------|---------------|---------------|---------------|---------------|
| Size (kSF) | | | 292 | 496 | 500 | 105 | 68 | 327 |
| Type | Office | Office | Office | Courthouse | Office | Office | Office | Office |
| Rating | 50 | 75 | 86 | 89 | 98 | 79 | 86 | 77 |
| Site EUI* | 118 | 87 | 71 | 48 | 43 | TBD | TBD | TBD |
| Source EUI* | 312 | 230 | 189 | 135 | 130 | TBD | TBD | TBD |

In addition, UFAD systems have layout flexibility, reduced life-cycle building costs, and reduced floor-to-floor height in new constructions (ASHRAE, 2013b). Some HVAC designers use UFAD systems to achieve higher scores when applying for Leadership in Energy and Environment Design (LEED) certificates because UFAD can contribute to a few LEED-New Construction credits due to the advantages stated above (Della Barba, 2005, Montanya et al., 2009, ASHRAE, 2013b). UFAD is commonly used in open-plan offices, data centers, call centers, libraries, auditoriums, and concert halls, where raised access floors are typically used to create access to power, voice, and data services. However, some specific facilities or spaces, including small non-residential buildings, wet spaces, kitchens and dining areas, and gymnasiums are not recommended to use UFAD systems, in that UFAD may result in especially difficult or costly designs (ASHRAE, 2013b).

1.1.3.3. Integrated design approach

Unlike the traditional linear design approach, it is essential to adopt an integrated design approach for UFAD system design, in order to achieve the potential benefits of UFAD.

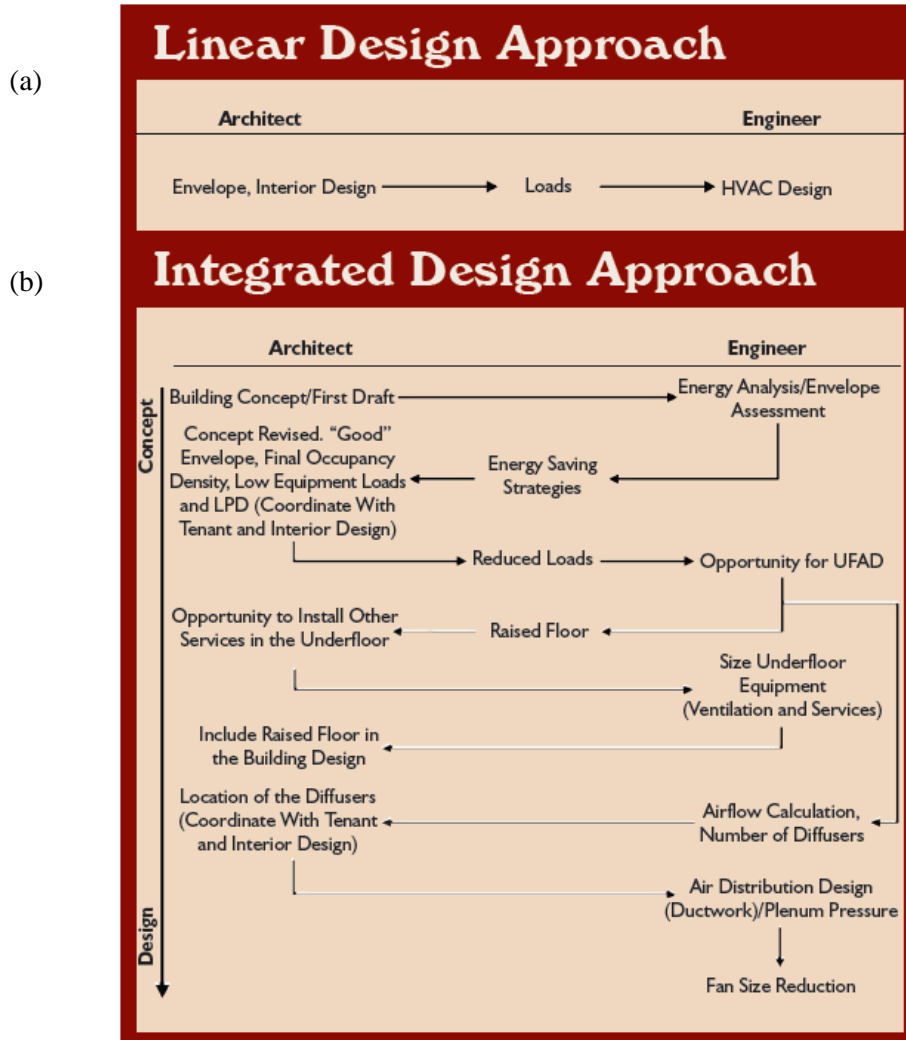


Figure 5 Information flow for (a) linear design approach, and (b) integrated design approach for UFAD system (Montanya et al., 2009).

In a linear design approach, an architect completes their design work and then hands it off to the engineer, as shown in Figure 5a. Similarly for other professionals on the design team, people tend to work in isolation in their own discipline. However, in an integrated design approach, building stakeholders collaborate at the beginning of the project to set the owner's project requirements (Figure 5b). The mechanical, electrical, and plumbing (MEP) engineers should engage with the project at the earliest possible state of the design. The architects should have MEP engineering guidance at the early design phase to include space needed for HVAC-related components, such as raised floor height, shafts, etc. This will help avoid compromises that could affect the performance of the UFAD system (Montanya et al., 2009, ASHRAE, 2013b). An integrated design approach is more common in contemporary, high-performance buildings, where the engineer is viewed as having a more relevant role both at early design stage, and throughout the design process.

An important architectural implication of the UFAD system is the potential to reduce floor-to-floor height in new construction, compared to an OH system. This is accomplished by reducing the overall height of service plenums and/or by changing from standard steel beam construction to a concrete (flat slab) structure approach, both of which are in the domain of the architect along with other design team professionals. As is shown in Figure 6, the underfloor/flat slab configuration allows 0.25 m (10 in.) to be saved in floor-to-floor height compared to overhead/steel system design (Bauman, 2003). For a typical OH system, the floor-to-floor height is 4.1 m (162 in.). Therefore, if a UFAD system is used, one floor height can be saved every 16 stories. This gives architects an opportunity to reduce the overall building height in order to save building materials and space.

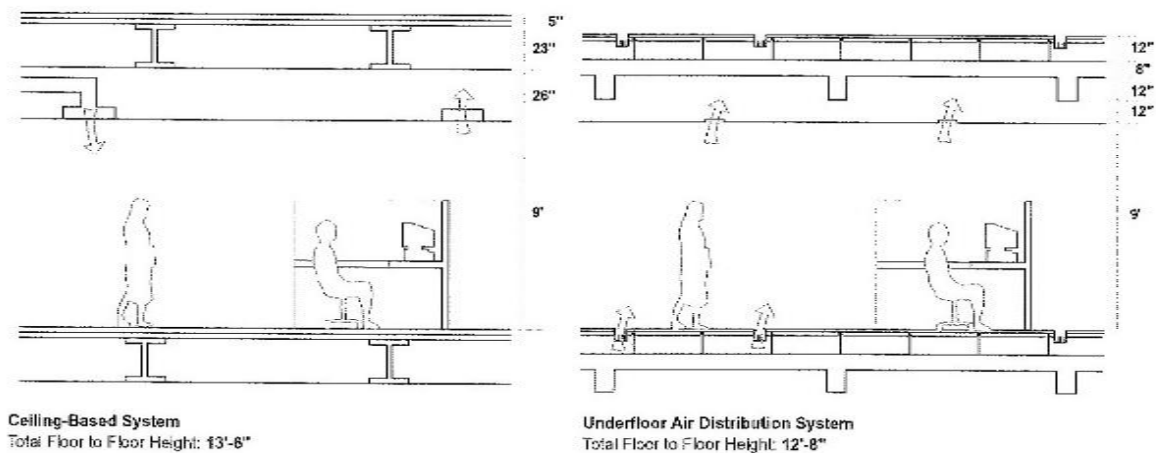


Figure 6 comparison of typical floor-to-floor heights for ceiling-based and UFAD system (Bauman, 2003).

The ceiling plenum can even be eliminated to reach even greater height savings. The concrete ceilings can be exposed, which provide another opportunity for architects to do more creative internal design, such as enhancing daylighting and artificial lighting effects. Figure 7 shows the Seattle Center Library, in Seattle, Washington. The library utilizes a UFAD system, as it provides better indoor air quality and energy efficiency, as well as allowing increased flexibility in technology-intensive spaces (Athens, 2007). The Seattle Center Library is a good example to illustrate how UFAD systems can be used to help architects maximize daylighting.



Figure 7 The Seattle Central Library (Source : <http://blog.historyofscience.com/2008/07/25-most-modern-libraries-in-world.html>)

Architects will also need to account for the raised floor height for the underfloor plenums, which is usually higher than those employed solely for cable management purposes. However, the additional height required for acceptable airflow performance is not large, based on research results (Bauman et al., 1999). Underfloor plenum heights are usually determined by the largest HVAC components located under the floor, requirements for cabling, and additional clear space for air flow (usually 76 mm (3 in.)) (Bauman, 2003). Maintaining the integrity of the supply air plenum is extremely important to the system operating properly. Therefore, the architects must be aware of sealing requirements and document them as appropriate. The sequence of construction also plays an important role in a properly operated UFAD system. Prior to installation of the raised floor system, the slab must be cleaned and sealed to reduce dust. When a well-planned construction sequence is employed, the finished raised floor surface is not installed until after most of the dirt-generating construction has been completed. Detailed information on the construction sequences can be found in chapter 13 of 2013 ASHRAE UFAD design guide (ASHRAE, 2013b).

In addition, the MEP engineers should coordinate with architects to determine zones for optimum supply air room locations and sizes of HVAC supply equipment. Early identification of spaces, which are suitable and unsuitable for UFAD such as wet areas for food preparation, is also very important. Careful attention should be paid to the room occupancies, especially furniture design, in order to coordinate with floor diffuser locations. In particular, it is challenging in spaces where room configurations are changed frequently, such as in multipurpose exhibitions, meeting, and dining spaces.

1.1.3.4. UFAD case study

Webster et al. (2008a) conducted a detailed field study of the Region 8 Headquarters buildings for the Environmental Protection Agency (EPA), named here the EPA building, in Denver, Colorado. The EPA building (Figure 8) is a 9-story structure, which was completed and occupied in

December 2006. Floors 4-9 of the building are served by a UFAD system, while the first three floors are conditioned by an OH system. A series of field investigations were conducted to assess the overall performance of the underfloor air distribution spaces, including temperature profile measurement, building energy use data collection, and occupant satisfaction surveys.



Figure 8 EPA Region 8 Headquarters, Denver, CO (Webster et al., 2008a).

It was concluded from the investigation results that the EPA building is a good example of a well performing building in terms of energy, IAQ, and occupant satisfaction. The UFAD systems performed well and both occupants and operators are satisfied with it. The EPA building achieved an Energy Star rating of 86, which is well above the threshold of 75 to qualify for an Energy Star label. The Energy Star rating system is developed by EPA to evaluate the energy performance of an individual building. It compares a building energy use to similar buildings nationwide and rate the energy performance on a scale of 1 to 100. The EPA building, in which the resource utilization is predominantly due to the UFAD portion of the building floor area (Webster et al., 2008a), has a very good energy performance. Second, the temperature measurements results showed that in most UFAD areas, the average occupied zone temperatures were within the comfort range calculated by ASHRAE procedures. The stratification in the occupied zone was also within the limit specified in ASHRAE standard 55 to ensure occupant thermal comfort. Third, the results from occupant surveys further verified the measurement results. Thermal comfort satisfaction reaches a high percentile ranking of 73% when compared to the CBE benchmark database. The air quality scores are very high with an 87% percentile ranking when compared to the CBE benchmark database, which further supports that UFAD systems provide higher ventilation effectiveness.

Webster et al. (2013) also conducted a post-occupancy monitored evaluation study of the UFAD systems in the New York Times Building (NYTB), in Manhattan, New York. NYTB is a 52-story high-rise building, with floors 2 through 21 being fully occupied by the NY Times Company since 2007. UFAD systems were implemented in the floors occupied by NY Times, due to its potential benefits, including reduced energy use, flexibility and reduced life-cycle building costs, improved

occupant control and comfort, and improved air change effectiveness. The results of the field measurements indicated that a reasonable amount of stratification (1.1-1.7 °C (2-3 °F)) was achieved in the occupied zone, which was less than the limit of 3 °C (5.4 °F) defined in ASHRAE Standard 55(ANSI/ASHRAE, 2010a). An on-line survey was issued to the occupants, in order to investigate the comfort and quality of the thermal environment. Responses were on a 7-point scale, where 1 is “very dissatisfied”, 4 is “neutral”, and 7 is “very satisfied”. The survey results showed that 46% of the occupants responded with greater than neutral satisfaction with the temperature in their workspace, with an average rating of 4.06 out of 7. There were 68% of the occupants that responded with greater than neutral satisfaction with the humidity level in their workspace, with an average rating of 5.26 out of 7.



Figure 9 Exterior of the tower portion of the Times Building. Copyright: The Times Company (Webster et al., 2013).

In summary, UFAD systems have several advantages over OH system, including improved IAQ, improved thermal comfort, reduced energy use in suitable climate, etc. The integrated design approach should be adopted between architects and MEP engineers to achieve the potential benefits of UFAD system. There are two unique aspects of thermal performance of UFAD systems under cooling operation, which distinguish UFAD from traditional OH systems and DV systems. They are room air stratification and the underfloor air supply plenums, which will be introduced in details in next section.

1.2. Room air stratification

UFAD systems create a partially stratified environment, resulting in the unique room air stratification profile compared to OH and DV systems. Figure 10 plots the dimensionless temperature vs. the room height to illustrate the typical temperature profile in OH, DV and UFAD system, where T , T_S and T_R represents the room point temperature, supply air temperature and return air temperature respectively. The main idea of the chart is to show the primary difference of the temperature profiles between UFAD, DV, and OH systems. In an ideal OH system, as the

room air is well mixed with the supply air, the temperature is the same everywhere in the space. For a fully stratified DV system, with the “50%-rule” described in (Skistad et al., 2011) for most practical purposes, the supply air temperature at the floor is approximated as half the temperature difference between the supply and return air temperature. The room air temperature increased linearly with the room height. However, a UFAD system with a partially mixed environment has a unique temperature profile as shown in the figure, which represents the temperature profile in the space away from the direct supply jets (ASHRAE, 2013b). The room air stratification profile for UFAD actually varies a lot depending on multiple impacting parameters, which will be discussed below.

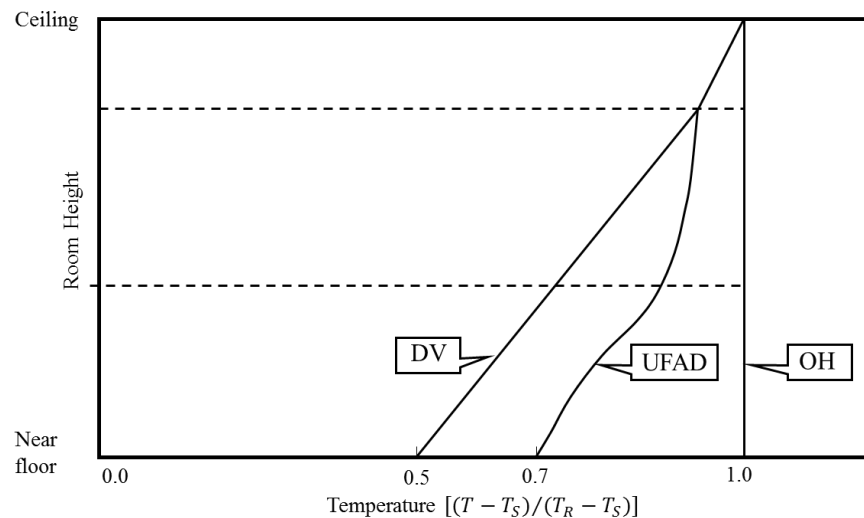


Figure 10 Comparison of typical vertical temperature profiles for OH, DV and UFAD system (ASHRAE, 2013b). The figure is revised based on Figure 2.7 in (ASHRAE, 2013b).

Many studies have been conducted analyzing the vertical thermal stratification in UFAD systems. Lin and Linden (2005) developed the Gamma (Γ)-Phi (Φ) model to predict thermal stratification for UFAD system from laboratory experimental study. The model was based on plume theory for the heat (Liu and Linden, 2006), and predicts a steady-state two-layer stratification in the room. It was concluded that the governing parameters on the flow pattern in a UFAD systems are the buoyancy flux of the heat source, and the volume and momentum fluxes of the cooling diffuser. Zheng et al. (2012) also developed a model, using the Archimedes number, Ar , to predict thermal stratification in UFAD systems. The model evaluates the overall effort of buoyancy and inertial forces, which are critical to an appropriate UFAD design. These two models will be further discussed in details in paragraph 2.1.3.

Webster et al. (2002a) performed a series of full-scale laboratory experiments to investigate the impact of room airflow, supply air temperature (SAT), and the effect of blinds on the thermal stratification of a UFAD system. Figure 11 shows the influence of room airflow on stratification performance, which indicates that a higher supply airflow rate results in less room air stratification, representing that the space is being “over-aired”, while a lower supply airflow rate leads to more stratification representing that the space is not being supplied at sufficient airflow rates.

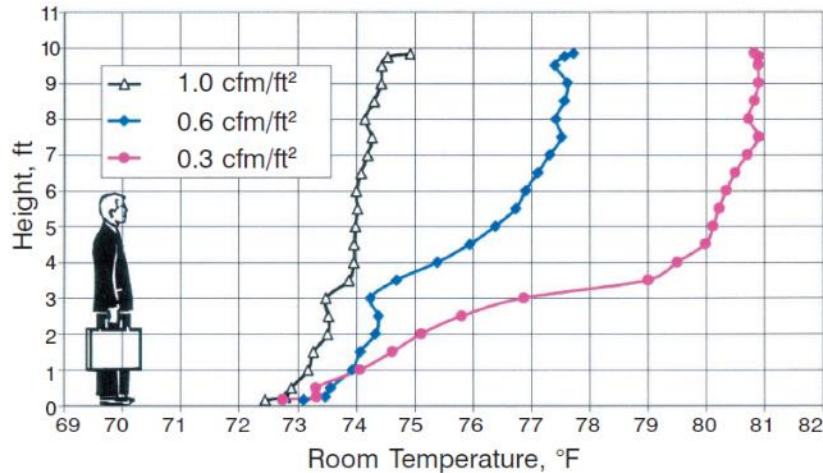


Figure 11 Effect of room airflow variation at constant heat input, swirl diffusers, interior zone (Webster et al., 2002a).

They also found that changing supply air temperature simply moved the stratification profile to higher or lower temperatures without changing its shape, which is shown in Figure 12a. Figure 12b indicates that room load is reduced when blinds are closed due to bypassing the window heat gains directly to the ceiling.

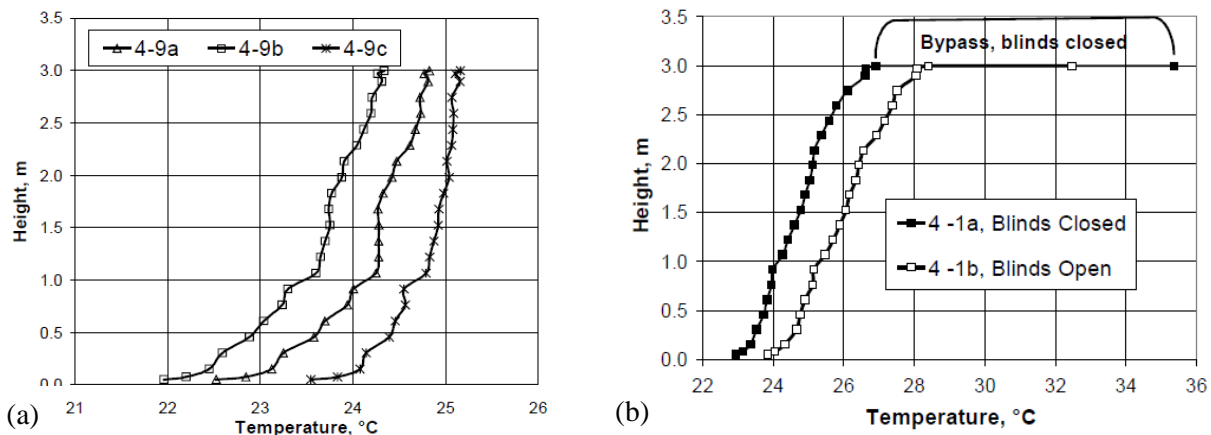


Figure 12 Effect of (a) supply air temperature in the interior zone and (b) blinds in the perimeter zone (Webster et al., 2002b)

There are other researchers also investigated the temperature stratification in UFAD systems. Wan and Chao (2005) investigated the temperature characteristics in a ventilated enclosure with a UFAD system using both numerical simulation and experimental tests. They concluded that the room air temperature stratification was a combined effect of supply jet conditions, jet height, and heat density. Kong and Yu (2008) did a similar study to investigate the temperature stratification in a UFAD system using a validated CFD model. They found that the room air temperature stratification in UFAD systems can be affected by three parameters: heat load, supply volume flux, and supply air velocity. However, these studies only qualitatively described the impacting factors

on thermal stratification, and was not able to come up with a quantitative model to predict the temperature stratification in UFAD systems.

In summary, room air stratification is a distinguishing aspect of UFAD systems. The temperature stratification profile is impacted by many factors, including zone cooling load, supply airflow rate, supply air velocity, and the effects of blinds in the perimeter zone. Two models to predict the temperature stratification, including the Γ - Φ model, and the Ar number model will be further compared in paragraph 2.1.3.

1.3. Underfloor air supply plenums

The use of space under a raised access floor system to deliver conditioned air directly into the occupied zone is the key feature that distinguishes UFAD systems from OH and DV systems. Cool supply air flowing through the underfloor plenum is exposed to heat gain from both the concrete slab in a multistory building and the raised floor panels. This results in an increase in temperature between the air entering the plenum and the air leaving through the diffuser, which used to be referred to as thermal decay (Lee et al., 2012b), but is now called temperature gain in the plenum. Through an EnergyPlus simulation study, Lee et al. (2012b) found that the temperature rise was considerable (annual median = 3.7 K, with 50% of the values between 2.4 and 4.7 K based on annual simulations). Through experimental tests and CFD modeling, Pasut (2011) proved that the use of ductwork to deliver fresh air into the plenum perimeter would improve the air distribution in underfloor plenum systems. In particular, fabric ductwork systems would reduce the air temperatures in the plenum perimeter.

Lee et al. (2012b) also investigated the influence of temperature gain in the plenum on UFAD energy consumption and the parameters that affect temperature gain in the plenum. For a typical series plenum configuration with temperature gain in the plenum, the annual HVAC energy use was greater than that of an idealized ducted system (with no temperature gain in the plenum); chiller and fan energy was increased by 23% and 10%, respectively. Several parameters influenced the temperature gain in the plenum, including central air handler supply air temperature, zone orientation, floor level, climate, interior load, and plenum configuration.

The amount of heat entering the underfloor plenum directly influences the design cooling airflow rate by reducing the amount of heat gain that must be removed by room air extraction. Schiavon et al. (2011) by an analysis of 87 EnergyPlus simulation results, found that the part of the cooling load that went to the supply plenum depended mainly on the floor level, and the position and orientation of the zone under analysis. For all cases considered, median values of the total cooling load going to the supply plenum were found to be 22% in the perimeter zone and 37% in the interior zone. Therefore, it is very important to capture this unique aspect of UFAD systems when doing UFAD load calculation.

In summary, the underfloor air supply plenum is another unique aspect of UFAD systems. Temperature gain in the plenum can be very significant and have a negative influence on UFAD energy consumption. The amount of heat that goes to the supply plenum directly impacts the supply airflow rate calculation for UFAD systems.

1.4. EnergyPlus UFAD model

There are a lot of energy simulation programs that HVAC designers can use to calculate the energy consumption for a building with traditional OH systems, such as eQUEST and DOE-2 etc. (Crawley et al., 2008). These programs assume that each space within a building is well mixed and calculate the heat balances within each individual space, characterized by a single temperature, due to convective, conductive, and radiative exchanges with the surfaces in the space. However, HVAC designers also need tools with which they can calculate the potential energy savings of a UFAD system, in which there are room air temperature stratification and supply plenum heat gains. To solve this problem, Bauman et al. (2007a) and Webster et al. (2008b) developed a module that is, for the first time, capable of simulating UFAD system in EnergyPlus, which is a free and publicly available whole-building energy simulation program maintained by the U.S. Department of Energy (US Department of Energy). This model for EnergyPlus captures two important elements of UFAD systems: the room air stratification under cooling load operation and the underfloor air supply plenum described above. These algorithms were developed over a five-year period of interdisciplinary work consisting of theory, bench-scale and full-scale experimental testing, and analytical, and empirical modeling.

Lin and Linden (2005) first developed the Gamma (Γ)-Phi (Φ) model for UFAD systems, which was further tested in the salt-water tank experiments by Liu and Linden (2006). Room air stratification full-scale testing was conducted by Webster et al. (2002b) to provide a detailed understanding of how room air stratification is influenced by room airflow rate, diffuser type and operating characteristics in typical office arrangements. These tests also provided data to support the development of the room air stratification model for EnergyPlus. In addition, a series of full-scale experiments of the underfloor air supply plenums were conducted to create the underfloor plenum model in order to predict the airflow and thermal performance of underfloor air supply plenums. Detailed information about the testing and models can be found in (Bauman et al., 2007a). The EnergyPlus UFAD module, which was based on a solid understanding of the fluid mechanics of UFAD systems and numerous experiments, was finally developed by Bauman et al. (2007a) and Webster et al. (2008b). It allows design practitioners to model the energy performance of UFAD systems accurately and to compare them with that of conventional systems.

In addition, researchers also used EnergyPlus to study energy performance of UFAD systems. Webster et al. (2012) compared the energy performance of UFAD system with an OH system through EnergyPlus simulation study. The study indicated that a UFAD system has an energy savings of 22% compared to conventional OH system. Alajmi and El-Amer (2010) investigated the effectiveness of UFAD systems in commercial buildings at different supply air temperatures in a hot climate using EnergyPlus. Their findings showed that UFAD systems can save up to 30% energy compared to OH systems, particularly in buildings with higher ceilings. Lim et al. (2012) did a similar EnergyPlus simulation study in Korea and found that UFAD systems consumes 18% less energy than OH systems in large spaces with high ceilings, such as theaters. These results further supported the energy benefits of UFAD systems described in paragraph 1.1.3.2.

1.5. Simplified UFAD design tool

As discussed above, EnergyPlus is capable of performing load and airflow rate calculations, as well as simplified thermal stratification prediction for UFAD systems. However, EnergyPlus is a complex software, and the cost and effort related to modeling a building for the cooling load calculation using EnergyPlus is, most of time, prohibitive for HVAC designers. Therefore, it is valuable to develop a simplified load calculation procedure for practitioners to use. Currently, there are two available design tools for determining zone airflow requirements for UFAD systems (ASHRAE, 2013b): one, named here the CBE UFAD Cooling Load Design Tool, was developed at Center for the Built Environment (CBE) at University of California, Berkeley (Schiavon et al., 2010a); the other one, named here the RP-1522 tool, was developed at Purdue University as result of the ASHRAE Research Project (RP-1522) (Jiang et al., 2012).

1.5.1. CBE UFAD cooling load design tool

Bauman et al. (2007b) developed a spreadsheet-based simplified tool in 2007 to help HVAC designers predict required cooling airflow rates and the amount of stratification in the occupied zone for UFAD systems. An improved CBE UFAD Cooling Load Design Tool was developed in 2010 by Schiavon et al. (2011), which is publicly available online at http://www.cbe.berkeley.edu/ufad-designtool_old/online.htm. The CBE UFAD Cooling Load Design Tool is capable of predicting the design cooling load, airflow rate, room air stratification, and plenum air temperature gain for both interior and perimeter zones of a typical multi-story office or other commercial building using UFAD (Schiavon et al., 2011, Schiavon et al., 2010b, Bauman et al., 2010). The CBE UFAD Cooling Load Design Tool does not calculate the UFAD cooling load from scratch, but instead uses the cooling load calculated for the same building under design with an OH system as input. This can be obtained from common load calculation programs, like TRACE 700, hourly analysis program (HAP), and eQUEST etc. (Crawley et al., 2008). The regression equation, which transforms the cooling load for an OH system to the same building with a UFAD system, was derived from 36 EnergyPlus simulations. A detailed description of the method used to obtain the regression equation is reported in (Schiavon et al., 2011). Users need to input the floor level, zone type and orientation, as well as the cooling load calculated for OH system to the design tool, and then the cooling load for the UFAD system will be calculated. In this way, using a familiar load calculation tool, the HVAC designer can account for such factors as building shell construction, internal loads, orientation, climate, etc.

The CBE UFAD Cooling Load Design Tool allows the user to select from three types of diffusers, including swirl diffusers for interior zones, variable air volume (VAV) directional diffusers for interior and perimeter zones, and linear bar grilles for perimeter zones. Figure 13a shows a typical swirl diffuser, which are commonly installed in the interior zone of UFAD systems. Swirl diffusers are generally installed as passive diffusers, requiring a pressurized underfloor plenum. Figure 13b shows a typical VAV directional diffuser, which operates with constant underfloor plenum pressure (i.e. 12.5 Pa (0.05 iwc)) and constant discharge air velocities. They employ a pulse-width modulation (PWM) valve that automatically adjusts individual terminals, using time-modulation logic and digital accuracy to maintain thermostat set points. The integrated motor uses a timed

sequence of fully open or closed positions, based on load, to supply cooling or heating to the space (YORK, 2006). Figure 13c shows a linear bar grille. Linear bar grilles are standard products that are routinely used in OH systems and are commonly employed in UFAD systems for heating and cooling in the perimeter zone. They come in various lengths and widths. The one used in the lab test is 0.15 m by 1.83 m (6 in. by 6 ft).

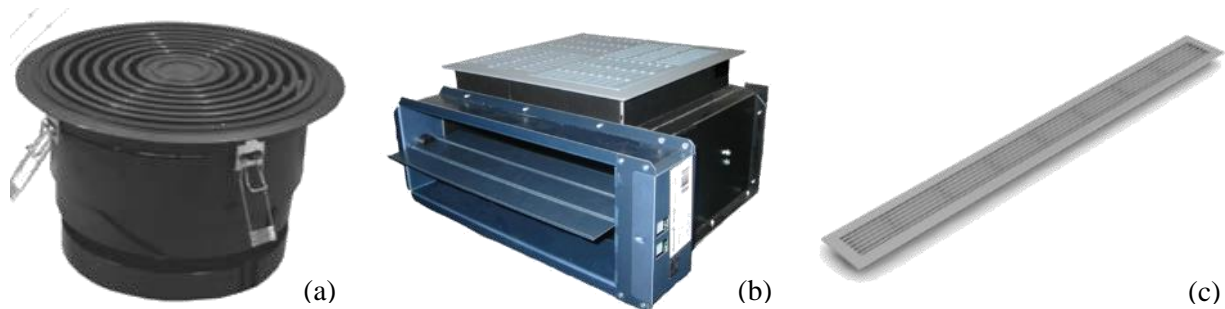


Figure 13 (a) Swirl diffuser (b) VAV directional diffuser (c) linear bar grille

The stratification models used in the CBE UFAD Cooling Load Design Tool were developed using the full-scale experimental testing database, which covers all three types of diffusers discussed above in either interior or perimeter zones (Lin and Linden, 2005, Liu and Linden, 2006, Webster et al., 2002b).

Experimental measurements give the relevant information concerning the thermal environment for various spaces under different thermo-fluid conditions. However, it is very expensive and time consuming to measure detailed information in an indoor space with a UFAD system. One of the limitations of this method is that it is often inflexible in changing the dimensions of the indoor spaces to be studied. Furthermore, the resolution of the measured data is normally not fine enough to obtain a complete picture of the ventilation performance in an indoor space (Zheng et al., 2012). This might bring uncertainties to a model developed from experimental measurements.

1.5.2. ASHRAE RP-1522 UFAD design tool

The ASHRAE RP-1522 tool is an airflow design tool, which was developed in 2010 in an ASHRAE research project. It is freely available to ASHRAE members. The RP-1522 tool is able to predict the vertical temperature difference between the head and ankle of occupants and the supply airflow rate for one zone under cooling conditions (Zheng et al., 2012). The RP-1522 tool requires the user to specify the zone cooling load and the fraction of the cooling load assigned to the underfloor plenum, if the supply air temperature at the air handler is specified. Otherwise, the user must specify the supply air temperature at the diffuser.

The stratification model that RP-1522 tool used was developed from an extensive CFD simulation database with 150 cases (Xue et al., 2012a). The database covers typical airflow and thermal conditions in multiple room spaces, including classrooms, offices, workshops, restaurants, retail shops, conference rooms and auditoriums. Similar to the development of the CBE UFAD Cooling Load Design Tool, three types of diffusers, including swirl, VAV directional and linear bar grille,

are simulated in both interior and perimeter zones. The database is based on the study of both Lee et al. (2009b) and Lee et al. (2011). Before conducting the parametric CFD simulation study, nine experimental tests were also performed to validate the CFD model. These nine cases cover three types of diffusers in office, classroom, and conference room. From the experimental results, they found that thermal stratification of UFAD systems varied depending on the diffuser type, zone type, and space type (Zheng et al., 2012). Therefore, a unique stratification model was developed for each type of diffuser. Lee et al. (2009a) examined the influence of several key design parameters on air distribution effectiveness by using a validated CFD program. An empirical equation was developed from 102 parametric CFD simulation database to calculate the air distribution effectiveness for UFAD, which was also implemented into RP-1522 tool.

The advantages of using CFD simulation is that it can quickly obtain detailed information concerning ventilation performance at very little cost (Zheng et al., 2012). However, there are also limitations. One of them is that it uses approximations to model the flow physics (Versteeg and Malalasekera, 1995). The approximations could bring uncertainties to the computational results. The uncertainties could come from grid resolution, wall surface and diffuser boundary conditions, and turbulence models. As mentioned before, the CFD model that the RP-1522 tool used to create the database is validated with the experiments tested in three type of building layouts. However, spaces with high ceilings like auditoriums are also simulated with the same CFD model. The fact that thermal characteristics in spaces with high ceilings, including the air velocity distributions, air temperature, and contaminant concentrations, are the same as those in spaces with normal ceiling height was not proved. Hence, this might bring uncertainties to the simulation results of cases with high ceilings.

1.6. Statement of the problem

The ASHRAE 2013 UFAD design guide is the main references for the building design, construction, and operations industry. The two simplified UFAD design tools, which were introduced in Chapter 11.7 of ASHRAE UFAD design guide (ASHRAE, 2013b), play an important role in helping HVAC engineers to determine zone airflow requirements and predict the thermal stratification in UFAD system. Zone airflow rate and thermal stratification have a direct impact on the energy performance, and indoor environment quality of the UFAD system. Currently there are not studies comparing the two design tools. This makes it difficult for HVAC designers to decide which design tool is more appropriate to use. HVAC designers would like to understand whether there are differences between these two design tools in regards to those aspects that distinguish UFAD systems from other air distribution methods. The relevant aspects include the design cooling load, thermal stratification profile, the air distribution models, diffuser types, supply plenum heat balance, plenum configuration and air distribution effectiveness.

Besides, the stratification model implemented in the current CBE UFAD cooling load design tool has been developed based on 79 experimental tests, the one for the RP-1522 is based on 31 CFD tests. Therefore, there's a possibility of expanding the CBE experiment database by adding the CFD simulation database from the RP-1522 tool. The CBE stratification model then could be

updated with the larger database, which would be expected to be more accurate and more robust than the original one.

1.7. Objectives

In order to address the previously identified problems, the objectives of this work are:

- To comprehensively compare the features of the CBE UFAD Cooling Load Design Tool and RP-1522 tool based on design cooling load, thermal stratification profile, air distribution models, diffuser types, supply plenum heat balance, plenum configuration and air distribution effectiveness.
- To quantitatively compare the accuracy of the thermal stratification predictions of the two tools using a combined database. The new database would be composed of both full-scale experiments (CBE) and CFD simulations (RP-1522).
- To develop a new stratification model for each type of diffuser based on the combined database.
- To update the CBE UFAD Cooling Load Design Tool with the newly developed stratification model and implementing new capabilities to CBE tool.

1.8. Significance

The comprehensive comparison of the two UFAD design tools will provide HVAC designers with a reference when deciding which design tool to use. It will help HVAC designers to understand the difference between the capabilities of these two tools and to choose the most appropriate one for the given task. It also gives an assessment of the accuracy of each design tool when predicting the thermal stratifications in a UFAD system.

The updated stratification model for the CBE UFAD Cooling Load Design Tool, which will be developed from larger data samples, would be expected to be more accurate and robust than the original one. If so, the updated CBE UFAD Cooling Load design tool will help calculate the supply airflow rate, and predict thermal stratification more accurately. This will help maximize the potential benefits of UFAD systems in energy savings, thermal comfort, and IAQ. As a member of the integrated design team, the engineer would be responsible for conducting the modeling, and communicating the results with the architect to evaluate the implications for architectural design decisions. In the big picture, it would also be beneficial for green building development and to reduce buildings' impact on the total U.S. energy consumption.

2. The comparison of two UFAD design tools

As introduced in paragraph 1.5, currently there are two available design tools for determining zone airflow requirements for UFAD systems, one is CBE UFAD tool, and the other one is RP-1522 tool. In order to provide design engineers with the reference to choose appropriate design tools, it is important to perform a comprehensive comparison of these two tools. This chapter will mainly discuss the differences and similarities between the two UFAD design tools. The comparison is composed of two parts, the first part is the feature comparison, including the design cooling load, thermal stratification profile, air distribution models, supply plenum cooling load, plenum configurations, diffuser types, air distribution effectiveness, work scheme and user interface. The second part is the numeric comparison, which was performed to provide a quantitative assessment of the accuracy of the two tools.

2.1. Feature comparison

2.1.1. Design cooling load

Previously, it was thought that the design cooling loads for a UFAD system and an overhead (OH) system were nearly identical. However, recent energy modeling research has demonstrated that cooling load profiles for UFAD and OH systems are different (Schiavon et al., 2011). Figure 14 shows a comparison between the predicted cooling load profiles for overhead (mixing) and UFAD systems for five zones of a middle floor from a 3-story prototype office building for a Baltimore, MD, summer design day. The HVAC system is operating between 5am and 8pm. During the night the HVAC system is off. The internal and external heat gains are almost the same for the two systems but the cooling load removed by the HVAC systems is different. The difference is primarily due to the reduced thermal storage effect of the lighter-weight raised floor panels, when compared to the heavier mass of a structural floor slab, as well as the enhanced rate of zone heat removal due to radiant heat transfer (Schiavon et al., 2010a). In an OH system, part of the heat is stored in the floor slab during the day, thus reducing peak zone cooling loads, and released at night when the air conditioning system is off; In a UFAD system the presence of the raised flooring transforms the solar-absorbing massive floor slab into a lighter weight material. This transformation reduces the ability of the slab to store heat, thereby resulting in relatively higher peak cooling load in the zone. The precise magnitude of the difference in design cooling loads between the overhead and UFAD system is still under further investigation, but mainly depends on zone orientation, floor level, and possibly the effects of furniture (ASHRAE, 2013b).

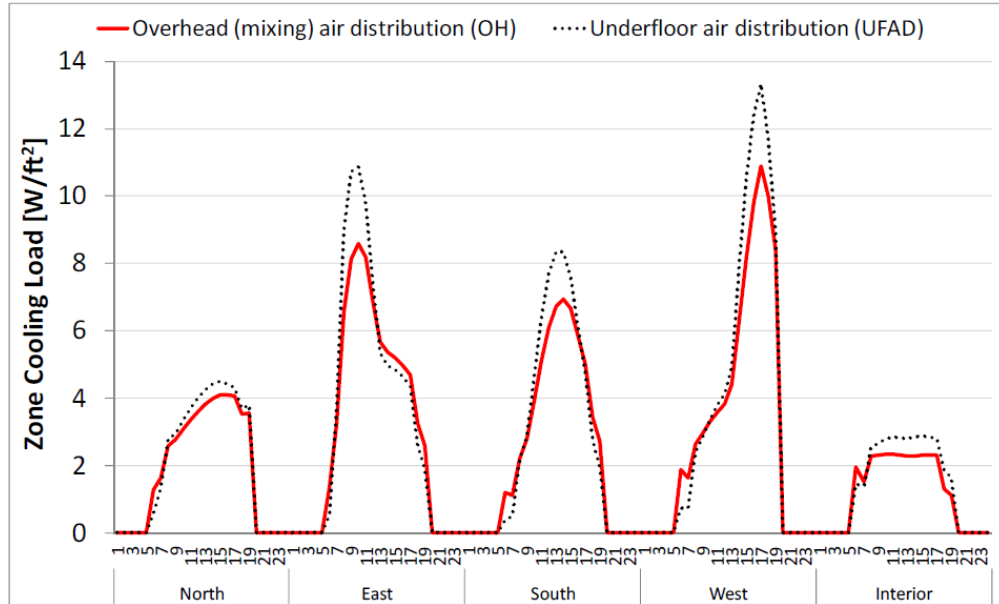


Figure 14 Cooling load profiles for overhead (mixing) vs. UFAD systems

Thermal mass is a relevant issue for architecture design, as it relates to basic design decisions about the buildings. Given that a UFAD system has higher peak cooling load than a traditional OH system, it is essential to reduce the load during the architectural design phase, in order to improve the energy performance of UFAD system. There are many ways to reduce the cooling load at the architecture design phase, such as choosing the best orientation to minimize excessive solar gain on the east and west facades, integrating concrete light shelves to add more mass to the building, etc. More strategies can be found in Brown and Dekay (2000).

Recent technology in the access raised floor also brings opportunities to compensate the higher peak cooling load of UFAD systems. A phase change panel, EcoCore, was recently developed to incorporate the latest advances in micro-encapsulated phase change materials to reduce building peak cooling load and save energy. The phase change materials within the EcoCore panel can absorb and store the heat gains from the solar radiation during the day, and release heat during non-peak hours (nighttime). In this way, the peak cooling load can be reduced in the space, resulting in the reduction of cooling energy (Tate Access Floor, 2012).

A new index, named UFAD cooling load ratio ($UCLR$), which is defined by the ratio of the peak cooling load calculated for UFAD (CL^{UFAD}) to the peak cooling load calculated for a well-mixed system (CL^{OH}) as described in Equation 1, was developed to calculate the cooling load for UFAD system. The CBE UFAD tool is able to calculate the UFAD cooling load for each zone with the $UCLR$ when the traditional peak cooling load has been calculated for an overhead (well-mixed) system.

$$UCLR = \frac{CL^{UFAD}}{CL^{OH}} \quad \text{Equation 1}$$

UCLR can be obtained with the empirical Equation 2 , developed by Schiavon et al. (2010b).

$$UCLR = 0.9528 + C_1X_1 + C_2X_2 \quad \text{Equation 2}$$

Where X_1 = floor level: ground, middle and top; $C_1=0$ if floor is the ground floor; $C_1=0.1572$ if floor is a middle floor; $C_1=0.2379$ if the floor is a top floor; X_2 = zone type: one interior zone and four perimeter zones, orientations east, south, west, and north; $C_2=0$ if the zone is north oriented; $C_2=0.1739$ if the zone is east; $C_2=0.0999$ if the zone is south; $C_2=0.1349$ if the zone is west; $C_2=0.0802$ if the zone is an interior zone.

The ASHRAE RP-1522 tool does not calculate the cooling load as it was not the objective of the project, but accepts two cooling loads as an input (“equipment, occupants and lighting” and “solar heat flux”). It requires users to obtain the UFAD design cooling load from energy simulation programs (like EnergyPlus) or those methods described in ASHRAE Fundamentals Handbook (Zheng et al., 2012). There are two limits with this approach. First, only EnergyPlus has the ability to calculate UFAD cooling load (Webster et al., 2008b), and if the HVAC designers use EnergyPlus, the two simplified tools are not needed. However, the simplified tool can still be used to obtain a more precise temperature profile. Second, the two inputs related to cooling load are “equipment, occupants and lighting” and “solar heat flux”, which are actually the zone heat gain. There are significant differences between heat gain and cooling load. According to the ASHRAE Fundamentals Handbook (ASHRAE, 2013a), the space heat gain is the rate at which heat enters into and/or is generated within a space, including the heat generated by occupants, lights and appliances and solar radiation through the window. While cooling load is the rate at which sensible and latent heat must be removed from the space to maintain a constant space air temperature and humidity. In particular, it underlines that the sum of all space instantaneous heat gains at any given time does not necessarily equal the cooling load for the space at that same time. Therefore, the RP-1522 tool is not capable of calculating the cooling load for a UFAD system.

2.1.2. Thermal stratification profile

As introduced in paragraph 1.2, in a properly controlled UFAD systems under cooling operation, temperature stratification will be produced in the conditioned space. This results in higher temperatures at the ceiling level that change the dynamics of heat transfer within a room, as well as between floors of a multi-story building (Bauman, 2003). Thermal stratification also affects occupants’ thermal comfort. In a well-mixed system the air temperature measured at 1.2 m is considered representative of the thermal environment. This assumption is no longer valid when UFAD is used, which produces temperature stratification in the conditioned space as shown in Figure 15. Wyon and Sandberg (1996) showed that local and whole-body discomfort sensations is slightly affected by thermal gradient, but is strongly affected by average operative temperature. The CBE UFAD design tool uses the average occupied zone temperature ($T_{oz,avg}$) to better represent the acceptable comfort condition for standing occupants in a stratified room, on the assumption that the thermal sensation perceived by an occupant exposed to a stratified

environment is close to that of an occupant exposed to a uniform air temperature equal to the average occupied zone temperature (Schiavon et al., 2010b).

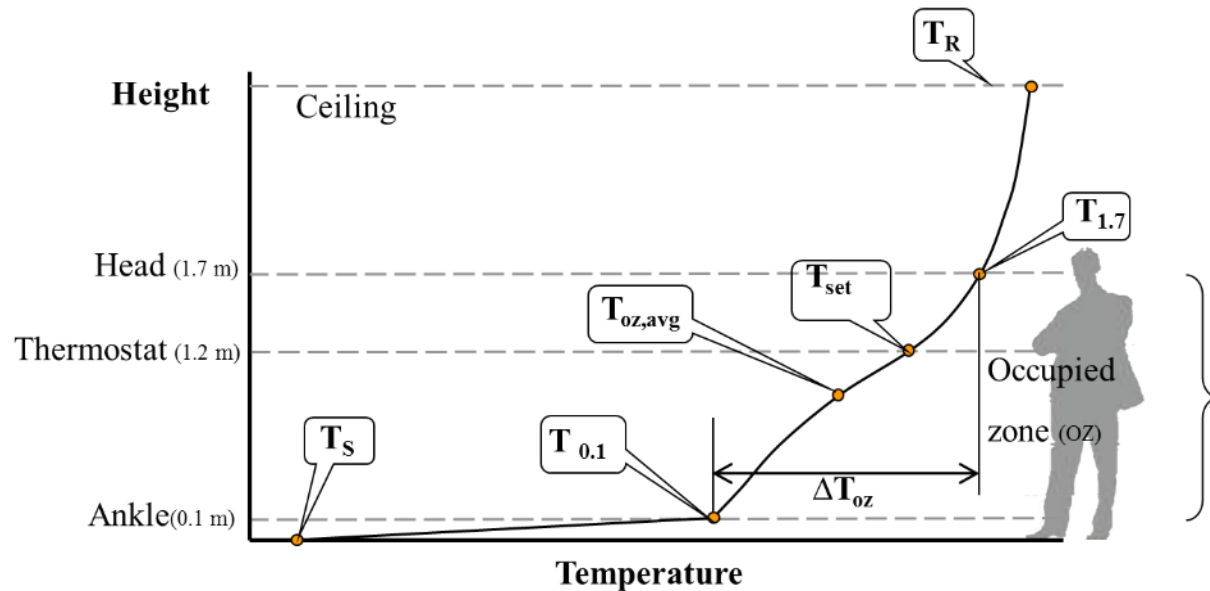


Figure 15 Example room air temperature profile in stratified UFAD room. (Schiavon et al., 2010b)

Besides, the CBE UFAD Cooling Load Design Tool is able to provide the temperature at the thermostat height (1.2 m), so that users know the actual setpoint for the thermostat in order to meet occupants' thermal comfort needs.

In ASHRAE RP-1522 tool, a different way of characterizing the temperature gradient is used to predict the thermal stratification of UFAD system as Figure 16 shows. The average temperature of occupied zone, $T_{oz,avg}$, is used to represent the comfort condition of the occupants in stratified thermal environment. $T_{oz,avg}$ equals the average temperature between the air temperature at standing head level (1.7 m), $T_{1.7}$, and air temperature at ankle level (0.1 m), $T_{0.1}$. It also assumes that the room design temperature T_x , which is the same as T_{set} in CBE UFAD tool equals the $T_{oz,avg}$ without considering the difference of occupants' thermal sensation between the stratified thermal environment and well-mixed condition. This might cause the calculation of supply airflow rate to be slightly larger than required.

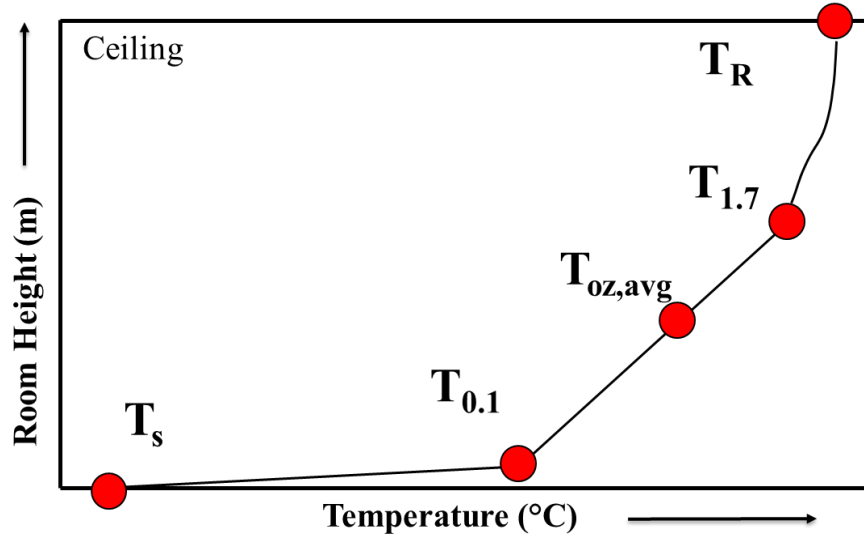


Figure 16 Computed temperature points in the thermal stratification model. (Jiang et al., 2012)

2.1.3. Air distribution models for predicting thermal stratification

The CBE UFAD tool uses the Gamma (I)-Phi (Φ) model to predict thermal stratification. Φ is the dimensionless temperature at a height in the room, which is generally defined by the following equation:

$$\Phi = \frac{T - T_s}{T_R - T_s} \quad \text{Equation 3}$$

Where T , T_s and T_R are, respectively, the point, supply and return air temperatures. The dimensionless temperature ratio at the ankle level (0.1 m), $\Phi_{0.1}$, at the occupied zone, Φ_{oz} , and at the head level for a standing person (1.7 m), $\Phi_{1.7}$, are defined in Equation 4, Equation 5 and Equation 6. In this project, the temperature at the occupied zone, T_{oz} , as the average of $T_{0.1}$ and $T_{1.7}$.

$$\Phi_{0.1} = \frac{T_{0.1} - T_s}{T_R - T_s} \quad \text{Equation 4}$$

$$\Phi_{oz} = \frac{T_{oz} - T_s}{T_R - T_s} \quad \text{Equation 5}$$

$$\Phi_{1.7} = \frac{T_{1.7} - T_s}{T_R - T_s} \quad \text{Equation 6}$$

For displacement ventilation systems according to Chen and Glicksman (2003), $\Phi_{0.1}$ varies between 0.2 and 0.7. According to Nielsen, $\Phi_{0.1}$ is between 0.3 and 0.7 (Nielsen, 1993). Mundt (1996) and Skistad et al. (2002) developed a model for the prediction of $\Phi_{0.1}$ for displacement ventilation systems that is a function of the airflow rate and it is based on a heat transfer model between the ceiling and the floor. Mundt's equation is used in a cooling airflow design modelling tool developed by Chen and Glicksman (2003).

According to Liu and Linden (2006), Γ is a non-dimensional parameter representing the relative strengths between buoyancy and momentum forces. It was also showed that the buoyancy flux generated by the heat source and the momentum flux from the diffuser discharge are the two governing parameters for the thermal stratification. Lin and Linden (2005), Liu and Linden (2006) and Liu and Linden (2008) theoretically developed and experimentally tested (in a small-scale salt-tank model) a prediction of Φ for UFAD system as a function of Γ . Their model was used to develop stratification prediction based on full-scale experiments by Webster et al. (2007). The formulation of Γ is different for the interior and perimeter zones, as reported in Equation 7 and Equation 8.

Γ for the interior zone:

$$\Gamma = \frac{(Q \cdot \cos \varphi)^{\frac{3}{2}}}{m \cdot \left(\frac{n}{m} \cdot A_d\right)^{\frac{5}{4}} \cdot (0.0281 \cdot W)^{\frac{1}{2}}} \quad \text{Equation 7}$$

Where Q = room airflow (m^3/s); A_d = Diffuser effective area; $\cos \varphi$ = discharge angle for diffuser flow; n = number of diffusers; m = number of plumes (i.e., occupants); and W = zone cooling load (supply and return plenum cooling loads are not included plenum) (kW).

Γ for the perimeter zone:

$$\Gamma = \frac{(Q \cdot \cos \varphi)}{(n \cdot A_d) \cdot (0.0281 \cdot W_L)^{\frac{1}{3}}} \quad \text{Equation 8}$$

Where Q = total perimeter zone airflow (m^3/s); A_d = diffuser effective area (m^2); $\cos \varphi$ = cosine of discharge angle for diffuser flow; n = number of diffusers; and W_L = zone extraction rate per unit length of zone (kW/m).

The empirical equations correlating Γ and Φ were developed from laboratory experiments for each type of diffusers (Schiavon et al., 2010b, Webster et al., 2007), which were shown in Table 2.

Table 2 Γ - Φ relationships at 0.1 and 1.7 m for the diffuser types used in the design tool

| Zone | Diffuser Type | Γ - $\Phi_{0.1}$ | Γ - $\Phi_{1.7}$ |
|-----------|-------------------|---|--|
| Interior | Swirl | $\Gamma \leq 7.0$; $\Phi_{0.1} = 0.4024$ | $\Phi_{1.7} = 0.951$ |
| | | $7 < \Gamma < 78.4$; $\Phi_{0.1} = 0.2075 \Gamma^{0.3403}$ | |
| | | $\Gamma > 78.4$; $\Phi_{0.1} = 0.9155$ | |
| Interior | VAV directional | $\Phi_{0.1} = 0.745$ | $\Phi_{1.7} = 0.956$ |
| Perimeter | VAV directional | $\Gamma \leq 2.9$; $\Phi_{0.1} = 0.5452$ | $\Gamma \leq 2.9$; $\Phi_{1.7} = 0.7719$ |
| | | $2.9 < \Gamma \leq 15$; $\Phi_{0.1} = 0.4605 + 0.0292\Gamma$ | $2.9 < \Gamma \leq 15$; $\Phi_{1.7} = 0.7168 + 0.0190\Gamma$ |
| | | $\Gamma > 15$; $\Phi_{0.1} = 0.8987$ | $\Gamma > 15$; $\Phi_{1.7} = 1.0018$ |
| | | Remove 0.13 if blinds are down | |
| Perimeter | Linear bar grille | $\Gamma \leq 2.7$; $\Phi_{0.1} = 0.3582$ | $\Gamma \leq 2.7$; $\Phi_{1.7} = 0.8305$ |
| | | $2.7 < \Gamma \leq 23$; $\Phi_{0.1} = 0.1282 + 0.0908\Gamma - 0.0021\Gamma^2$ | $2.7 < \Gamma \leq 23$; $\Phi_{1.7} = 0.7742 + 0.0208\Gamma$ |
| | | $\Gamma > 23$; $\Phi_{0.1} = 1.1074$ | $\Gamma > 23$; $\Phi_{1.7} = 1.2535$ |
| | | Remove 0.13 if blinds are down | |

Because the experimental data for the Γ - Φ model was primarily focusing on office layouts, the CBE UFAD tool has the limitation that it is mainly applicable to office buildings. Γ - Φ model requires the users to specify the number of thermal plumes for the design calculation, which is referred as the number of occupants in CBE UFAD tool.

The RP-1522 tool uses the Archimedes number (Ar), which is defined in Equation 9. Ar is the ratio between the buoyancy and inertial forces in heat transfer and thermal fluid flow problems. Xue et al. (2012b) showed that the convective heat gain in the occupied zone contributes to room air thermal stratification due to buoyancy while the inertial force from the diffuser discharge provides mixing. An empirical quadratic regression model was developed from the CFD simulation database. The model correlates Ar with the temperature difference in the occupied zone $\Delta T_{oc} = T_{1.7} - T_{0.1}$, and is implemented in RP-1522 tool.

$$Ar = \frac{G_r}{Re} = \frac{\frac{g\beta(T_R - T_S)L^3}{\nu^2}}{\frac{uL}{\nu}} = \frac{gWHA_d^2}{C_P Q_d^2 Q \rho (T_x + 273.15)} \quad \text{Equation 9}$$

Where

G_r = Grashof number; Re = Reynolds number; g = gravitational constant ($m^3/kg \cdot s^2$);

β = thermal expansion coefficient ($m/m \cdot K$); T_R = return air temperature ($^{\circ}C$);

T_S = supply air temperature at diffuser ($^{\circ}C$); L = characteristic length (m);

ν = kinematic viscosity ($g/cm \cdot s$); u = air velocity (m/s); W = room heat extraction rate (W);

H = room height (m); A_d = diffuser effective area (m²); C_p =specific heat capacity of air (kJ/kg·K); Q_d = diffuser design airflow rate (L/s); and Q = supply airflow rate (L/s).

Equation 10 shows the regression equation between $\Phi_{1.7}$ and Ar :

$$\Phi_{1.7} = \frac{\Delta T_{oc}}{T_R - T_S} = \frac{T_{1.7} - T_{0.1}}{T_R - T_S} = aAr^2 + bAr + c \quad \text{Equation 10}$$

Note that a , b and c are varying among different types of diffusers, see Table 3.

Table 3 Summary of coefficients in Equation 10

| | a | b | c |
|-------------------|---------|--------|--------|
| Swirl | -0.0720 | 0.2385 | 0.1480 |
| VAV directional | -0.0362 | 0.2316 | 0.1076 |
| Linear bar grille | -0.1623 | 0.4902 | 0.0594 |

In order to develop RP-1522 UFAD design tool, the ankle temperature, $T_{0.1}$ is also correlated to Ar . Equation 11 shows the regression equation, which correlates $T_{0.1}$ with the temperature difference in the occupied zone.

$$\frac{\Delta T_{oc}}{T_{0.1} - T_S} = a'Ar^2 + b'Ar + c' \quad \text{Equation 11}$$

Note that a' , b' and c' varies among different type of diffusers, as shown in Table 4.

Table 4 Summary of coefficients in Equation 11

| | a' | b' | c' |
|-------------------|---------|--------|--------|
| Swirl | -0.3052 | 0.6382 | 0.2094 |
| VAV directional | -0.0673 | 0.4645 | 0.0860 |
| Linear bar grille | -0.2888 | 0.8963 | 0.0247 |

The main advantage of RP-1522 tool is that it can be applied to various types of building layouts, such as classrooms, workshops, restaurants, retail shops, conference rooms and auditoriums, as well as offices. However, there's no input in the tool's interface to allow the users to specify the height of the zone and it has the default built-in value of 2.43 m. This limits the RP-1522 tool's application to spaces with high ceilings, like auditoriums. Besides, For RP-1522 tool, power equation was selected at first to model room air thermal stratification in UFAD systems. However, other forms of equations were not compared to elaborate the accuracy of the model. Furthermore, quadratic function was finally chosen to implement in the tool in order to simplify the calculation process.

2.1.4. Supply plenum cooling load

For UFAD systems, the cool supply air warms up significantly in the supply plenum, as described by Lee et al. (2012b). The amount of heat entering the underfloor plenum directly influences the design cooling airflow rate. Hence, the UFAD cooling load is split into supply plenum, zone and return plenum cooling loads. Based on the research results from Schiavon et al. (2010b), three new indexes, which are supply plenum fraction (*SPF*), zone fraction (*ZF*) and return plenum fraction (*RPF*) were developed to split the total UFAD cooling load into three fractions in order to calculate the cooling airflow rate more accurately. Similar to *UCLR*, a regression equation for each of those indexes was developed based on EnergyPlus simulation results (Schiavon et al., 2011), as summarized in Equation 12, Equation 13, and Equation 14.

$$SPF = 0.6179 + C_1 + C_2 + C_3 \quad \text{Equation 12}$$

$$ZF = 1 - SPF - RPF \quad \text{Equation 13}$$

$$RPF = C_4 \quad \text{Equation 14}$$

Where $C_1 = 0$ if the zone is an interior zone; $C_1 = -0.2095$ if the zone is a perimeter zone; $C_2 = 0$ if the floor level is ground; $C_2 = 0.1242$ if the floor level is middle; $C_2 = -0.0896$ if the floor level is top; $C_3 = 0$ if the zone is interior zone and the floor is the ground floor; $C_3 = 0.0396$ if the zone is a perimeter zone and the floor a middle floor; $C_3 = 0.1642$ if the zone is a perimeter zone and the floor level is a top floor; $C_4 = 0.01$ if floor level is ground; $C_4 = -0.2095$ if floor level is middle; $C_4 = 0.30$ if floor level is top.

The CBE UFAD Cooling Load Design Tool is able to predict *SPF* with the user input of floor level, zone type and orientation as Equation 12 shows. Figure 17 illustrates how the modeling process works to transform the cooling load calculated for a well-mixed zone into a UFAD cooling load and split the UFAD cooling load into the three components, which helps to predict the thermal stratification later.

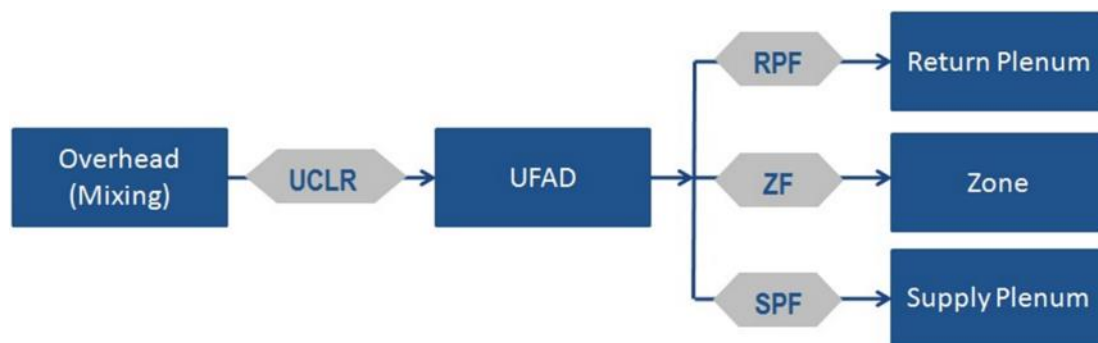


Figure 17 Schematic flow diagram of CBE design tool showing transformation from cooling load calculated for an overhead mixing system into a UFAD cooling load and then divided between the supply plenum, zone (room), and return plenum.

ASHRAE RP-1522 tool requires the user to specify the fraction of the cooling load assigned to the supply plenum (η), as is defined in Equation 15.

$$W = (1 - \eta)W_{tot} \quad \text{Equation 15}$$

Where W = Room heat extraction rate (W); W_{tot} = Total summer design cooling load (W); η = supply plenum heat gain ratio.

This is a limitation because only with an advanced energy simulation (like EnergyPlus) can this be determined. Design load tools are not able to predict it. Zheng et al. (2012) developed an analytical heat transfer model for predicting heat loss to the supply plenum of the UFAD system, however it is not directly implemented into the design tool. Instead Jiang et al. suggested to use 30% to 40% according to the results of (Bauman et al., 2006) which is less accurate than the method used in the CBE UFAD tool.

2.1.5. Plenum configurations

The CBE UFAD Cooling Load Design Tool is able to model four plenum configurations. They are series, reverse series, independent and common plenum configurations, which are shown in Figure 18, Figure 19, Figure 20 and Figure 21. The supply plenum is a key component of a UFAD system, and can have an important impact on peak cooling loads for UFAD compared to an OH system. Due to the plenum temperature rise effect, the air temperature at the diffusers is warmer than the one supplied to the plenum. Taking series plenum as an example, the supply air temperature entering the plenum is 15.6 °C (60 °F). However, because of the supply plenum heat gain, the diffuser discharge temperature in interior zone increases 2.2 °C (4 °F), which is 17.8 °C (64 °F). When the supply air enters the perimeter zone, it has already raised up to 20 °C (68 °F). Besides, the supply air may take many different paths in the supply plenum, which will impact the temperature of the air leaving the diffusers. Therefore, providing different options for plenum configurations is essential to accurately predict the thermal stratification and comfort. The CBE UFAD Cooling Load Design Tool allows the user to specify the temperature at the inlet of the plenum, representing the supply air temperature from the central air handler.

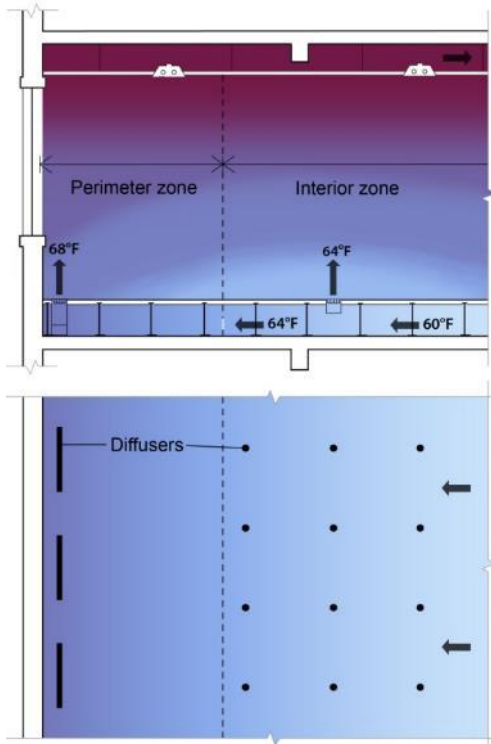


Figure 18 Series plenum configuration

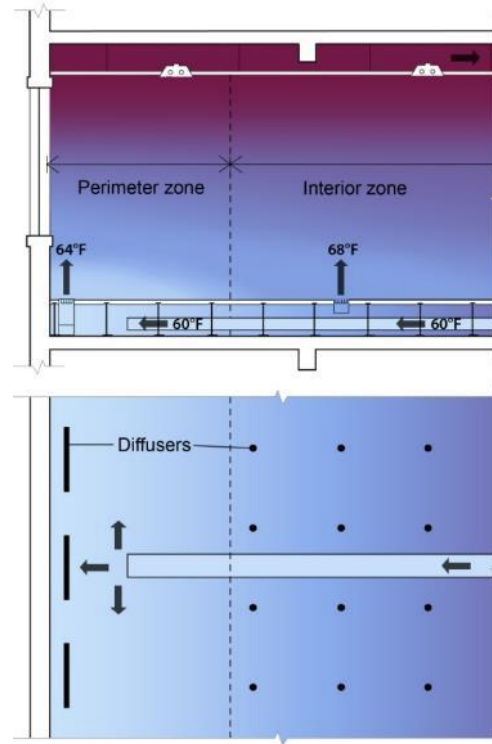


Figure 19 Reverse series plenum configuration

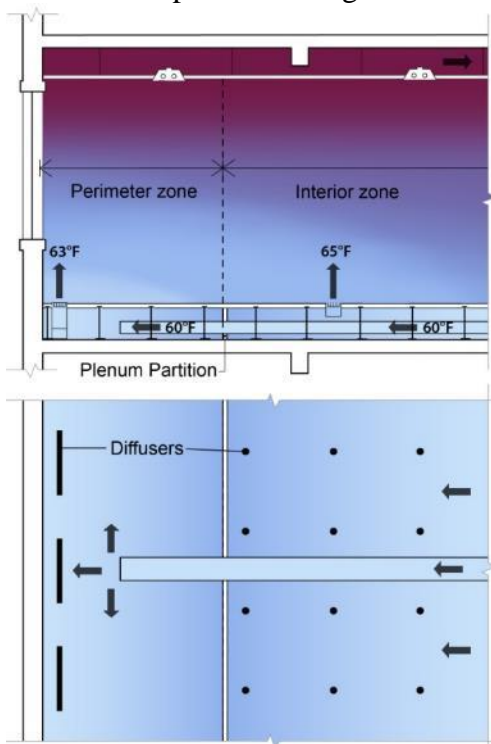


Figure 20 Independent plenums configuration

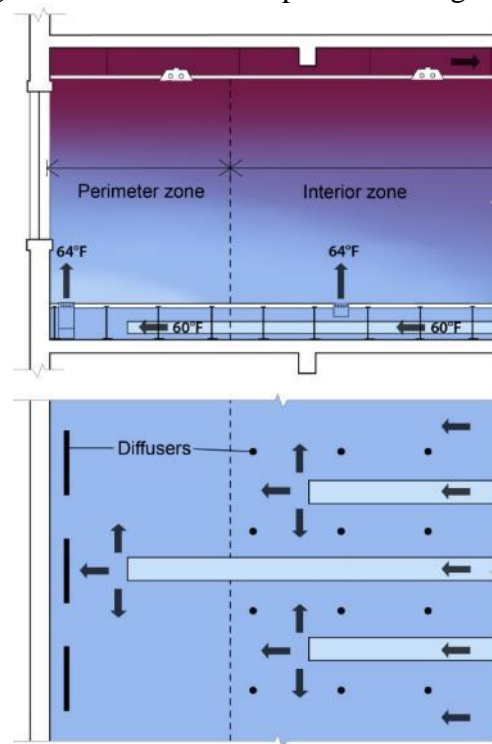


Figure 21 Common plenum configuration

The ASHRAE RP-1522 tool does not consider different plenum configurations and it is only able to calculate one zone at a time. It requires users to specify the supply air temperature at the diffuser or the ratio of plenum flow rate to zonal supply flow rate, which is difficult to get at the design stage.

2.1.6. Diffuser types

Both tools cover three diffuser types: swirl, VAV directional and linear bar grille. However there are slight differences in the specific diffusers that each tool used to build their models. As Table 5 shows, there are differences in the effective outlet area (A_d) of linear bar grille of the two tools, and the design air flow rate (Q_d) for diffusers in the RP-1522 tool varies case by case.

Table 5 Comparison of diffuser types in two UFAD design tools

| Type | | Diffuser Effective Area | Design Airflow Rate | Angle Specific to Diffuser Type | Angle Factor Specific to Diffuser Type |
|-------------------|---------|-------------------------|---------------------------|---------------------------------|--|
| | | A_d (m ²) | Q_d (m ³ /h) | θ (°) | Cos θ |
| Swirl | CBE | 0.0075 | 122 | 28 | 0.883 |
| | RP-1522 | 0.0075 | variable | 28 | 0.883 |
| VAV directional | CBE | 0.0350 | 250 | 45 | 0.707 |
| | RP-1522 | 0.0350 | variable | 45 | 0.707 |
| Linear bar grille | CBE | 0.0152 | 247 | 15 | 0.966 |
| | RP-1522 | 0.0276 | variable | 15 | 0.966 |

For CBE UFAD tool, users can select from swirl and VAV directional diffuser for interior zones, VAV directional and linear bar grille for perimeter zones. The value of A_d and θ have the default settings built in CBE UFAD tool. In the current version of the tool, the user cannot change those values to match different diffuser designs. For RP-1522 tool, users are required to input the operating airflow rate (Q_d), and the effective outlet area (A_d) for each diffuser. This gives users more power to edit the characteristics of the diffusers. However, users have to check the diffuser catalogues or contact the manufacturers to get the precise information to use the tool.

2.1.7. Air distribution effectiveness

One of the advantages of RP-1522 tool is that it is able to calculate the air distribution effectiveness E_z . E_z is a description of an air distribution system's ability to remove internally generated pollutants from a building, zone or space. In ASHRAE Fundamental Handbook (ASHRAE, 2005), ventilation effectiveness is defined as

$$E_z = \frac{C_e - C_s}{C_b - C_s} \quad \text{Equation 16}$$

Where E_z = ventilation effectiveness; C_e = contaminant concentration at the exhaust; C_s = contaminant concentration at the supply; C_b = contaminant concentration at the breathing zone.

According to ASHRAE standard 62.1 (ANSI/ASHRAE, 2010b), E_z for spaces with ceiling supply of cool air is equal to 1.0. For spaces with floor supply of warm air and ceiling return, E_z equals 0.7. In the latest version of ASHRAE standard 62.1(ANSI/ASHRAE, 2013b), it is said that for a UFAD system that provides low velocity air at 4.5 ft above the floor (less than 50 fpm), E_z is assigned to be 1.2. Lee et al. (2009a) shows that UFAD has higher ventilation effectiveness, and spaces with a high ceiling such as workshops and auditoriums have higher E_z than those with a low ceiling.

ASHRAE (ANSI/ASHRAE, 2010b) defines the minimum airflow rate required in the breathing zone of the occupiable space, V_{bz} , which is based on mixing ventilation where the ventilation effectiveness is 1.0. V_{bz} is defined in Equation 17.

$$V_{bz} = R_p \cdot P_z + R_a \cdot A_z \quad \text{Equation 17}$$

Where A_z = zone floor area: the net occupiable floor area of the ventilation zone (m^2); P_z = zone population: the number of people in the ventilation zone during typical usage; R_p = outdoor airflow rate required per person (L/s-person); R_a = outdoor airflow rate required per unit area (L/s- m^2). Note that R_p and R_a are determined from Table 6-1 in ASHRAE Standard 62.1(ANSI/ASHRAE, 2010b).

The required supply airflow rate (V_f) of fresh air in UFAD can be calculated by Equation 18.

$$V_f = V_{bz}/E_z \quad \text{Equation 18}$$

Where V_f = the minimum airflow rate of fresh air (L/s); V_{bz} = the required minimum supply airflow rate for breathing zone (L/s); E_z = air distribution effectiveness. It is essential to calculate E_z , so that V_f can be determined to check whether the predicted supply airflow rate meets ASHRAE requirements for acceptable indoor air quality.

According to the study of Lee et al. (2009a), an empirical equation was developed based on a database, which contained 102 cases of CFD parametric cases. This study identifies six most important parameters, including the diffuser type, total airflow rate, airflow rate per diffuser, supply air temperature, cooling load and the diffuser density, to follow in developing the correlation equation for calculating E_z through statistical analysis. The empirical equation used to predict E_z in the stratified air distribution systems was defined in Equation 19.

$$E_z = 1.9 + 0.9252 \frac{QW}{A_f^2} + 37.8 \frac{QT_s}{A_f H} + 103.68 \frac{Q^2 T_s}{A_f H n} - 1288.8 \frac{Q}{A_f H} - 3240 \frac{Q^2}{A_f H n} + 0.00591 \frac{W}{A_f} \quad (SI \text{ units}) \quad \text{Equation 19}$$

Where n = the number of diffusers; Q = supply airflow rate (m^3/s); W = room heat extraction rate (W); A_f = Zone floor area (m^2); H = Room height (m); T_s = supply air temperature at the diffuser ($^\circ\text{C}$). This equation has been implemented in RP-1522 tool. However, the CBE UFAD tool currently does not have the capability to calculate E_z .

2.1.8. Work scheme of the tools

A working scheme chart was made for each tool in order to compare the calculation process. Figure 22 shows the work scheme for an independent plenum configuration in CBE UFAD cooling load design tool. Variables with grey background are the inputs of the tool, and the ones with blue background are intermediate variables or the outputs. In general, the whole process can be divided into two parts: the first one is cooling load calculation, the second one is using the solver to vary the supply airflow rate in order to make $T_{oz,avg}$ equals the room design temperature.

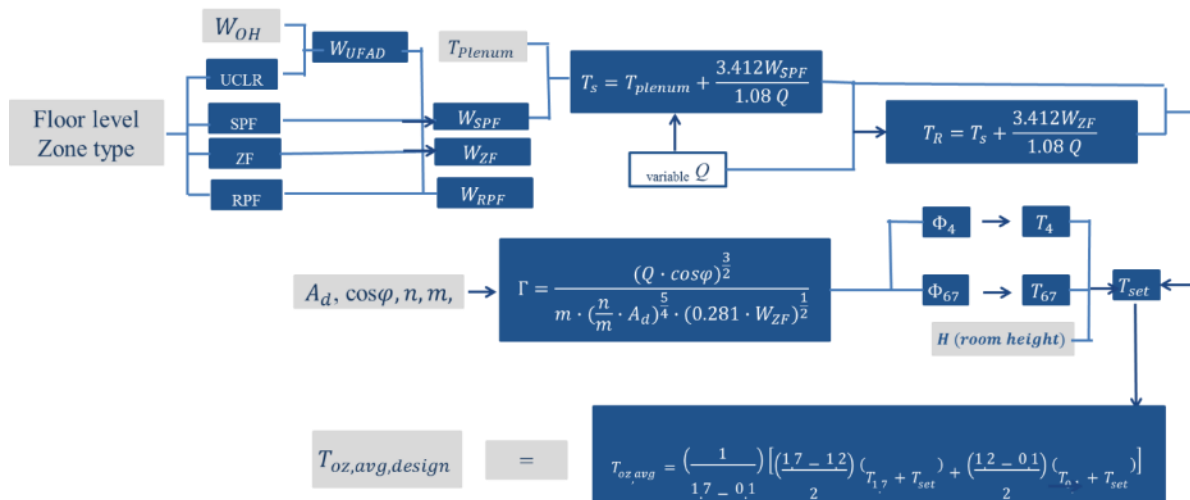


Figure 22 work scheme of CBE UFAD cooling load design tool

Figure 23 describes the work scheme of RP-1522 tool. The solver of RP-1522 tool will vary the supply airflow rate for several times in order to make the difference between two ΔT_{oc} less than the convergence criteria and finally get the outputs of ΔT_{oc} and V .

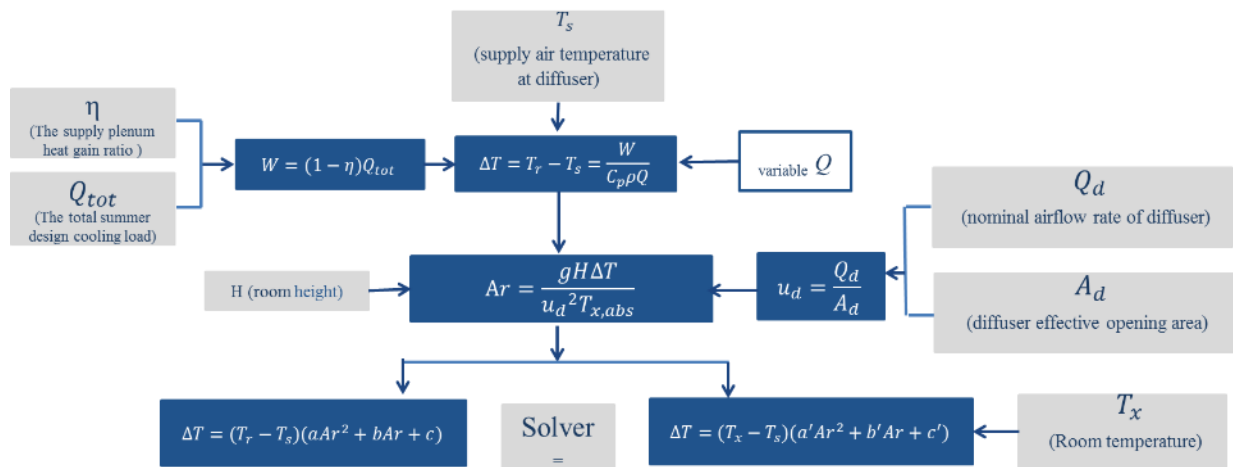


Figure 23 work scheme of ASHRAE RP-1522 UFAD design tool

2.1.9. User interfaces

CBE tool has both online web-based version and spreadsheet version, as shown in Figure 24. It is publicly available to all the users. It has three panels, including the input, results and stratification profile visualization. Figure 25 is a screen shot of the RP-1522 UFAD design tool. It was a program available to ASHRAE members, which to some extent constrains its popularization.

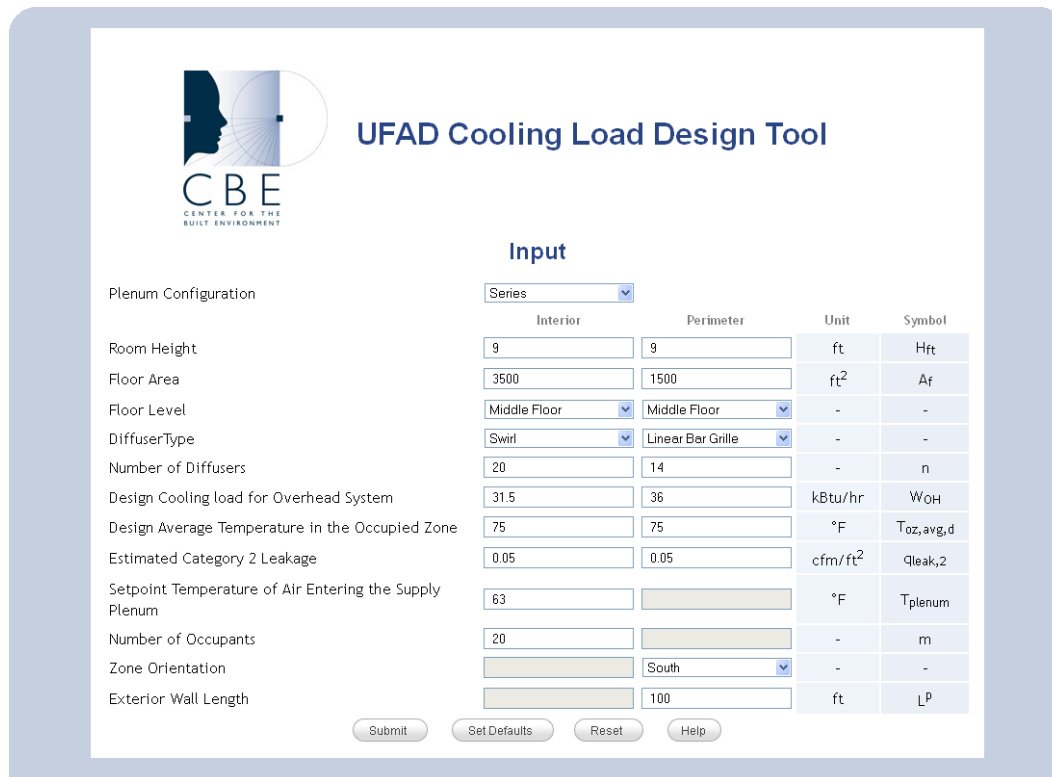


Figure 24 web based version of CBE tool

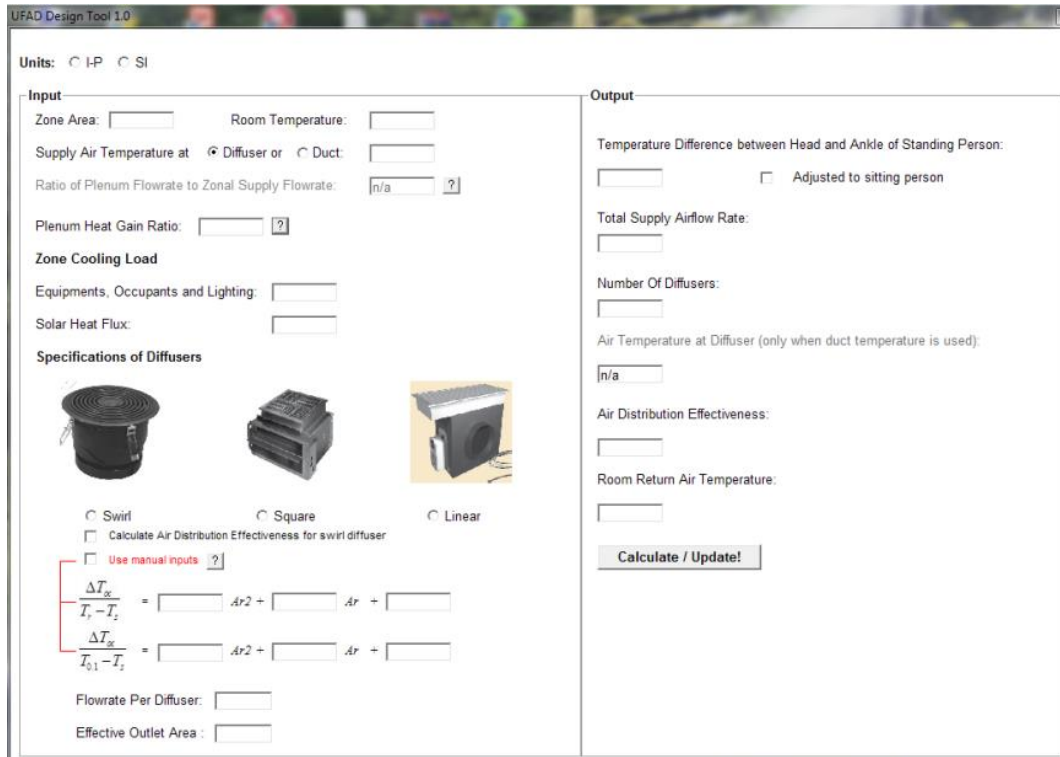


Figure 25 screenshot of the ASHRAE RP-1522 tool

2.2. Numeric comparison

2.2.1. Method

A numeric comparison was performed to provide a quantitative assessment of the accuracy of the two tools. Given that the users could only specify the supply air temperature entering the plenum in CBE UFAD Cooling Load Design Tool, it is not feasible to feed exactly the same inputs to both tools in order to keep the supply air temperature at the diffuser level (T_S) and return air temperature (T_R) the same. Therefore, only the air distribution model for predicting the thermal stratification is compared using a new UFAD database. In this case, the supply air temperature at the diffuser (T_S) and return air temperature (T_R) are kept the same for both models. The predicted temperature at the ankle level ($T_{0.1}$) and at the head level ($T_{1.7}$) will be compared.

The new UFAD database is a combination of 79 cases from the CBE full-scale experiments and 31 cases from the RP-1522 CFD simulations. All the cases are office building layout and the diffuser configurations are shown in Table 6.

Table 6 Case configuration of combined database

| | Swirl | VAV directional | | Linear bar grille | Total |
|-----------|----------|-----------------|----------|-------------------|-------|
| Zone type | Interior | Interior | Exterior | Exterior | |
| RP-1522 | 13 | 6 | 6 | 6 | 31 |
| CBE | 18 | 8 | 30 | 23 | 79 |

For CBE UFAD tool, Γ is calculated according to Equation 7 and Equation 8 with the inputs of room airflow, diffuser effective area (A_d), discharge angle for diffuser flow (θ), number of diffusers, number of plumes and zone cooling load. Based on the Γ - Φ equations shown in Table 2, $T_{0.1}$ and $T_{1.7}$ can be obtained. For RP-1522 tool, zone area, room temperature, supply air temperature at diffuser (T_s), zone cooling load, diffuser design airflow rate (Q_d) and effective area (A_d) of the diffuser were fed into the tool to calculate the temperature difference between head and ankle of a standing person ($\Delta T_{oc} = T_{1.7} - T_{0.1}$). Then the ankle temperature could be calculated with Equation 20, the head temperature can be obtained with Equation 21 because T_{set} is known.

$$T_{0.1} = T_{set} - \frac{1}{2} \Delta T_{oc} \quad \text{Equation 20}$$

$$T_{1.7} = T_{0.1} + \Delta T_{oc} \quad \text{Equation 21}$$

The comparison is done by calculating the coefficient of variation of the root mean square deviation, CVRMSD, of $T_{0.1}$ and $T_{1.7}$ determined by results from two tools versus those from the database. CVRMSD is defined in Equation 22. It represents how well a mathematical model describes the variability in measured data (ASHRAE, 2002). A model with smaller CVRMSD better describes the variability in the measured temperature and is more accurate.

$$CVRMSD = \frac{RMSD}{\bar{T}_i} = \frac{\sqrt{(\sum_{i=1}^n (T_i - \hat{T}_i)^2 / n')}}{\bar{T}_i} \quad \text{Equation 22}$$

Where T_i is the measured temperature of the experiment ($^{\circ}\text{C}$), \hat{T}_i is the predicted temperature ($^{\circ}\text{C}$), \bar{T}_i is the averaged measured temperature of the experiment ($^{\circ}\text{C}$) and n' is the number of cases.

Given that there's no rule of thumb value for CVRMSD that can be used to assess whether a model is acceptable to be used, a model prediction test as in the Mean Magnitude of Relative Error (MMRE) needs to be performed as an auxiliary reference to help the comparison. MMRE is the most widely used evaluation criterion to assess the performance of software prediction models (Briand and Wiczorek). Conte et al. (1986) consider $\text{MMRE} \leq 25\%$ as acceptable for effort prediction models. MMRE is defined in Equation 23. Note that MMRE is widely used in assessing software prediction models. To author's knowledge, MMRE has not been used for simple regression model analysis as in the case of this project.

$$MMRE = \frac{100}{n} \sum_{i=1}^n \left| \frac{T_i - \hat{T}_i}{T_i} \right| \quad \text{Equation 23}$$

Where T_i are measured temperatures from the database ($^{\circ}\text{C}$), \hat{T}_i are predicted temperatures from each model ($^{\circ}\text{C}$), and n is the number of cases.

2.2.2. Result

Figure 26 shows the comparison results of $T_{0.1}$ from two prediction models, with X axis representing the measured $T_{0.1}$ from the database and Y axis representing the predicted $T_{0.1}$ from CBE and RP-1522 models. Blue dots represents the predicted results from CBE model and yellow triangle represents predicted results from RP1522 model. The diagonal line represents the perfect prediction model, in which the predicted $T_{0.1}$ equals to measured $T_{0.1}$. Therefore, the closer the dots or triangles are to the diagonal line, the more accurate the model is for predicting $T_{0.1}$.

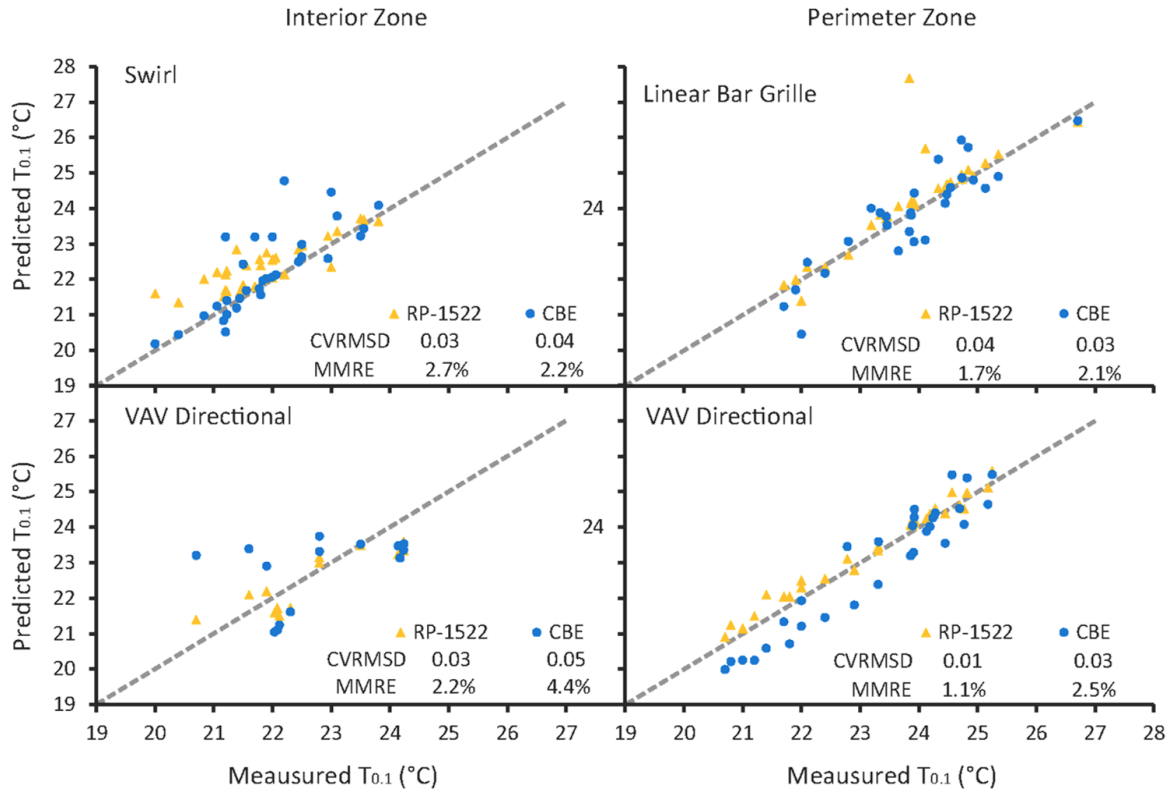


Figure 26 The comparison of $T_{0.1}$ with cases using swirl for interior zone, VAV directional diffuser for interior and perimeter zone, linear bar grille for perimeter zone.

From the comparison of CVRMSD, it is concluded that the RP-1522 tool predicts slightly more accurately than the CBE UFAD Cooling Load Design Tool for swirl (0.03 vs. 0.04), VAV directional diffusers in the interior zone (0.03 vs. 0.05), and VAV directional diffusers in the perimeter zone (0.01 vs. 0.03). Same conclusion can be reached by analyzing the plots in Figure 26. Most of the blue dots and yellow triangles are very close to the diagonal line, except for one or two blue dots from swirl and VAV directional diffusers plots a little bit far away from the diagonal line. This indicates that there are only one or two cases in which the prediction error of CBE model is a little bit larger than the RP-1522 model.

For linear bar grille, the CBE UFAD Cooling Load Design Tool is slightly more accurate than the RP-1522 tool, with CVRMSD at 0.03 vs. 0.04. For all the other cases, two models have relatively similar performance. The MMRE of both models in four cases are significantly less than 25%. The MMRE of CBE UFAD Cooling Load Design Tool is less than RP-1522 tool around 0.5% for swirl diffusers and linear bar grille, around 1% for VAV directional diffuser in the perimeter zone. For VAV directional diffuser in the interior zone, the MMRE of CBE model is greater than RP-1522 model by 2.2. This indicates that the difference between the prediction accuracy of two design tools in VAV directional diffuser in the interior zone might be larger than that in other diffuser types. However, due to the low values of MMRE, both models are comparably accurate prediction models to predict $T_{0.1}$ for design purposes.

The results of $T_{1.7}$ prediction for all three diffusers are shown in Figure 27.

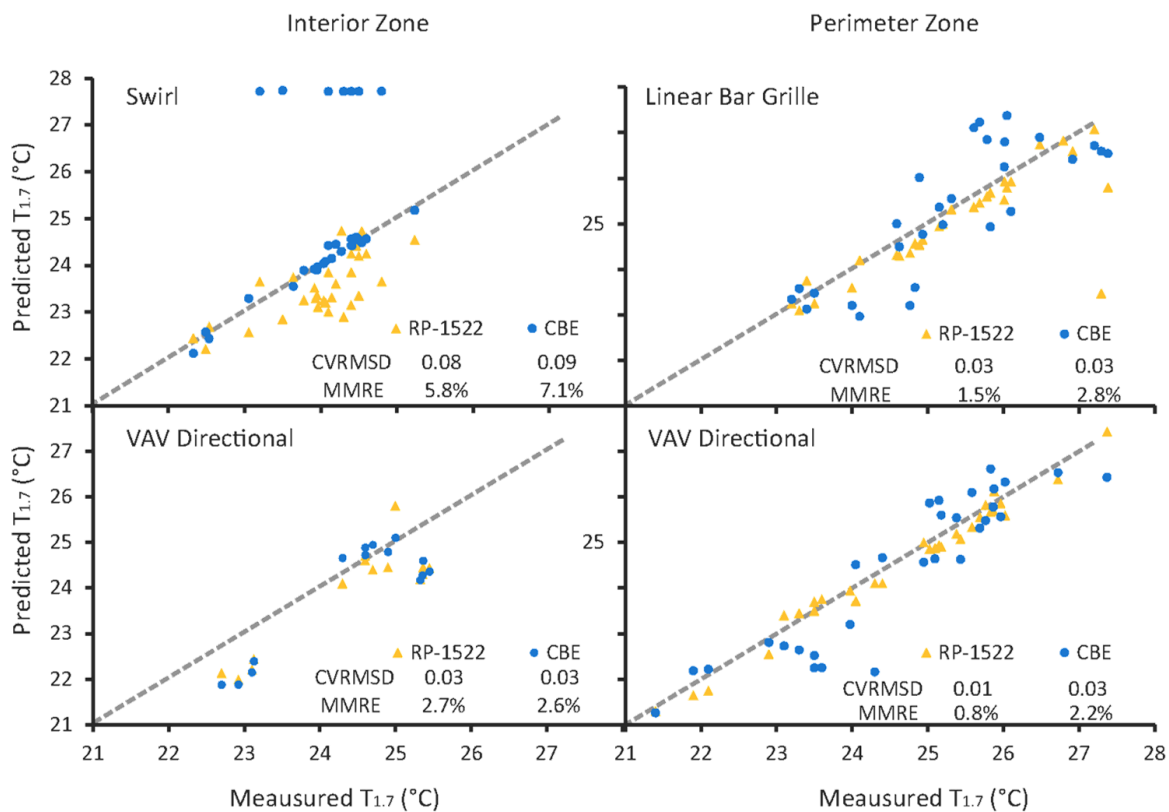


Figure 27 The comparison of $T_{1.7}$ with cases using swirl for interior zone, VAV directional diffuser for interior and perimeter zone, linear bar grille for perimeter zone.

The comparison of predicted $T_{1.7}$ has the similar results of $T_{0.1}$. Figure 27 shows that for interior swirl diffuser, 77% of the yellow triangles are under the diagonal line and 74% of the blue dots are above the diagonal line. This indicates that RP-1522 model tends to under-predict $T_{1.7}$ while CBE model tends to over-predict $T_{1.7}$. From the comparison of CVRMSD, the RP-1522 tool predicts slightly more accurately than the CBE UFAD Cooling Load Design Tool for swirl (0.08

vs. 0.09) and VAV directional diffusers in the perimeter zone (0.01 vs. 0.03). For linear bar grille and VAV directional diffuser in the interior zone, the accuracy of both tools are about the same (0.03 vs. 0.03). Given that the MMRE of both models in four cases are far less than 25%, both model are comparably good prediction models for predicting $T_{1.7}$.

2.3. Conclusion and discussion

Both tools have practical advantages and limitations. CBE UFAD tool has the key advantage of being able to predict the UFAD cooling load, calculate heat gain in the supply plenum, model different plenum configurations and zone types. It has the limitation of primarily being used in office buildings and not able to calculate air distribution effectiveness. RP-1522 tool covers more buildings types (classrooms, offices, workshops, restaurants, retail shops, conference rooms and auditoriums), and is able to calculate the air distribution effectiveness. However it requires users to input the zone cooling load, supply plenum factor and the supply airflow rate of each diffuser, which is difficult to get during the design stage for UFAD system.

There are slight differences in terms of the accuracy to predict the thermal stratification of two tools. The RP-1522 tool predicts thermal stratification slightly more accurately than the CBE model in cases using swirl and VAV directional diffusers, while CBE model is slightly more accurate than RP-1522 model in cases using linear bar grille. However, both models are acceptably accurate prediction models for design purposes.

3. Updated $\Gamma - \Phi$ model

A new database including 79 tests from the CBE full-scale experimental database and 31 tests from RP-1522 CFD simulation database has been developed (see paragraph 0). The total number of cases in the combined UFAD database is 110. New Γ - Φ equations (see Table 11) are developed based on the combined database. This chapter describes how the Γ - Φ regression equation for each type of diffusers was developed, a numeric and visual comparison of the old and updated Γ - Φ equations, and an example in which the old and updated equations are compared.

3.1. Combined UFAD database

The Γ - Φ model that is implemented in CBE UFAD Cooling Load Design Tool was developed from CBE experimental measurement database. The 79 experimental tests in the database covered a large variation in Γ in order to build a practical stratification prediction model. However, there is a possibility that adding 31 CFD simulation cases from RP-1522 database could expand the range of Γ for certain type of diffusers to make the CBE stratification model more robust. Besides, the regression based model would be expected to be more representative with a larger number of data samples. Therefore, the CBE database and RP-1522 database were combined. New $\Gamma - \Phi$ equations for each type of diffusers were developed from the combined database with larger data samples.

The combined database is reported in Appendix 7.1 and 7.2. It is also publicly available online at <http://tinyurl.com/UFADdatabase>. The database includes two parts: Part I is the input parameters for each case, Part II is the results of each case. Those parameters reported in the database were selected based on the inputs to calculate Γ , including the diffuser type, zone type, the number of diffusers, number of thermal plumes (same as the number of occupants), window blinds condition, the cooling load from the work station, lighting and solar heat gain, the supply airflow rate for the zone (Q) and the zone extraction rate per unit length of the perimeter zone (W_L). Part II includes T_s , $T_{0.1}$, the air temperature in the occupied zone (T_{OZ}), $T_{1.7}$, T_R , Γ , $\Phi_{0.1}$, Φ_{OZ} , and $\Phi_{1.7}$.

3.2. Method

3.2.1. Statistical analysis

The statistical analysis includes two sequential steps. The first step is plotting all the data points of Γ - Φ for each type of diffusers to identify patterns. The data distribution are described with median, first, and third quartile in parenthesis.

The second step is to develop the regression model of Γ and Φ . As there is only one explanatory variable (Γ) in the regression model, one variable linear regression is selected to develop Γ - Φ equations. The regression analysis starts with visually checking the shape of the data. Five common linear regression models were considered, including linear, logarithmic, second and third order polynomial, and power. The regression line has been visually evaluated by plotting the residuals. Regression models were selected based on R-square adjusted values and the method of

cross validation, which will be introduced in detail in the next section. The statistical analysis was performed with R version 3.0.2 (R Development Core Team, 2013).

3.2.2. Model selection indexes

R-squared, the coefficient of determination of the regression line, is defined as the proportion of the total sample variability explained by the regression model. It has been widely used as a measure of the adequacy of a regression model. R-squared varies between 0 and 1. One indicates that the regression model is a perfect fit to the data. Generally models having large values of R-squared are preferred. However, R-squared can simply increase by adding more regressors. To avoid the difficulties of interpreting R-squared, some analysts prefer to use the adjusted R-squared. Because the adjusted R-squared statistic does not necessarily increase as additional regressors are introduced into the model. One criterion for selection of an optimum model is to choose the model that has maximum adjusted R-squared (Montgomery et al., 2012).

Cross validation is a method for model selection according to the predictive ability of the proposed models (Shao, 1992). Zucchini (2000) describe cross validations as following: “The idea here is to split the sample data into two subsamples, a calibration sample of size $(n-m)$ and a validation sample of size m ; the first is used to fit the model and the second to estimate the expected discrepancy. Such an estimator is called a cross-validation criterion”. In each case, all the datasets will be randomly divided into n/m groups. For each time, one group of dataset will be used as the testing set, as the rest $(n/m-1)$ groups will be used to generate the regression model for testing. After (n/m) times, the discrepancy will be averaged as an indicator to assess the predictive ability of the models. Models with the least average error is preferred (Zucchini, 2000). Cross validation is used here as an auxiliary method to help select the best model in addition to adjusted R-squared, aka when two models have the same or similar adjusted R-squared value, the one with smaller average error will be selected. The cross validation analysis is performed with DAAG and cvTools in R, which is introduced in Appendix 7.4 .

3.3. Results

3.3.1. Γ - Φ plots

Figure 28 and Figure 29 show the Γ - Φ plots for swirl, VAV directional diffusers and linear bar grilles for three values of Φ ($\Phi_{0.1}$, $\Phi_{0.2}$, and $\Phi_{1.7}$). The plots have been grouped by zone type (interior or perimeter), including swirl and VAV directional diffusers for the interior zone, and VAV directional and linear bar grille for the perimeter zone. From Figure 28, it is found that for VAV directional diffusers in the interior zone, the lower range of Γ is expanded by adding the datasets from RP-1522 database. For other diffuser types, the ranges of Γ stay the same as before.

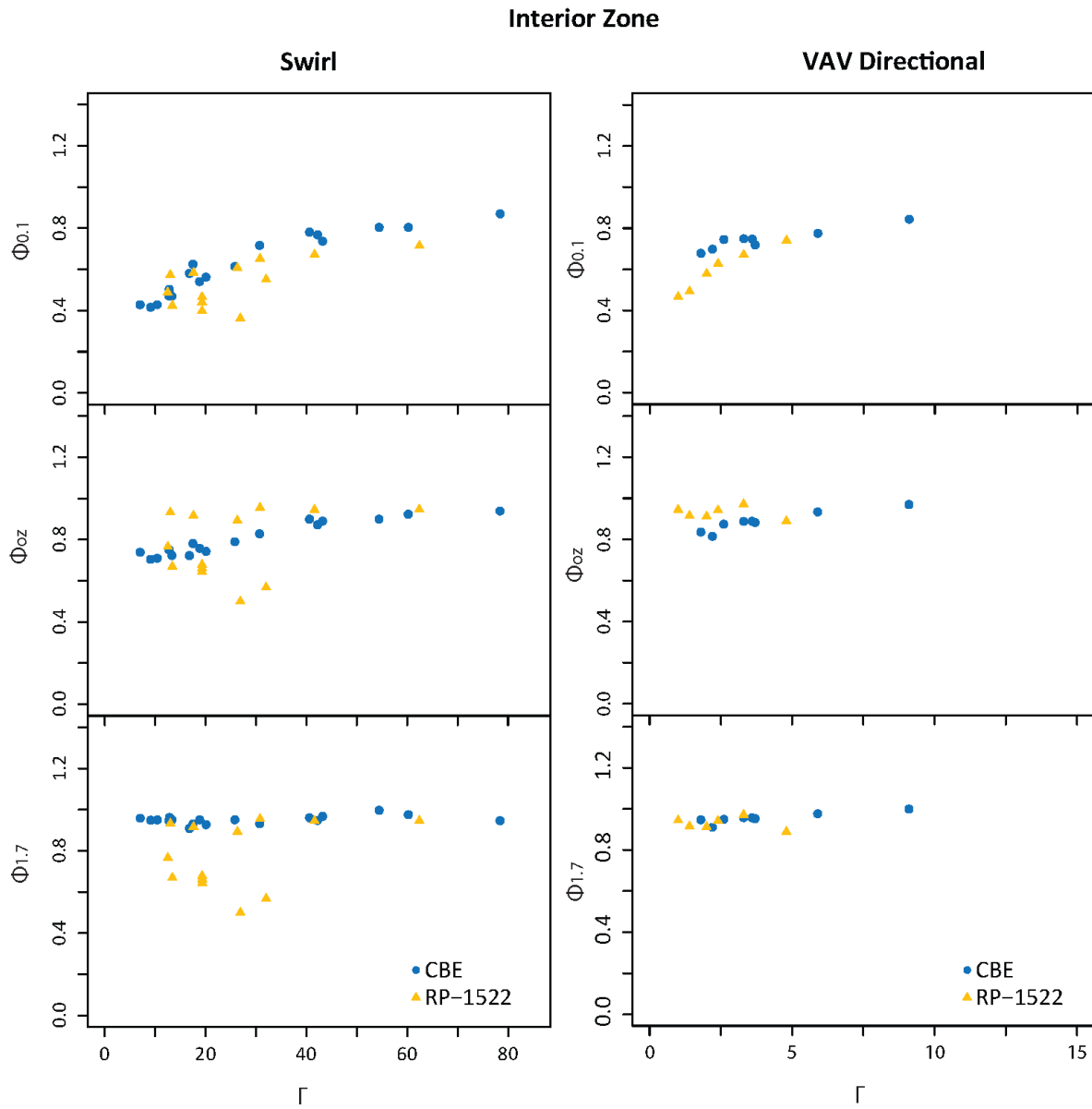


Figure 28 Γ - Φ plots for swirl and VAV directional diffusers in the interior zone

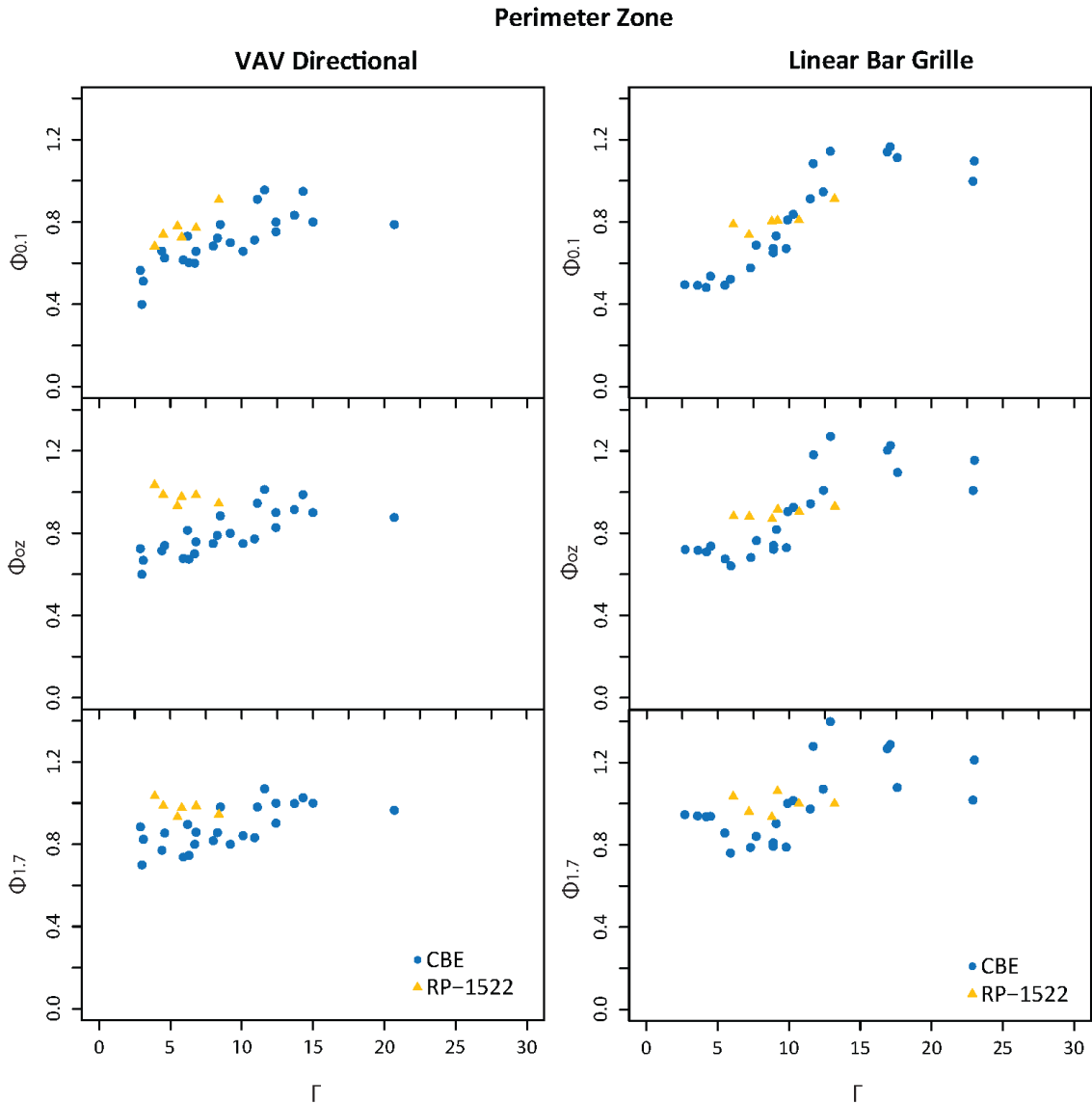


Figure 29 Γ - Φ plots for VAV directional diffusers and linear bar grille in perimeter zone

It can be seen from Figure 28 and Figure 29 that as Γ increases, the variation in $\Phi_{1.7}$ is much less than that of $\Phi_{0.1}$. $\Phi_{1.7}$ appears to be a constant value throughout the range of Γ for swirl diffusers and VAV directional diffusers in the interior zone. Therefore, the simple linear regression model can be considered. For Γ - $\Phi_{0.1}$, as Γ increases, the increasing speed of $\Phi_{0.1}$ first is very fast and gradually slows down in the upper range of Γ . Therefore, polynomial second order model can be considered. No obvious patterns can be found in other Γ - Φ plots.

The results of Φ are described with median and first and third quartile in parenthesis, which are summarized in Table 7. It can be seen from Table 7 that for each type of diffusers, Φ is strongly

dependent on height for this stratified UFAD environment. Taking swirl diffusers in the interior zone as an example, $\Phi_{1.7}$, 0.946 (0.901-0.951) is greater than Φ_{oz} , 0.751 (0.707-0.830), and Φ_{oz} is greater than $\Phi_{0.1}$, 0.573 (0.468-0.693). $\Phi_{1.7}$ of all three type of diffusers are very close to one, which represents that the temperature at the head height is very close to the return air temperature. Linear bar grilles generate less stratification than swirl and VAV directional diffusers, considering that $\Phi_{0.1}$ for linear bar grilles (0.803 (0.651-0.947)) is greater than that of swirl diffusers (0.573 (0.468-0.693)), VAV directional diffusers in the interior zone (0.709 (0.639-0.747)), and VAV directional diffusers in the perimeter zone (0.724 (0.658-0.788)).

Table 7 Statistical summaries of Φ

| | | First quartile | Median | Third quartile |
|-----------------------------|--------------|----------------|--------|----------------|
| Swirl interior | $\Phi_{0.1}$ | 0.468 | 0.573 | 0.693 |
| | Φ_{oz} | 0.707 | 0.751 | 0.830 |
| | $\Phi_{1.7}$ | 0.901 | 0.946 | 0.951 |
| VAV directional interior | $\Phi_{0.1}$ | 0.639 | 0.709 | 0.747 |
| | Φ_{oz} | 0.798 | 0.825 | 0.886 |
| | $\Phi_{1.7}$ | 0.922 | 0.948 | 0.958 |
| VAV directional perimeter | $\Phi_{0.1}$ | 0.658 | 0.724 | 0.788 |
| | Φ_{oz} | 0.742 | 0.821 | 0.900 |
| | $\Phi_{1.7}$ | 0.826 | 0.899 | 0.985 |
| Linear bar grille perimeter | $\Phi_{0.1}$ | 0.651 | 0.803 | 0.947 |
| | Φ_{oz} | 0.730 | 0.882 | 1.008 |
| | $\Phi_{1.7}$ | 0.903 | 0.974 | 1.060 |

3.3.2. Regression model selection result

Table 1 shows the results of model selection indexes for Γ - $\Phi_{0.1}$ equation. For swirl diffusers in the interior zone a second order polynomial is selected. Both second order polynomial, logarithmic and third order polynomial have highest adjusted R-squared value. However, second order polynomial has the least average error in cross validation results. Therefore, second order polynomial is an optimal model for swirl diffusers in the interior zone. Same selection process was performed for other types of diffusers. Logarithmic is selected for VAV directional diffusers in both interior and perimeter zone. Second order polynomial is selected for linear bar grille in the perimeter zone.

Table 8 Results of statistical analysis for Γ - $\Phi_{0.1}$ regression model selection

| Diffuser type | Model | Adjusted R ² | Cross validation average error |
|-----------------|-----------------------|-------------------------|--------------------------------|
| Swirl Interior | linear | | - |
| | logarithmic | 0.82 | 0.020 |
| | polynomial (2) | 0.82 | 0.004 |
| | polynomial (3) | 0.82 | 0.007 |
| | power | 0.81 | - |
| VAV directional | linear | 0.57 | - |

| | | | |
|-----------------------------|-----------------------|-------------|--------------|
| Interior | logarithmic | 0.78 | 0.017 |
| | polynomial (2) | 0.71 | - |
| | polynomial (3) | 0.79 | 0.037 |
| | power | 0.74 | - |
| VAV directional Perimeter | linear | 0.49 | - |
| | logarithmic | 0.54 | 0.009 |
| | polynomial (2) | 0.50 | - |
| | polynomial (3) | 0.50 | - |
| Linear bar grille Perimeter | power | 0.54 | 0.018 |
| | linear | 0.78 | - |
| | logarithmic | 0.78 | - |
| | polynomial (2) | 0.83 | 0.012 |
| | polynomial (3) | 0.86 | 0.014 |
| | power | 0.81 | - |

Table 9 shows the results of model selection indexes for Γ - Φ oz equation. For swirl diffusers in the interior zone, the adjusted R-square values for second and third order polynomials are very close (0.37 vs. 0.38). However, the average error from cross validation result of third order polynomial is much larger than second order polynomial. This indicates that third order polynomial model is overfitting the data by adding more parameters. Therefore, second order polynomial is finally selected for the Γ - Φ oz for swirl diffusers in the interior zone. Linear model is selected for VAV directional diffusers in both interior and perimeter zone, and for linear bar grilles in perimeter zone with the same statistical analysis.

Table 9 Results of statistical analysis for Γ - Φ oz regression model selection

| Diffuser type | Model | Adjusted R ² | Cross validation average error |
|-----------------------------|-----------------------|-------------------------|--------------------------------|
| Swirl Interior | linear | 0.28 | - |
| | logarithmic | 0.33 | - |
| | polynomial (2) | 0.37 | 0.009 |
| | polynomial (3) | 0.38 | 0.020 |
| | power | 0.26 | - |
| VAV directional Interior | linear | 0.56 | 0.002 |
| | logarithmic | 0.55 | 0.022 |
| | polynomial (2) | 0.53 | - |
| | polynomial (3) | 0.49 | - |
| | power | 0.53 | - |
| VAV directional Perimeter | linear | 0.33 | 0.008 |
| | logarithmic | 0.33 | 0.010 |
| | polynomial (2) | 0.30 | - |
| | polynomial (3) | 0.28 | - |
| | power | 0.34 | 0.009 |
| Linear bar grille Perimeter | linear | 0.66 | 0.014 |
| | logarithmic | 0.60 | - |
| | polynomial (2) | 0.65 | - |
| | polynomial (3) | 0.72 | 0.029 |

| | | | |
|--|-------|------|---|
| | power | 0.61 | - |
|--|-------|------|---|

Table 10 shows the results of model selection indexes for $\Gamma-\Phi_{1.7}$ equation. For swirl diffusers, the adjusted R-squared value of all the models are very low. This indicates that all models explain little variability of the response data around its mean. Therefore, the median value of the sample is used to represent the $\Gamma-\Phi_{1.7}$ for swirl diffusers in the interior zone. Linear model is selected for VAV directional diffusers in both interior and perimeter zone, and for linear bar grilles in the perimeter zone.

Table 10 Results of statistical analysis for $\Gamma-\Phi_{1.7}$ regression model selection

| Diffuser type | Model | Adjusted R ² | Cross validation average error |
|-----------------------------|----------------|-------------------------|--------------------------------|
| Swirl Interior | linear | 0.02 | - |
| | logarithmic | -0.01 | - |
| | polynomial (2) | -0.01 | - |
| | polynomial (3) | 0.05 | - |
| | power | -0.02 | - |
| VAV directional Interior | linear | 0.26 | 0.001 |
| | logarithmic | 0.18 | - |
| | polynomial (2) | 0.22 | 0.020 |
| | polynomial (3) | 0.05 | - |
| | power | 0.16 | - |
| VAV directional Perimeter | linear | 0.19 | 0.0097 |
| | logarithmic | 0.15 | - |
| | polynomial (2) | 0.18 | 0.0100 |
| | polynomial (3) | 0.15 | - |
| | power | 0.15 | - |
| Linear bar grille Perimeter | linear | 0.39 | 0.018 |
| | logarithmic | 0.29 | - |
| | polynomial (2) | 0.37 | - |
| | polynomial (3) | 0.48 | 0.051 |
| | power | 0.28 | - |

All the updated $\Gamma-\Phi$ equations are reported in Table 11.

Table 11 Updated $\Gamma-\Phi$ relationships at 0.1, occupied zone, and 1.7 m.

| Diffuser Type | $\Gamma-\Phi_{0.1}$ | $\Gamma-\Phi_{oz}$ | $\Gamma-\Phi_{1.7}$ |
|----------------|---|--|---|
| Swirl interior | $\Gamma < 7.0$; $\Phi_{0.1} = 0.4207$ | $\Gamma < 7.0$; $\Phi_{oz} = 0.6626$ | $\Phi_{1.7} = 0.946$ |
| | $7.0 \leq \Gamma \leq 78.4$; $\Phi_{0.1} = 0.339 + 0.0122\Gamma - 7.55e-5\Gamma^2$ | $7.0 \leq \Gamma \leq 78.4$; $\Phi_{oz} = 0.6281 + 0.0050\Gamma - 9.874e-6\Gamma^2$ | |
| | $\Gamma > 78.4$; $\Phi_{0.1} = 0.8314$ | $\Gamma > 78.4$; $\Phi_{oz} = 0.9593$ | |
| | $R^2_{adj} = 0.82$ | $R^2_{adj} = 0.37$ | |
| | $\Gamma < 1.0$; $\Phi_{0.1} = 0.5076$ | $\Gamma < 1.0$; $\Phi_{oz} = 0.7824$ | $\Gamma < 1.0$; $\Phi_{1.7} = 0.9264$ |
| | $1.0 \leq \Gamma \leq 9.1$; $\Phi_{0.1} = 0.1645\ln(\Gamma) + 0.5076$ | $1.0 \leq \Gamma \leq 9.1$; $\Phi_{oz} = 0.7577 + 0.0247\Gamma$ | $1.0 \leq \Gamma \leq 9.1$; $\Phi_{1.7} = 0.0078\Gamma + 0.9186$ |

| | | | |
|-----------------------------|--|---|--|
| VAV directional interior | $\Gamma > 9.1; \Phi_{0.1} = 0.8700$ | $\Gamma > 9.1; \Phi_{oz} = 0.9825$ | $\Gamma > 9.1; \Phi_{1.7} = 0.9896$ |
| | $R^2_{adj} = 0.78$ | $R^2_{adj} = 0.56$ | $R^2_{adj} = 0.26$ |
| VAV directional perimeter | $\Gamma < 2.9; \Phi_{0.1} = 0.5553$ | $\Gamma \leq 2.9; \Phi_{oz} = 0.7274$ | $\Gamma < 2.9; \Phi_{1.7} = 0.8379$ |
| | $2.9 \leq \Gamma \leq 15;$ $\Phi_{0.1} = 0.174 \ln(\Gamma) + 0.37$ | $2.9 < \Gamma \leq 15;$ $\Phi_{oz} = 0.6758 + 0.0178\Gamma$ | $2.9 \leq \Gamma \leq 15;$ $\Phi_{1.7} = 0.8057 + 0.0111\Gamma$ |
| | $\Gamma > 15; \Phi_{0.1} = 0.8412$ Remove 0.13 if blinds are down | $\Gamma > 15;$ $\Phi_{oz} = 0.9428$ | $\Gamma > 15;$ $\Phi_{1.7} = 0.9722$ |
| | $R^2_{adj} = 0.54$ | $R^2_{adj} = 0.33$ | $R^2_{adj} = 0.19$ |
| Linear bar grille Perimeter | $\Gamma < 2.7; \Phi_{0.1} = 0.3903$ | $\Gamma < 2.7; \Phi_{oz} = 0.6576$ | $\Gamma < 2.7; \Phi_{1.7} = 0.8301$ |
| | $2.7 \leq \Gamma \leq 23; \Phi_{0.1} = 0.1834 + 0.0810$ $\Gamma - 0.0016\Gamma^2$ | $2.7 \leq \Gamma \leq 23;$ $\Phi_{oz} = 0.5696 + 0.0326\Gamma$ | $2.7 \leq \Gamma \leq 23;$ $\Phi_{1.7} = 0.768 + 0.023\Gamma$ |
| | $\Gamma > 23; \Phi_{0.1} = 1.1798$ Remove 0.13 if blinds are down | $\Gamma > 23;$ $\Phi_{oz} = 1.3194$ | $\Gamma > 23;$ $\Phi_{1.7} = 1.297$ |
| | $R^2_{adj} = 0.83$ | $R^2_{adj} = 0.66$ | $R^2_{adj} = 0.39$ |

3.4. Comparison between old and updated Γ - Φ equation

The updated Γ - Φ equations have been developed from the combined database (see Table 11). They are expected to be more accurate than the old Γ - Φ equations. This section will compare the old and updated Γ - Φ equations in detail. First, the Γ - Φ equations are plotted in Figure 30 and Figure 31 to visually compare the difference between the equations. The impact of the difference on thermal stratification prediction will be analyzed. Second, a real case example is fed into both the old and updated Γ - Φ equations. The predicted $T_{0.1}$ and $T_{1.7}$ are compared to check whether the change of the equation will make a difference in impacting the design. Since ASHRAE Standard 55 updated the requirement for the maximum temperature difference between $T_{0.1}$ and $T_{1.7}$ to be less than 4 °C (7.2 °F), which will be expected in the next release of (ANSI/ASHRAE, 2013a), ΔT_{oz} is compared in addition to $T_{0.1}$ and $T_{1.7}$, in order to check compliance with Standard 55. The calculated supply airflow rate is also compared to see the difference in the supply airflow rate calculation between the old and updated Γ - Φ equations, given the same cooling load input.

3.4.1.1. Γ - Φ equation comparison

Table 12 reports the old Γ - Φ equations for each type of diffusers, which were implemented in the CBE UFAD Cooling Load Design Tool.

Table 12 Old Γ - Φ equations for each type of diffusers

| Diffuser Type | Γ - $\Phi_{0.1}$ | Γ - Φ_{oz} | Γ - $\Phi_{1.7}$ |
|---------------|-------------------------------------|------------------------------------|-------------------------|
| Swirl | $\Gamma < 7.0; \Phi_{0.1} = 0.4024$ | $\Gamma < 7.0; \Phi_{oz} = 0.6994$ | $\Phi_{1.7} = 0.951$ |

| | | | |
|-----------------------------------|--|--|---|
| interior | $7.0 \leq \Gamma \leq 78.4; \Phi_{0.1} = 0.2075\Gamma^{0.3403}$ | $7.0 \leq \Gamma \leq 78.4; \Phi_{oz} = 0.653$ $1 + 0.0069\Gamma - 4e^{-5\Gamma^2}$ | |
| | $\Gamma > 78.4; \Phi_{0.1} = 0.9155$ | $\Gamma > 78.4; \Phi_{oz} = 0.9482$ | |
| | $R^2_{adj} = 0.82$ | $R^2_{adj} = 0.93$ | |
| VAV directional interior | $\Phi_{0.1} = 0.745$ | $\Gamma < 1.8; \Phi_{oz} = 0.8436$ | $\Phi_{1.7} = 0.956$ |
| | | $1.0 \leq \Gamma \leq 9.1;$ $\Phi_{oz} = 0.8094 + 0.019\Gamma$ | |
| | | $\Gamma > 9.1; \Phi_{oz} = 0.9823$ | |
| | | $R^2_{adj} = 0.844$ | |
| VAV directional perimeter | $\Gamma < 2.9; \Phi_{0.1} = 0.5452$ | $\Gamma \leq 2.9; \Phi_{oz} = 0.6652$ | $\Gamma < 2.9; \Phi_{1.7} = 0.7719$ |
| | $2.9 \leq \Gamma \leq 15;$ $\Phi_{0.1} = 0.4605 + 0.0292\Gamma$ | $2.9 < \Gamma \leq 15;$ $\Phi_{oz} = 0.5977 + 0.0233\Gamma$ | $2.9 \leq \Gamma \leq 15;$ $\Phi_{1.7} = 0.7168 + 0.0190\Gamma$ |
| | $\Gamma > 15; \Phi_{0.1} = 0.8987$ Remove 0.13 if blinds are down | $\Gamma > 15;$ $\Phi_{oz} = 0.9472$ | $\Gamma > 15;$ $\Phi_{1.7} = 1.0018$ |
| | $R^2_{adj} = 0.64$ | $R^2_{adj} = 0.65$ | $R^2_{adj} = 0.36$ |
| Linear bar grille Perimeter | $\Gamma < 2.7; \Phi_{0.1} = 0.3582$ | $\Gamma < 2.7; \Phi_{oz} = 0.6484$ | $\Gamma < 2.7; \Phi_{1.7} = 0.8305$ |
| | $2.7 \leq \Gamma \leq 23; \Phi_{0.1} = 0.1282 + 0.0908$ $\Gamma - 0.0021\Gamma^2$ | $2.7 \leq \Gamma \leq 23; \Phi_{oz} = 0.5671$ $+ 0.0301\Gamma$ | $2.7 \leq \Gamma \leq 23; \Phi_{1.7} = 0.7742 + 0.02$ 08Γ |
| | $\Gamma > 23; \Phi_{0.1} = 1.1074$ Remove 0.13 if blinds are down | $\Gamma > 23;$ $\Phi_{oz} = 1.2594$ | $\Gamma > 23;$ $\Phi_{1.7} = 1.2535$ |
| | $R^2_{adj} = 0.86$ | $R^2_{adj} = 0.60$ | $R^2_{adj} = 0.36$ |

Figure 30 and Figure 31 are the plots of the old and updated Γ - Φ equations for swirl and VAV directional diffusers in the interior zone, and VAV directional diffusers and linear bar grilles in the perimeter zone.

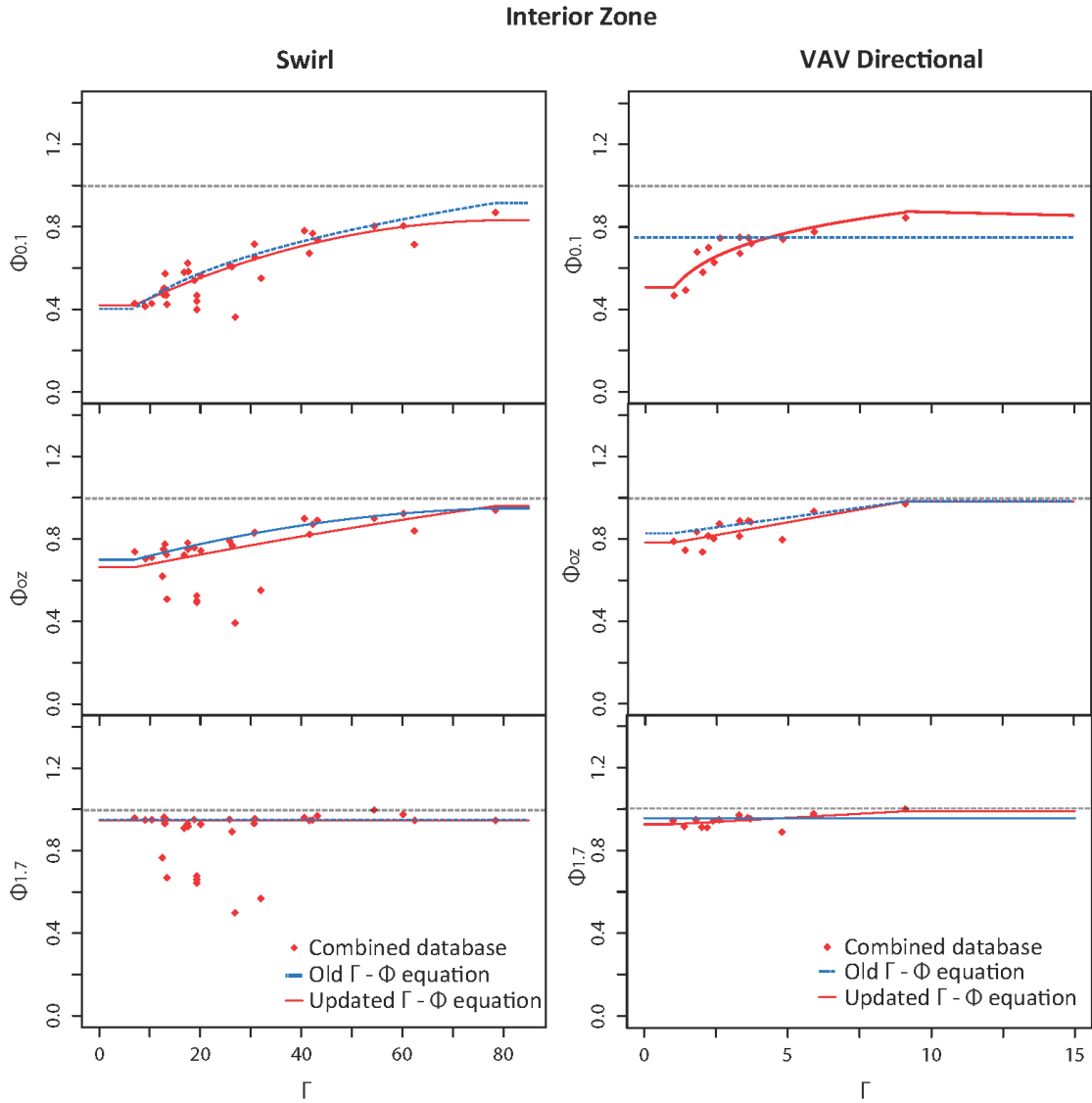


Figure 30 Comparison of old and updated Γ - Φ equation for swirl and VAV directional diffusers in the interior zone

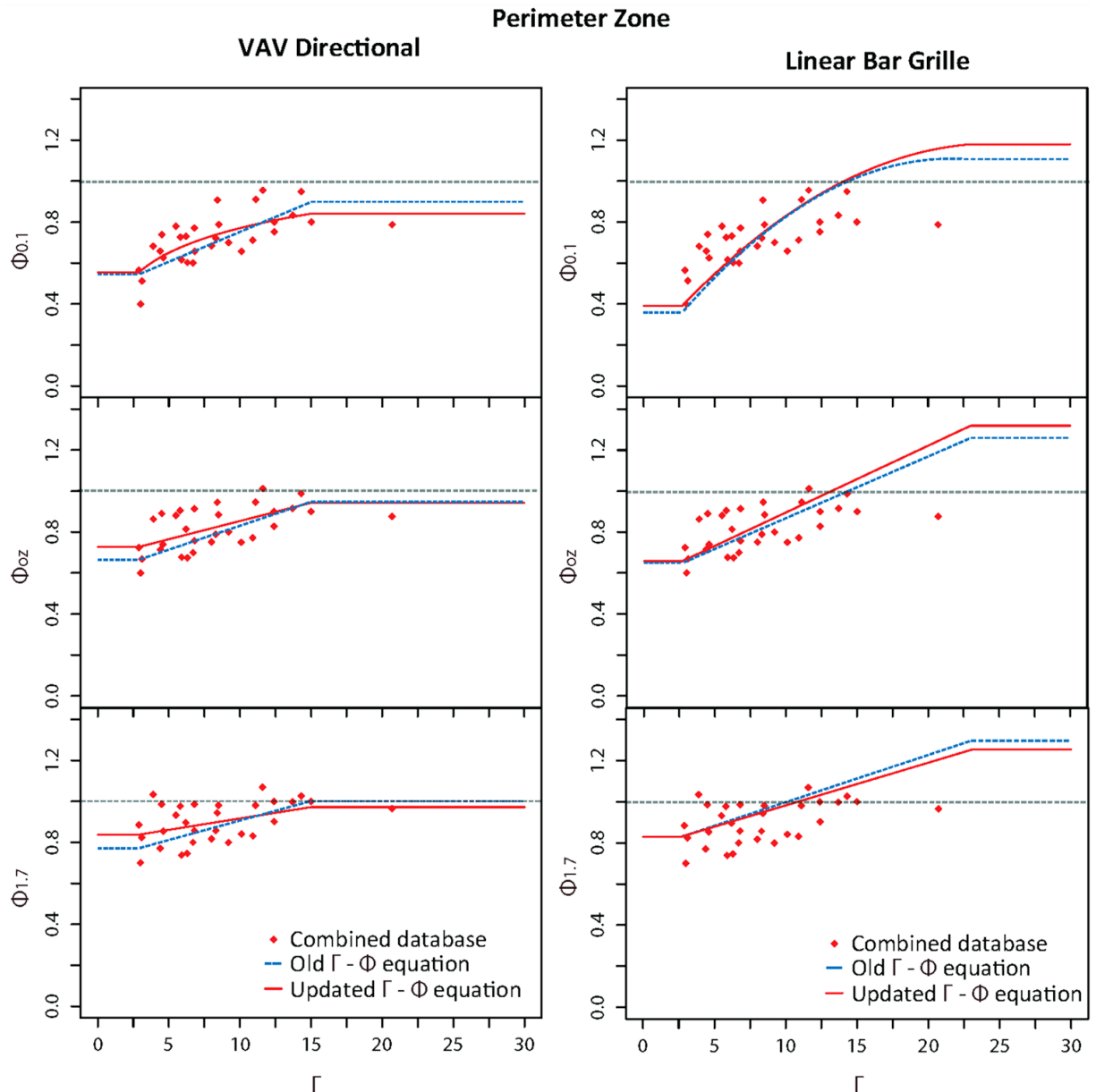


Figure 31 Comparison of old and updated Γ - Φ equation for VAV directional diffusers and linear bar grille in the perimeter zone

From Figure 30 it can be deduced that for swirl diffusers in the interior zone, the old and updated Γ - $\Phi_{0.1}$ and Γ - Φ_{0z} are basically the same. The added 13 cases from RP-1522 database does not make a difference in terms of improving the accuracy of Γ - $\Phi_{0.1}$ for swirl diffusers. There is no difference for Γ - $\Phi_{1.7}$ for swirl diffusers as well. Since both models use a constant value and the difference of predicted $\Phi_{1.7}$ between two models is only 0.005, which is negligible.

The new Γ - $\Phi_{0.1}$ equation for VAV directional diffusers in interior zone is quite different from the old one. As shown in Figure 30, $\Phi_{0.1}$ is kept at a constant value of 0.745 for all Γ . With the larger

data samples, the new $\Gamma-\Phi_{0.1}$ is able to better describe the positive correlation between $\Phi_{0.1}$ and Γ for VAV directional diffusers in the interior zone. As a result, when $\Gamma < 4.23$, $\Phi_{0.1}$ from the old $\Gamma-\Phi_{0.1}$ equation is larger than the one from the new $\Gamma-\Phi_{0.1}$ equation, aka the predicted $T_{0.1}$ from the old $\Gamma-\Phi_{0.1}$ is higher than the one from the new $\Gamma-\Phi_{0.1}$ equation. This indicates that the old $\Gamma-\Phi_{0.1}$ equation tends to underestimate the thermal stratification for VAV directional diffusers in interior zone. When $\Gamma > 4.23$, $\Phi_{0.1}$ from the old $\Gamma-\Phi_{0.1}$ equation is smaller than the one from the new $\Gamma-\Phi_{0.1}$ equation, aka the old $\Gamma-\Phi_{0.1}$ equation tends to overestimate the thermal stratification in the higher range of Γ .

The $\Gamma-\Phi_{0z}$ and $\Gamma-\Phi_{1.7}$ for VAV directional in the interior zone is basically the same between the old and updated equations. Both the old and updated $\Gamma-\Phi_{0z}$ use linear regression equations. For $\Gamma-\Phi_{1.7}$, the updated equation selects linear model instead of using a constant value. This helps describes the little variation in $\Phi_{1.7}$, but the difference can be negligible.

It is found in Figure 31 that there is little difference between the old and updated $\Gamma-\Phi$ equations for VAV directional and linear bar grille in the perimeter zone. This may be due to the fact that only six cases were added to each type of diffusers. Moreover, all those added cases falls in the existing range and trend of Γ .

In summary, there are not significant differences between the old and the updated $\Gamma-\Phi$ equations, except for $\Gamma-\Phi_{0.1}$ of VAV directional diffusers in the interior zone. Several explanations might lead to this result, including:

- The range of Γ for all the type of diffusers was not expanded as expected by adding cases from RP-1522 database, except for VAV directional diffusers in the interior zone.
- The trend between Γ and Φ for cases in RP-1522 database are very similar to CBE database. In regression analysis, if two datasets have similar trend between the independent variable and dependent variable, there will be little difference between the regression model from the combined datasets and the one from each dataset, respectively.
- The number of added cases for VAV directional diffusers and linear bar grilles in the perimeter zone is much smaller than that of the original CBE database, as is shown in Table 6. Taking linear bar grille as an example, there are only 6 cases from RP-1522 database, but 23 cases from CBE database. It can be expected that those 6 cases will not have a big impact on the overall regression analysis. Besides, the Γ range of the cases from RP-1522 database are within the one of CBE database. And the trend between Γ and Φ from those 6 cases are similar to that of CBE database. Therefore, there's no difference between old and updated $\Gamma-\Phi$ equations.

3.4.1.2. Case comparison

To compare the predictions of $T_{0.1}$, $T_{1.7}$, ΔT_{oc} , and supply airflow rate between the old and updated $\Gamma-\Phi$ models, an example of a 5,000 ft² (464 m²) office space is presented. This example is taken

from the example described in (Bauman et al., 2010). The design input parameters are summarized in Table 13 for a series plenum. Figure 32 shows a plan view indicating that air is delivered through swirl diffusers in the interior zone and linear bar grilles in the perimeter zone

Table 13 Design input parameters for the modeled UFAD system (series plenum).

| Parameter | Interior | Perimeter |
|--|--|--|
| Room height | 9 ft (2.7 m) | 9ft (2.7 m) |
| Floor level | Middle floor | Middle floor |
| Diffuser type | Swirl | Linear bar grille #1 48 in. (1.2 m) |
| Number of diffusers | 20 | 18 |
| Design cooling load calculated for a mixing system | 31.4 kBtu/hr (9.2 kW) | 36.2 kBtu/hr (10.6 kW) |
| Design average temperature in the occupied zone | 75 °F (23.9 °C) | 75°F (23.9 °C) |
| Estimated category 2 leakage | 0.05 cfm/ft ² (0.25 L/s/m ²) | 0.05 cfm/ft ² (0.25 L/s/m ²) |
| Setpoint temperature of air entering supply plenum | 63 °F (17.2 °C) | - |
| Number of occupants | 20 | - |
| Windows blinds | - | Up |
| Zone orientation | - | South |
| Length of the external wall of the perimeter zone | - | 100 ft (30.5m) |

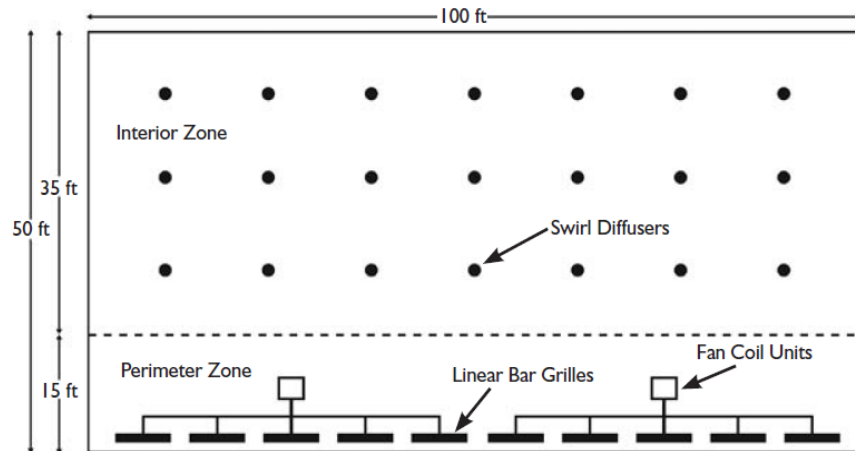


Figure 32 Floor plan for design tool example showing diffusers and underfloor fan coil units.

Table 14 shows the results of the three case comparisons. All the inputs are kept the same for the three cases, except the number of diffusers to target different values of Γ . The design airflow rate for the swirl diffusers implemented in the CBE UFAD Cooling Load Design Tool is 35 L/s (75 cfm). Case 1 represents the case with the design airflow rate per diffuser. Case 2 represents the case where each diffuser is below their design airflow rate; Case 3 represent the condition where there's a higher airflow rate than the recommended design value per diffuser.

Table 14 Interior swirl diffusers case comparison

| | Case 1 | | Case 2 | | Case3 | |
|--------------------------------------|-------------|-------------|-------------|-------------|-------------|-------------|
| | Old | Updated | Old | Updated | Old | Updated |
| No. of diffuser | 18 | 18 | 30 | 30 | 13 | 13 |
| Γ | 28.0 | 27.0 | 13.4 | 13.1 | 45.3 | 43.9 |
| $\Phi_{0.1}$ | 0.645 | 0.614 | 0.502 | 0.485 | 0.759 | 0.729 |
| $\Phi_{1.7}$ | 0.951 | 0.946 | 0.951 | 0.946 | 0.951 | 0.946 |
| ΔT_{oc} , °C (°F) | 1.8 (3.2) | 1.9 (3.5) | 2.7 (4.9) | 2.8 (5.1) | 1.1 (1.9) | 1.2 (2.2) |
| $T_{0.1}$, °C (°F) | 22.8 (73.1) | 22.7 (72.9) | 22.2 (71.9) | 22.1 (71.8) | 23.3 (73.9) | 23.2 (73.7) |
| T_{set} , °C (°F) | 24.4 (76.0) | 24.5 (76.1) | 24.8 (76.9) | 24.8 (76.6) | 24.4 (75.5) | 24.2 (75.6) |
| $T_{1.7}$, °C (°F) | 24.6 (76.2) | 24.7 (76.4) | 24.9 (76.8) | 24.9 (76.9) | 24.3 (75.8) | 24.4 (75.9) |
| Airflow rate per diffuser, L/s (cfm) | 34 (72) | 34 (71) | 19 (41) | 19 (40) | 50 (105) | 49 (103) |

It is shown in Table 14 that the old and updated Γ - Φ equation for swirl diffusers give similar results. There is only 0.1 to 0.2 °C (0.2 to 0.3 °F) difference in both $T_{0.1}$ and $T_{1.7}$ and ΔT_{oc} in all three cases, which is negligible. The calculated supply airflow rate from both the old and updated Γ - Φ models are the same for all three cases. The results fall in line with the analysis above.

Table 15 shows the compared cases for VAV directional diffusers in the interior zone. The design airflow rate for the VAV directional diffusers implemented in the CBE UFAD Cooling Load Design Tool is 72 L/s (150 cfm). Case 1, Case 2, and Case 3 represent the condition when the airflow rate of each diffuser is equal to, below, or above its design value, respectively.

Table 15 Interior VAV directional diffusers case comparison

| | Case 1 | | Case 2 | | Case 3 | |
|--------------------------------------|-------------|-------------|-------------|-------------|-------------|-------------|
| | Old | Updated | Old | Updated | Old | Updated |
| No. of diffuser | 10 | 10 | 15 | 15 | 7 | 7 |
| Γ | 6.6 | 7.1 | 4.0 | 5.9 | 10.2 | 11.6 |
| $\Phi_{0.1}$ | 0.745 | 0.829 | 0.745 | 0.799 | 0.745 | 0.870 |
| $\Phi_{1.7}$ | 0.956 | 0.974 | 0.956 | 0.964 | 0.956 | 0.990 |
| ΔT_{oc} , °C (°F) | 1.2 (2.1) | 0.8 (1.4) | 1.2 (2.1) | 0.8 (1.5) | 1.2 (2.1) | 0.6 (1.1) |
| $T_{0.1}$, °C (°F) | 23.2 (73.7) | 23.4 (74.2) | 23.2 (73.7) | 23.4 (74.1) | 23.2 (73.7) | 23.5 (74.3) |
| T_{set} , °C (°F) | 24.2 (75.6) | 24.1 (75.4) | 24.2 (75.6) | 24.2 (75.5) | 24.2 (75.6) | 24.1 (75.4) |
| $T_{1.7}$, °C (°F) | 24.3 (75.8) | 24.2 (75.5) | 24.3 (75.8) | 24.2 (75.6) | 24.3 (75.8) | 24.1 (75.4) |
| Airflow rate per diffuser, L/s (cfm) | 64 (136) | 67 (143) | 43 (91) | 60 (128) | 92 (195) | 100 (212) |

From Table 15 it can be deduced that the air stratification profile from the old Γ - Φ equations is kept the same for all the three cases, aka ΔT_{oc} , $T_{0.1}$, T_{set} , and $T_{1.7}$ from the old Γ - Φ equations are the same for all three cases. It is because in the old Γ - Φ model for VAV directional diffusers, both $\Phi_{0.1}$ and $\Phi_{1.7}$ are kept as a constant value over the range of Γ . For case 1, the old Γ - Φ equation tends to slightly overestimate ΔT_{oc} by 0.4 °C (0.7 °F). This results in the under prediction of the total required supply airflow rate, which might lead to undercooling of the space and bring discomfort to occupants. For Case 2 the old Γ - Φ equation tends to overestimate ΔT_{oc} by 0.4 °C (0.6 °F). For the same number of diffusers and cooling load, the calculated supply airflow rate per diffuser from the old Γ - Φ model is less than the one from updated Γ - Φ model by 17 L/s (37 cfm). This indicates that the results from the old tool will lead to warmer space than planned and this would have a negative impact on occupant thermal comfort. By comparing case 1 and case 2, it is found that the difference between the old and updated Γ - Φ equation is larger when the airflow rate per diffuser is below its design value. In case 3, the difference of ΔT_{oc} between the old and updated Γ - Φ equation is 0.6 °C (1.1 °F). Similar to case 1 and case 3, the calculated supply airflow rate from the old Γ - Φ model is smaller than the one from the updated Γ - Φ model. However, the difference is smaller compared to case 2.

Two typical cases for VAV directional and linear bar grille in the perimeter zone were fed into the old and updated Γ - Φ model, which are shown in Table 16. For both cases the design airflow rate is used. The design airflow rate for a 1.2 m (48 in.) long linear bar grille implemented in the CBE UFAD Cooling Load Design Tool is 106 L/s (225 cfm) (Webster et al., 2007).

Table 16 Case comparison for VAV directional diffusers and linear bar grille in perimeter zone

| | Case 1 (VAV directional diffusers) | | Case 2 (linear bar grilles) | |
|--------------------------------------|------------------------------------|-------------|-----------------------------|-------------|
| | Old | Updated | Old | Updated |
| No. of diffuser | 25 | 25 | 18 | 18 |
| Γ | 7.5 | 7.7 | 7.8 | 7.9 |
| $\Phi_{0.1}$ | 0.678 | 0.725 | 0.708 | 0.720 |
| $\Phi_{1.7}$ | 0.859 | 0.893 | 0.936 | 0.949 |
| ΔT_{oc} , °C (°F) | 0.7 (1.2) | 0.6 (1.1) | 0.8 (1.5) | 0.8 (1.5) |
| $T_{0.1}$, °C (°F) | 23.6 (74.4) | 23.6 (74.4) | 23.4 (74.1) | 23.4 (74.1) |
| T_{set} , °C (°F) | 24 (75.2) | 24 (75.2) | 24.1 (75.4) | 24.1 (75.4) |
| $T_{1.7}$, °C (°F) | 24.2 (75.6) | 24.2 (75.5) | 24.2 (75.6) | 24.2 (75.6) |
| Airflow rate per diffuser, L/s (cfm) | 73 (155) | 76 (160) | 107 (226) | 108 (229) |

From Table 16 it can be concluded that there are no differences between the old and updated Γ - Φ equations for both VAV directional diffusers and linear bar grilles in the perimeter zone. There is 0.1 °C (0.1 °F) difference in ΔT_{oc} for VAV directional diffusers, which can be negligible.

In summary, there are no differences between the old and updated Γ - Φ equations for swirl diffusers in the interior zone, and VAV directional diffusers and linear bar grilles in the perimeter zone, in terms of $T_{0.1}, T_{1.7}, \Delta T_{oc}$, and supply airflow rate prediction. The updated Γ - Φ equations for VAV directional diffusers in the interior zone are significantly different from the old one. For a practical range of Γ (4.0 -11.6) in the examples, the old Γ - Φ model tends to overestimate ΔT_{oc} by 0.4-0.6 °C (0.7-1.1 °F), and underestimate the supply airflow rate by 3-17 L/s (7-37 cfm). This may result in undersized cooling system and reduced ability to keep the space within comfort conditions. These results fall in line with the ones from paragraph 3.4.1.1.

3.5. Numeric comparison of the accuracy between the old and updated Γ - Φ equations

In order to quantify the improvement of the updated Γ - Φ equation compared to the old one, an assessment similar to the one described in paragraph 2.2.1 is used. Each case in the combined database will be fed into both the old, updated Γ - Φ model, and the RP-1522 model. The results of predicted $T_{0.1}$ and $T_{1.7}$ will be compared. Same statistical analysis, as in paragraph 2.2.1, is performed with the results.

The results of $T_{0.1}$ prediction comparison between the new Γ - Φ equation and the old ones are shown in Figure 33. The diagonal line in the figures represents the “perfect” prediction model, on which the predicted $T_{0.1}$ is exactly the same as the measured $T_{0.1}$ in the database. Therefore, the closer the dots are to the diagonal line, the more accurate the prediction model is.

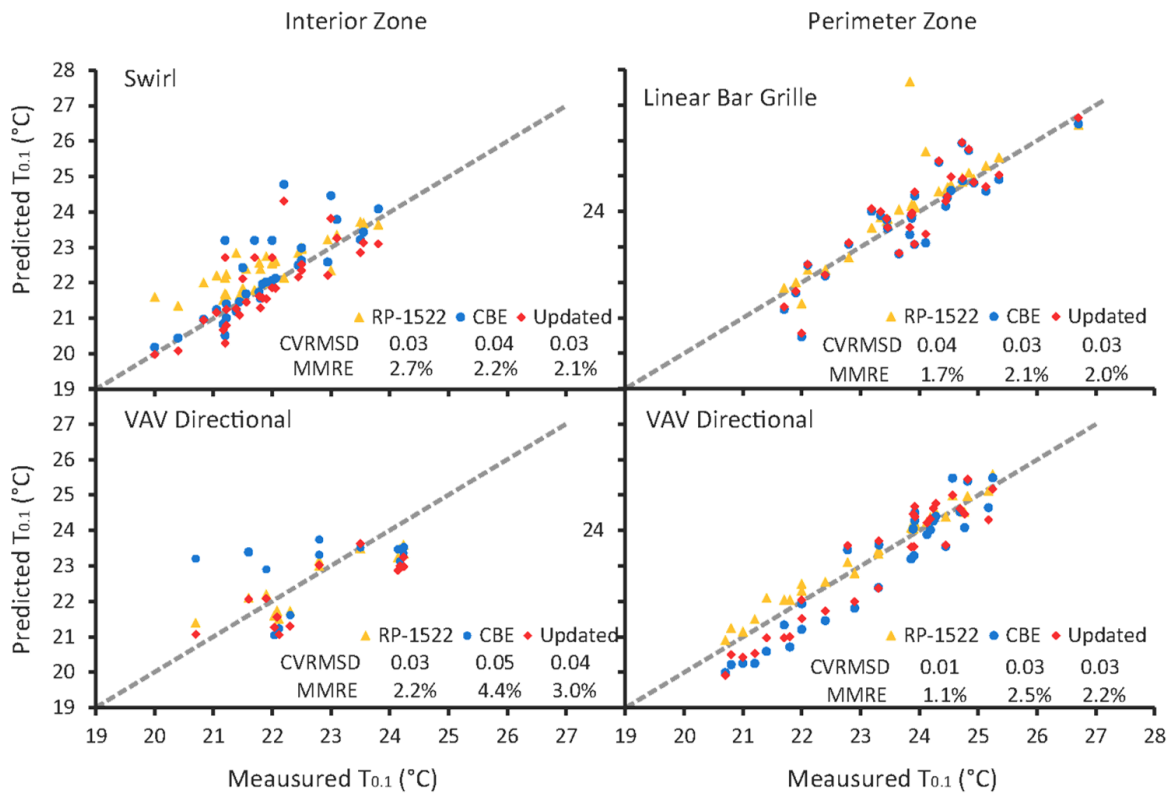


Figure 33 The comparison of $T_{0.1}$ with cases using swirl and VAV directional for the interior zone, and VAV directional diffusers for the perimeter zone.

For all the diffuser types the updated equations improved the accuracy compared to the original CBE database. The accuracy improved the most for the VAV directional diffusers in the interior zone. For VAV directional diffusers the CVRMSD of the new Γ - Φ model improved from 0.05 to 0.04. The MMRE value of the new Γ - Φ model was reduced from 4.4% to 3.0%. The CVRMSD of RP-1522 model is smaller than the updated Γ - Φ model (0.03 vs. 0.04). However, both models

are comparably accurate, given that the value of MMRE is far less than 25%. For VAV directional and linear bar grilles in perimeter zone, there is very little difference in terms of the improvement in the prediction accuracy, because the CVRMSD of the old and updated $\Gamma-\Phi$ model are the same and MMRE slightly reduced. For the swirl diffusers, the prediction accuracy of $T_{0.1}$ for the updated $\Gamma-\Phi$ model is slightly increased compared to the old one, because the CVRMSD of the updated $\Gamma-\Phi$ model is slightly smaller than the old one (0.030 vs. 0.036). These differences are minor.

The results of $T_{1.7}$ prediction comparison between updated $\Gamma-\Phi$ equations, the old one, and RP-1522 model are shown in Figure 34.

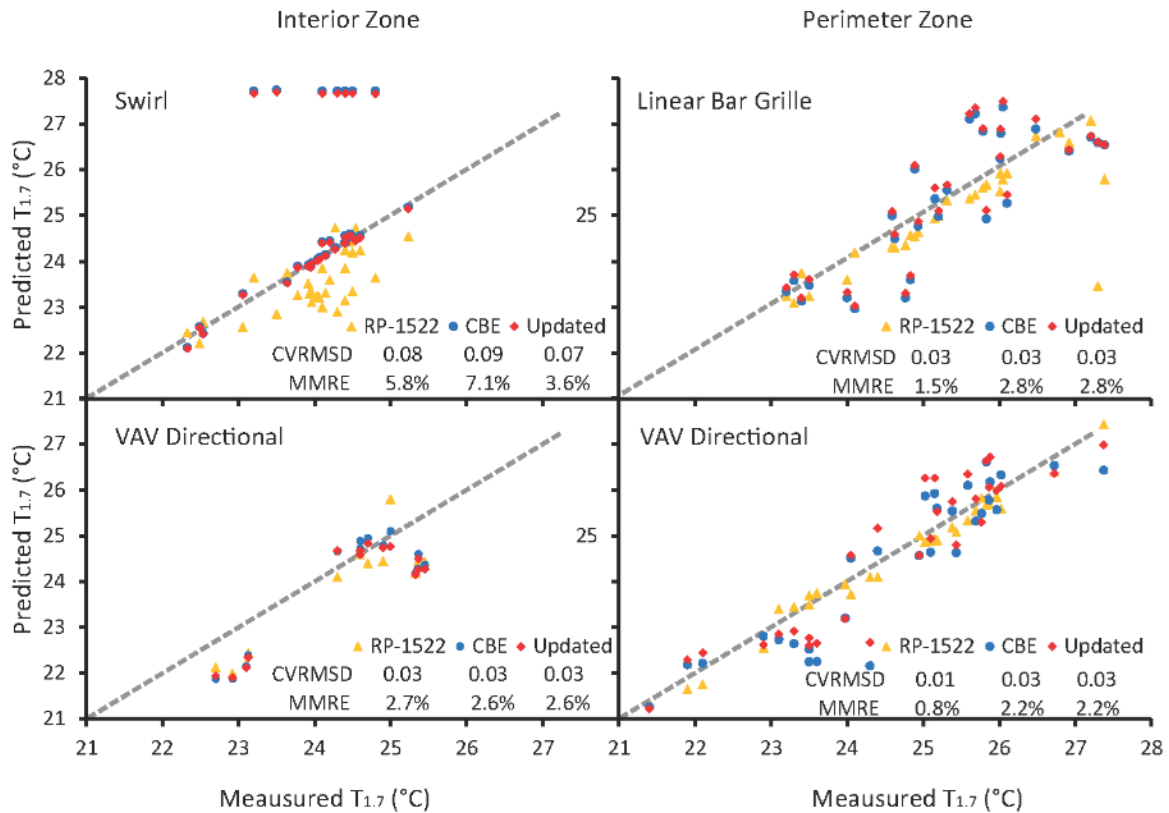


Figure 34 The comparison of $T_{1.7}$ with cases using swirl and VAV directional for the interior zone, and VAV directional diffusers for the perimeter zone

It is found in Figure 34 that for VAV directional diffusers in the interior and perimeter zones, and linear bar grilles in the perimeter zone, the prediction accuracy of $T_{1.7}$ is not improved from the updated $\Gamma-\Phi_{1.7}$ equation. This is due to the results that both values of CVRMSD and MMRE stay the same between the old and updated $\Gamma-\Phi_{1.7}$ models. For swirl diffusers in the interior zone, the updated $\Gamma-\Phi_{1.7}$ model is more accurate than the old one and RP-1522 model, considering the decrease in CVRMSD (0.07 vs. (0.09 and 0.08)).

3.6. Conclusion

New Γ - Φ equations were developed for each type of diffusers based on an expanded database including 79 cases from CBE full-scale experimental database and 31 tests from RP-1522 CFD simulation database. The CBE stratification model and RP-1522 model were developed independently by two reputable research institutions. Figure 28 and Figure 29 shows that the results of RP-1522 database and the CBE database agree very well. This is a good validation of both CBE and RP-1522 air distribution models for thermal stratification prediction. Since those two stratification models agree so well, the updated Γ - Φ equations developed from the combined database (CBE and RP-1522 database) does not make significant differences in the stratification prediction compared to the old Γ - Φ equations.

For swirl diffusers, there's slight improvement from the updated Γ - Φ equation in terms of the decrease in CVRMSD and MMRE. However, the difference can be negligible in practical cases.

For VAV directional diffusers in the interior zone the improvement is significant (CVRMSD improved from 0.05 to 0.04 and MMRE improved from 4.4% to 3.0%). The old Γ - Φ equation for VAV directional diffusers in the interior zone tends to underestimate the cooling supply airflow rate, which might lead to warmer spaces and discomfort to occupants.

For VAV directional diffusers and linear bar grilles in the perimeter zone, there is no difference between the old and updated Γ - Φ model.

Except for swirl diffusers, the updated Γ - Φ equations have still slightly less or comparable accuracy than the RP-1522 model.

In summary, the combined database with larger data samples does not make a significant difference in terms of increasing the accuracy of the Γ - Φ model, except for the VAV directional diffusers in the interior zone. It is possibly due to

- The range of Γ for all the types of diffusers was not expanded as much as expected by adding cases from RP-1522 database, except for VAV directional diffusers in the interior zone. This coincides with the fact that there is significant difference between old and updated Γ - Φ equations only for VAV directional diffusers in the interior zone.
- The trend between Γ and Φ for cases in RP-1522 database are very similar to CBE database.
- The number of added cases for VAV directional diffusers and linear bar grilles in the perimeter zone is much smaller than that of the original CBE database, as is shown in Table 6.

The updated Γ - Φ equations for VAV directional diffusers in the interior zone will be added to the CBE UFAD Cooling Load Design Tool because it has a significant improvement accuracy in terms of air stratification prediction and supply airflow rate calculation.

4. Updated CBE UFAD Cooling Load Design Tool

This chapter will introduce the new features of the updated CBE UFAD Cooling Load Design Tool, including the alert function to prevent reverse stratification in the perimeter zone, the added new diffuser type, the dual-unit system, the new data visualization of the thermal stratification profile, and the in-floor cooling unit. To illustrate the capabilities of the updated UFAD Cooling Load Design Tool, an example of a 464 m² (5,000 ft²) office space is presented. Given that the updated Γ - Φ equations for VAV directional diffuser in the interior zone have a significant improvement in terms of the thermal stratification prediction and airflow rate calculation, they have been implemented in the updated CBE UFAD Cooling Load Design Tool. It is publicly available online at <http://www.cbe.berkeley.edu/ufad-designtool/online.htm>.

4.1. New features

4.1.1. Alert function to prevent reverse stratification

Figure 35 shows the old Γ - Φ equations for the linear bar grille in the perimeter zone. It can be seen in Figure 35 that there is a certain range of Γ , above which the value of Φ is greater than one. When Γ is over 14.4, $\Phi_{0.1}$ is greater than one; when Γ is over 10.9, $\Phi_{1.7}$ is greater than one. When $\Phi_{0.1}$ and/or $\Phi_{1.7}$ is over one, it means that $T_{0.1}$ and/or $T_{1.7}$ is higher than T_R . This phenomenon is named the reverse thermal stratification effect. The discharging velocity of the airflow through the linear bar grille is too high that it blows the cool air all the way up to the ceiling, which reduces the return air temperature and produce Φ values greater than one. This is not preferred since the high airflow rates creates greater mixing in the space, which reduces or eliminates the thermal stratification. In general, the amount of air mixing should be controlled to maintain the stratification in UFAD systems.



Figure 35 The Γ - Φ equation for linear bar grille in perimeter zone

HVAC designers have to prevent reverse stratification because it has a negative impact on energy performance, indoor air quality, and possibly on occupant’s thermal comfort. The updated CBE UFAD Cooling Load Design Tool now has the capability to alert the users whenever their design parameters result in reverse stratification (i.e. when $\Phi_{0.1}$ and/or $\Phi_{1.7}$ is greater than one). The tool also provides suggestions to help users prevent reverse stratification from happening. These suggestions are shown in Figure 36:

- (1) Increase the number of diffusers;
- (2) Reduce the cooling load for the perimeter zone.

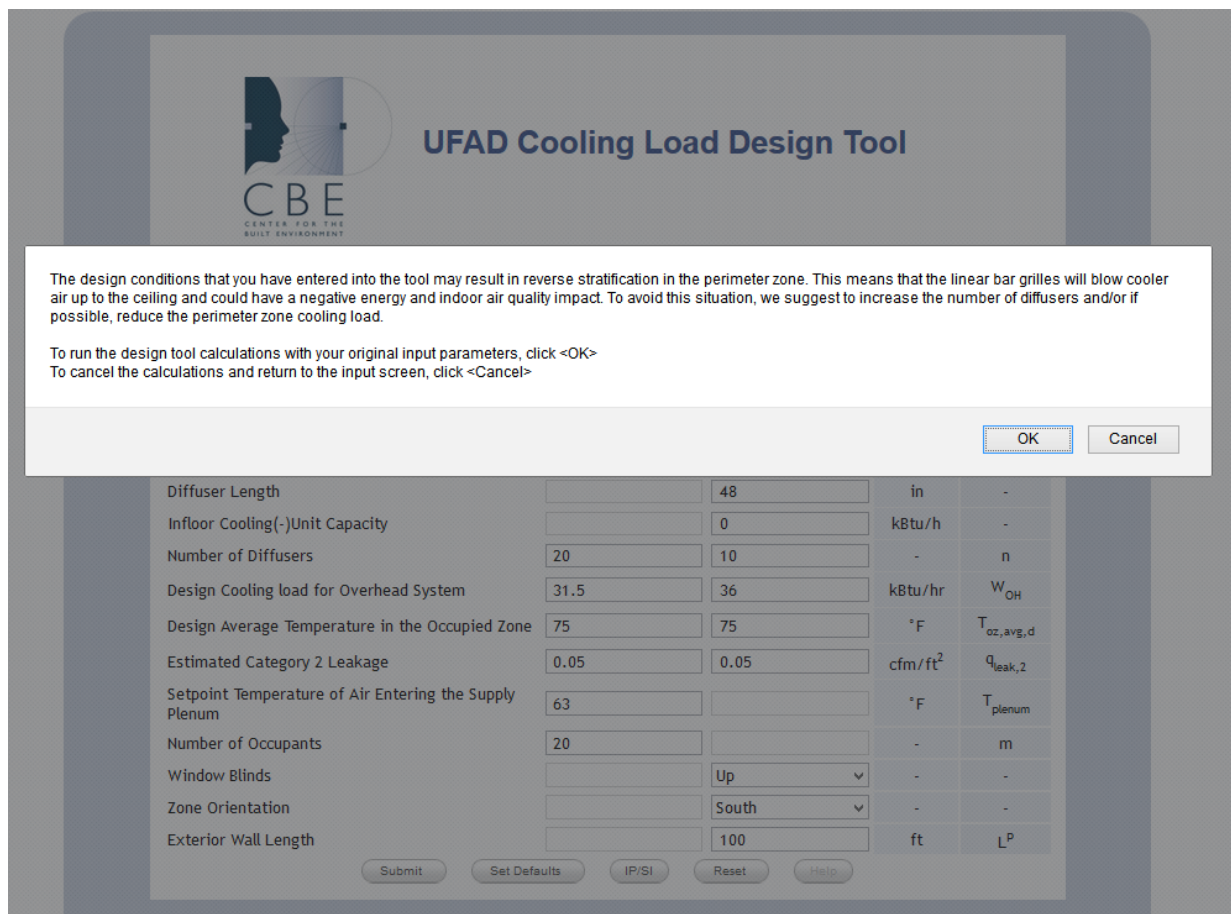


Figure 36 Screenshot of the alert information when reverse stratification happens

Users have the ability to choose whether or not to continue the calculation. If they click “OK”, then the tool will keep running, giving the results of the reversed stratification profile. If they press “Cancel”, then they can adjust the inputs according to the suggestions and prevent the reverse stratification.

4.1.2. New diffuser type

The old CBE UFAD Cooling Load Design Tool only offered text drop-down menus for users to select the diffuser type, including swirl and VAV directional diffusers for the interior zone, and VAV directional diffusers and linear bar grilles for the perimeter zone (as shown in Figure 37). However, in the updated CBE UFAD Cooling Load Design Tool, the users are able to choose the diffuser type with the reference of the diffuser picture along with a more detailed description of the diffuser, as is shown in Figure 38. This will help users choose the right diffuser type and get the right calculation results for supply airflow rate and thermal stratification.

The screenshot shows the 'Input' section of the old CBE UFAD design tool. It features a table with columns for 'Interior' and 'Perimeter' zones, and rows for various input parameters. The 'Diffuser Type' row is highlighted with a red dashed box, showing a dropdown menu with options: 'Swirl', 'VAV Directional Int.', 'Linear Bar Grille', 'VAV Directional Per.', and 'Linear Bar Grille'. The 'Unit' and 'Symbol' columns are also visible.

| Parameter | Interior | Perimeter | Unit | Symbol |
|---|--------------|-------------------|-----------------|----------------|
| Room Height | 9 | 9 | ft | H_{ft} |
| Floor Area | 3500 | 1500 | ft ² | A_f |
| Floor Level | Middle Floor | Middle Floor | - | - |
| Diffuser Type | Swirl | Linear Bar Grille | - | - |
| Number of Diffusers | | | - | n |
| Design Cooling load for Overhead System | 31.5 | | kBtu/hr | W_{OH} |
| Design Average Temperature in the Occupied Zone | 75 | 75 | °F | $T_{oz,avg,d}$ |

Figure 37 Dropdown menu of diffuser type in old CBE UFAD design tool

The screenshot shows the 'Input' section of the updated CBE UFAD cooling load design tool. It features a table with columns for 'Interior' and 'Perimeter' zones, and rows for various input parameters. The 'Diffuser Type' row is highlighted with a red dashed box, showing a dropdown menu with options: 'Swirl', 'Linear Bar Grille #1', 'VAV directional VAV Directional Diffuser for perimeter zone', 'Linear Bar Grille #1', and 'Linear Bar Grille #2'. The 'Unit' and 'Symbol' columns are also visible.

| Parameter | Interior | Perimeter | Unit | Symbol |
|--|--------------|----------------------|-----------------|--------|
| Room Height | 9 | 9 | ft | H |
| Floor Area | 3500 | 1500 | ft ² | A_f |
| Floor Level | Middle Floor | Middle Floor | - | - |
| Diffuser Type | Swirl | Linear Bar Grille #1 | - | - |
| Diffuser Length | | | | |
| Infloor Cooling(-)Unit Capacity | | | | |
| Number of Diffusers | 20 | | | |
| Design Cooling load for Overhead System | 31.5 | | | |
| Design Average Temperature in the Occupied Zone | 75 | | | |
| Estimated Category 2 Leakage | 0.05 | | | |
| Setpoint Temperature of Air Entering the Supply Plenum | 63 | | | |
| Number of Occupants | 20 | | - | m |

Figure 38 Dropdown menu for diffuser selection in updated CBE UFAD cooling load design tool

Besides, a new type of linear bar grille, which is the one tested in RP-1522 (named as Linear Bar Grille #2 in the tool shown in Figure 38), has been added to the updated CBE UFAD Cooling Load Design Tool. It is Price linear floor grille (LFG-F) with the size of 0.406 m (16 in.) in length and 0.203 m (8 in.) in width. The effective area of this type of diffuser is 0.028 m² (0.297 ft²). It is rated for approximately 94.4 L/s (200 cfm) when fed by a supply plenum pressurized to 12 Pa. (Zheng et al., 2012). Figure 39 shows the Γ - Φ plots of cases using linear bar grilles from CBE and RP-1522 database. It can be seen in Figure 39 that the six data points (yellow triangles) from RP-1522 database using LFG-F diffuser align well with the twenty-three data points from CBE database. Therefore, it is reasonable to use the same Γ - Φ equation for both types of linear bar grilles.

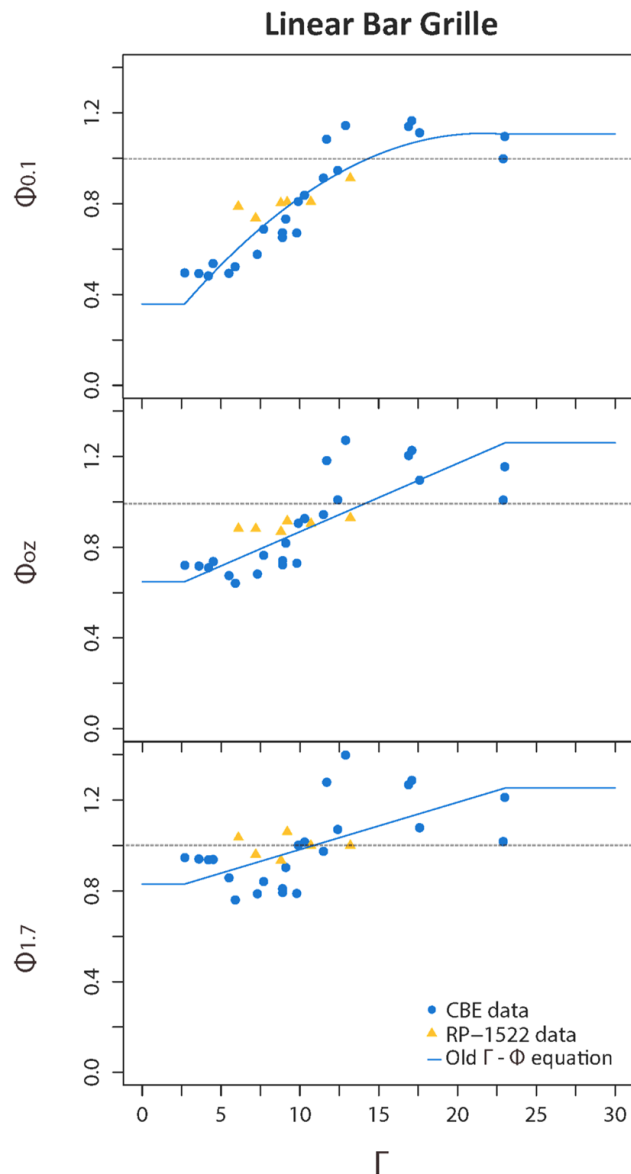
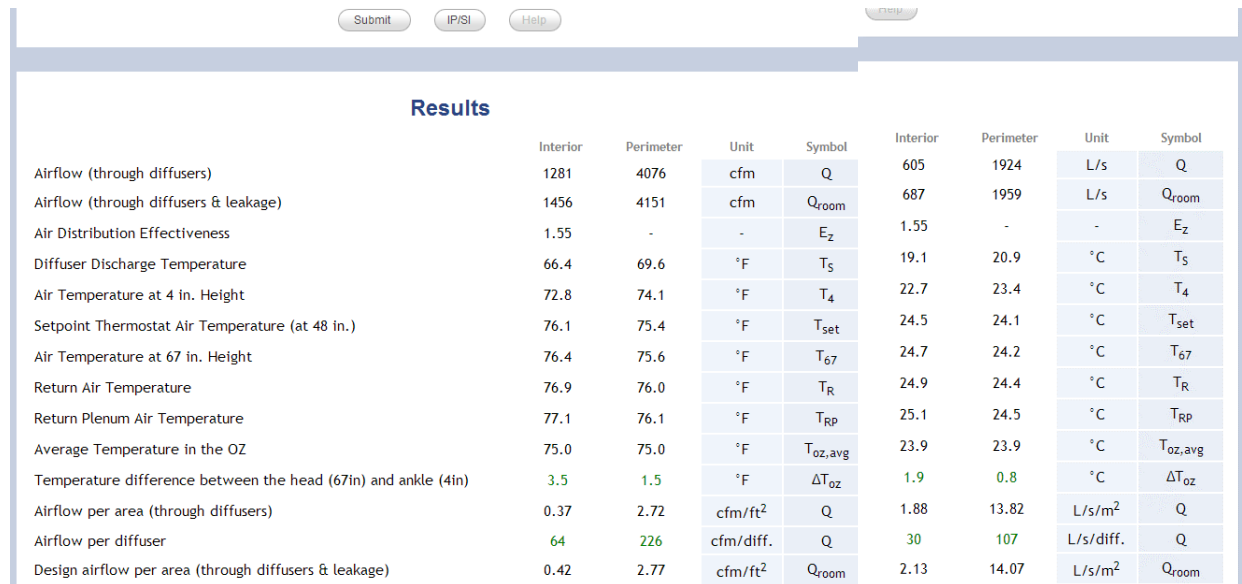


Figure 39 Γ - Φ plots of linear bar grille from CBE and RP-1522 database

4.1.3. Dual-unit system

The old CBE UFAD Cooling Load Design Tool only has imperial units for all the design parameters. To make it compatible with ASHRAE dual-unit policy (i.e., all the values can be reported in SI and IP units), SI units were added. The users can input values and see the results in either unit simply by clicking a button, as shown in Figure 40.



| | Interior | Perimeter | Unit | Symbol | Interior | Perimeter | Unit | Symbol |
|--|----------|-----------|---------------------|---------------------|----------|-----------|--------------------|---------------------|
| Airflow (through diffusers) | 1281 | 4076 | cfm | Q | 605 | 1924 | L/s | Q |
| Airflow (through diffusers & leakage) | 1456 | 4151 | cfm | Q _{room} | 687 | 1959 | L/s | Q _{room} |
| Air Distribution Effectiveness | 1.55 | - | - | E _z | 1.55 | - | - | E _z |
| Diffuser Discharge Temperature | 66.4 | 69.6 | °F | T _s | 19.1 | 20.9 | °C | T _s |
| Air Temperature at 4 in. Height | 72.8 | 74.1 | °F | T ₄ | 22.7 | 23.4 | °C | T ₄ |
| Setpoint Thermostat Air Temperature (at 48 in.) | 76.1 | 75.4 | °F | T _{set} | 24.5 | 24.1 | °C | T _{set} |
| Air Temperature at 67 in. Height | 76.4 | 75.6 | °F | T ₆₇ | 24.7 | 24.2 | °C | T ₆₇ |
| Return Air Temperature | 76.9 | 76.0 | °F | T _R | 24.9 | 24.4 | °C | T _R |
| Return Plenum Air Temperature | 77.1 | 76.1 | °F | T _{RP} | 25.1 | 24.5 | °C | T _{RP} |
| Average Temperature in the OZ | 75.0 | 75.0 | °F | T _{oz,avg} | 23.9 | 23.9 | °C | T _{oz,avg} |
| Temperature difference between the head (67in) and ankle (4in) | 3.5 | 1.5 | °F | ΔT _{oz} | 1.9 | 0.8 | °C | ΔT _{oz} |
| Airflow per area (through diffusers) | 0.37 | 2.72 | cfm/ft ² | Q | 1.88 | 13.82 | L/s/m ² | Q |
| Airflow per diffuser | 64 | 226 | cfm/diff. | Q | 30 | 107 | L/s/diff. | Q |
| Design airflow per area (through diffusers & leakage) | 0.42 | 2.77 | cfm/ft ² | Q _{room} | 2.13 | 14.07 | L/s/m ² | Q _{room} |

Figure 40 Screenshot of dual unit system of updated CBE UFAD Cooling Load Design Tool

4.1.4. Air distribution effectiveness

As discussed in paragraph 2.1.7, the capability of calculating air distribution effectiveness is one of the advantages of the RP-1522 tool over the original CBE UFAD Cooling Load Design Tool. The zone air distribution effectiveness plays an important role in determining the minimum required amount of outside air for a space to meet the indoor air quality requirements in ASHRAE Standard 62.1 (ANSI/ASHRAE, 2013b). For the traditional overhead (well-mixed) system, the air distribution effectiveness is usually equal to one. According to (Lee et al., 2009a), stratified air distribution systems, such as displacement ventilation and UFAD systems have higher ventilation effectiveness. For the office layout building type, the air distribution effectiveness at the breathing zone was at 1.1 ~ 1.6. (Lee et al., 2009a) developed an empirical model to predict the ventilation effectiveness based on a database from 102 CFD parametric simulation cases. The model is described in Equation 19 in SI units, and Equation 24 in IP units.

$$\begin{aligned}
 E_z = 1.9 + 0.01489244 \frac{QW}{A_f^2} + 0.0058333 \frac{QT_s}{A_f H} & \quad \text{Equation 24} \\
 + 0.00000755 \frac{Q^2 T_s}{A_f H n} - 0.5446667 \frac{Q}{A_f H} \\
 - 0.0006639 \frac{Q^2}{A_f H n} + 0.01864412 \frac{W}{A_f} & \quad (IP \text{ units})
 \end{aligned}$$

Where n = the number of diffusers; Q = supply airflow rate (cfm); W = room heat extraction rate (Btu/hr); A_f = Zone floor area (ft²); H = Room height (ft); T_s = supply air temperature at the diffuser (°F). Note that the equation is only valid for UFAD low throw diffuser, which is defined as a situation in which the air velocity from a supply jet decays to less than 0.3 m/s (60 fpm) at height of 1.35 m (4.5 ft) above the floor (Lee et al., 2009a).

These regression equations have been implemented into the updated CBE UFAD Cooling Load Design Tool. Since Equation 19 and Equation 24 were developed from the CFD simulation database, which includes seven office layout cases using swirl diffusers under cooling conditions in the interior zone, they are only applicable to the interior zone when swirl diffusers are at their design airflow rate in offices. Users now are able to see the calculated air distribution effectiveness for the interior zone swirl diffusers when the airflow per diffuser is around its design value in the results panel (as is shown in Figure 41).

| Results | | | | |
|---------------------------------------|----------|-----------|------|------------|
| | Interior | Perimeter | Unit | Symbol |
| Airflow (through diffusers) | 1281 | 4076 | cfm | Q |
| Airflow (through diffusers & leakage) | 1456 | 4151 | cfm | Q_{room} |
| Air Distribution Effectiveness | 1.20 | - | - | E_z |

Figure 41 Screenshot of results panel showing air distribution effectiveness

4.1.5. In-floor cooling unit

An in-floor cooling unit (Figure 42) can be installed as a linear grille in the perimeter zone to provide extra cooling capacity. This is mainly aimed to offset the temperature gain in the supply air plenum. The unit uses a water-based coil to cool down the plenum air before delivering it through a linear bar grille into the perimeter zone. Users should select Linear Bar Grille #1 when using the in-floor cooling unit. (Tate Access Floor, 2011).



Figure 42 Tate in-floor cooling unit

In the updated CBE UFAD Cooling Load Design Tool, users are able to specify the cooling capacity provided by the in-floor cooling unit, as is shown in Figure 43. The supply air temperature at the diffuser in the perimeter zone, T_s^P , will be recalculated to take into account the extra cooling capacity from the in-floor cooling unit, as is shown in Equation 25. It also will adjust the perimeter zone airflow rate, as well as the interior zone airflow rate, due to the lower perimeter zone supply air temperature.

| | Interior | Perimeter | Unit | Symbol |
|---------------------------------|--------------|----------------------|-----------------|----------------|
| Plenum Configuration | Series | | | |
| Room Height | 9 | 9 | ft | H |
| Floor Area | 3500 | 1500 | ft ² | A _f |
| Floor Level | Middle Floor | Middle Floor | - | - |
| Diffuser Type | Swirl | Linear Bar Grille #1 | - | - |
| Diffuser Length | | 48 | in | - |
| Infloor Cooling(-)Unit Capacity | | 0 | kBtu/hr | - |

Figure 43 Screenshot of input panel of the updated CBE Cooling Load Design Tool

$$T_s^P = T_{plenum}^P + \frac{3.412(SPF^P W^P - W_{unit})}{1.08 Q_{room}^T} \quad \text{Equation 25}$$

Where T_s^P = Temperature of air supplied at diffuser of the perimeter zone (°F); T_{plenum}^P = Temperature of air entering supply plenum of the perimeter zone (°F); SPF^P = Supply plenum fraction for the perimeter zone; W^P = Design cooling load for UFAD of the perimeter zone (kBtu/hr); W_{unit} = cooling capacity of the in-floor cooling unit (kBtu/hr); Q_{room}^T = Total airflow (through diffusers plus category II leakage (cfm)).

4.1.6. New data visualization

The updated CBE UFAD cooling load design tool has an improved visualization of thermal stratification profile, as is shown in Figure 44b. Each temperature point is color coded, with red representing higher temperature and blue representing lower temperature, which makes it easier for users to understand the thermal stratification effect. Besides, users can view the detailed height and temperature information by hovering over each temperature point. A correlated text box will pop out with the color coded background without blocking other temperature points and two dashed lines will point to the axis, which guides users to understand the right relationship between the temperature and the height. However for the old CBE UFAD Cooling Load Design Tool, the illustration box will block the view of the chart (as is shown in Figure 44a), which to some extent impacts users' view of the chart.

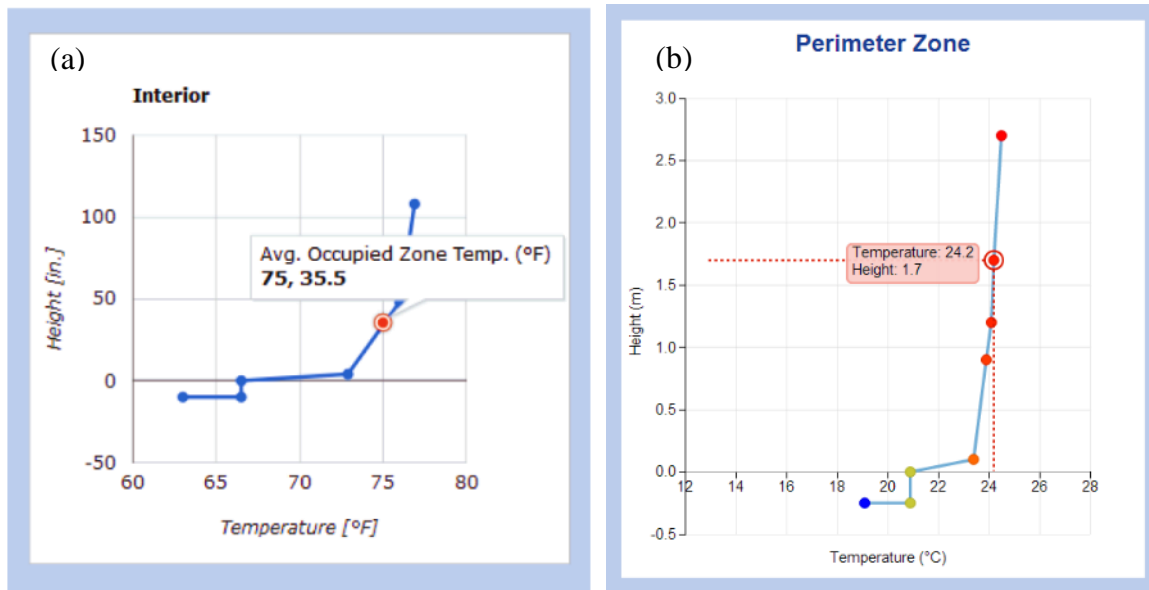


Figure 44 Thermal stratification profile visualization from (a) old (b) updated CBE UFAD Cooling Load Design Tool

4.2. The updated CBE UFAD cooling load design tool example

To demonstrate how the design tool can help HVAC designers make decisions during the design phase, the same example will be used as Table 13 shows. It is a 464 m² (5,000 ft²) office space, with 20 people working in an interior zone. For the number of diffusers, which is a design parameter a designer would like to get from the tool, I will start with 13 swirl diffusers for the interior zone and 12 linear bar grille for the perimeter zone. Figure 45 shows the input panel of the design tool with the default inputs.

UFAD Cooling Load Design Tool

Input

Plenum Configuration: Series

| | Interior | Perimeter | Unit | Symbol |
|--|--------------|----------------------|--------------------|-----------------------|
| Room Height | 2.7 | 2.7 | m | H |
| Floor Area | 325.1 | 139.3 | m ² | A _f |
| Floor Level | Middle Floor | Middle Floor | - | - |
| Diffuser Type | Swirl | Linear Bar Grille #1 | - | - |
| Diffuser Length | | 1.2 | m | - |
| In-floor Cooling(-)Unit Capacity | | 0 | kW | W _{unit} |
| Number of Diffusers | 13 | 12 | - | n |
| Design Cooling load for Overhead System | 9.2 | 10.6 | kW | W _{OH} |
| Design Average Temperature in the Occupied Zone | 23.9 | 23.9 | °C | T _{oz,avg,d} |
| Estimated Category 2 Leakage | 0.25 | 0.25 | L/s/m ² | q _{leak,2} |
| Setpoint Temperature of Air Entering the Supply Plenum | 17.2 | -17.8 | °C | T _{plenum} |
| Number of Occupants | 20 | | - | m |
| Window Blinds | | Up | - | - |
| Zone Orientation | | South | - | - |
| Exterior Wall Length | | 30.5 | m | LP |

Buttons: Submit, IP/SI, Help

Figure 45 Inputs of the example

4.2.1. Preventing reverse stratification in the perimeter zone

After entering the inputs to the updated CBE UFAD Cooling Load Design Tool according to paragraph 4.1.1, a notification text box popped up as Figure 36 shows. It alerts the users that the current inputs for the perimeter zone will result in reverse stratification condition. In order to further verify this thought, the “OK” button is clicked to check the calculation result. As is shown in Figure 46, the predicted thermal stratification profile for the perimeter zone does have the reverse stratification condition, as T_R (23.8 °C (74.8 °F)) is actually cooler than $T_{1.7}$ (23.9 °C (75.1 °F)) and T_{set} (24 °C (75.2 °F)). Based on the feedback information from the design tool, each of the suggested solutions will be tried to see whether reverse stratification problem can be solved.

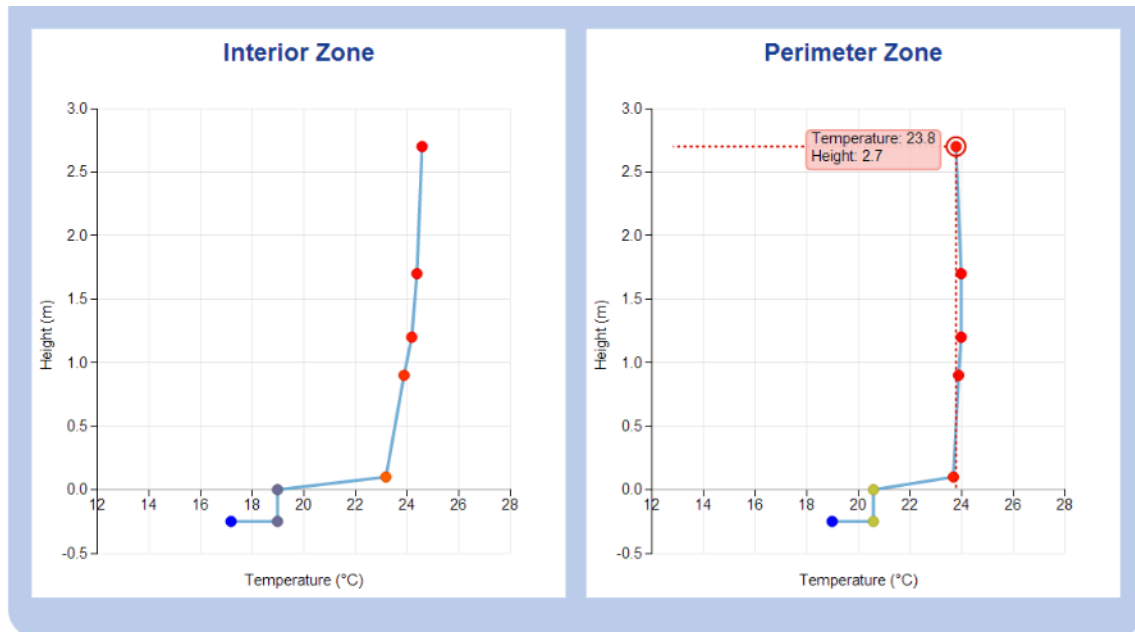


Figure 46 Screenshot of the first case calculation result

4.2.1.1. Adding the number of diffuser

As in the default case, there are twelve 1.2 m (4 ft) long linear bar grille in the perimeter zone. In this case, three more linear bar grilles are added to see whether the reverse stratification condition will be eliminated. As is shown in Figure 47a, the reverse stratification problem is solved. However there's very little thermal stratification between the head and the ankle (only 0.6 °C (1°F)). More diffusers can be added to create more stratification. Given that the length of the exterior wall is 30.5 m (100 ft), three more linear bar grilles (the total is 18 linear bar grille) are added to the perimeter zone. As is shown in Figure 47b, there is 0.8 °C (1.5 °F) stratification between $T_{1.7}$ and $T_{0.1}$. Note that linear bar grilles in general produce little stratification in practice based on the tests results (Webster et al., 2007). New advanced designs for linear bar grille includes vanes and less stratification angles to help reduce the vertical throw of the diffuser. Therefore, the amount of thermal stratification can be better maintained by reduced air mixing from the diffuser.

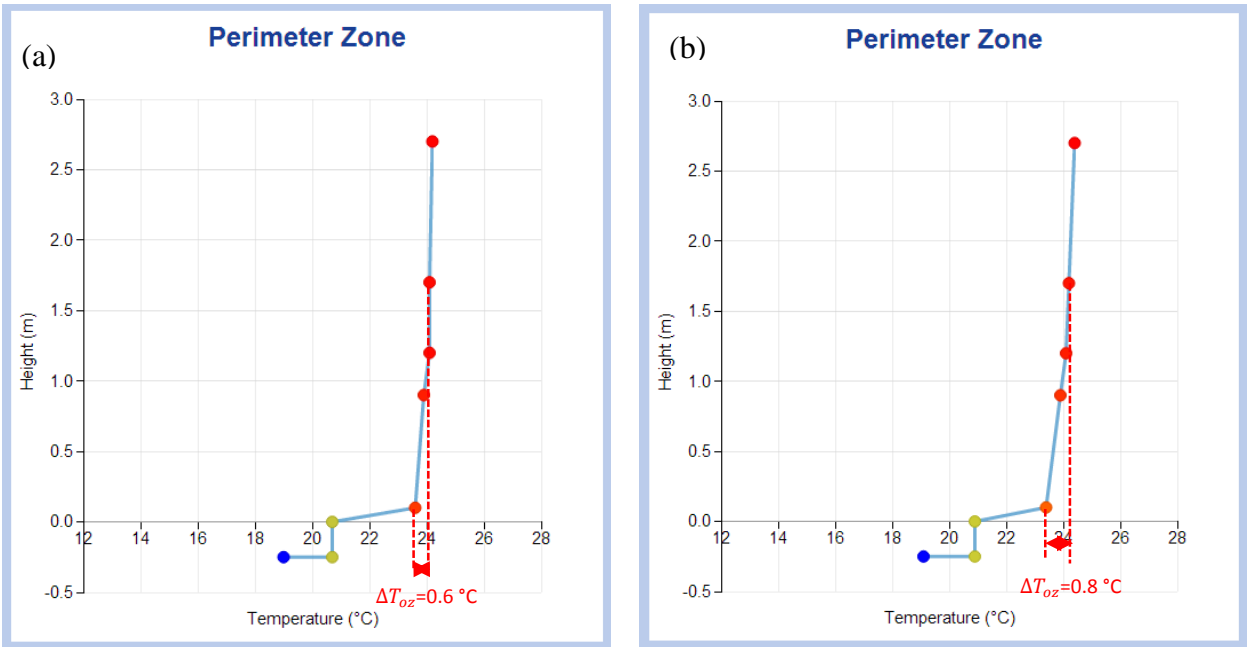


Figure 47 Temperature Profile with (a) 15 linear bar grille (b) 18 linear bar grille

4.2.1.2. Reducing the cooling load for perimeter zone

As is suggested from the design tool, in this scenario, the cooling load for the perimeter zone will be reduced to eliminate the reverse stratification. The cooling load is reduced from 10.6 kW (36 kBtu/hr) to 8.5 kW (29 kBtu/hr) in order to solve the reverse stratification problem. The prediction result is shown in Figure 48. Reducing this amount of cooling can be achieved by various ways, such as adding exterior shadings to reduce the solar heat gain from the windows, changing the lighting fixture or using dynamic lighting control to reduce the heat gains from lighting, etc.

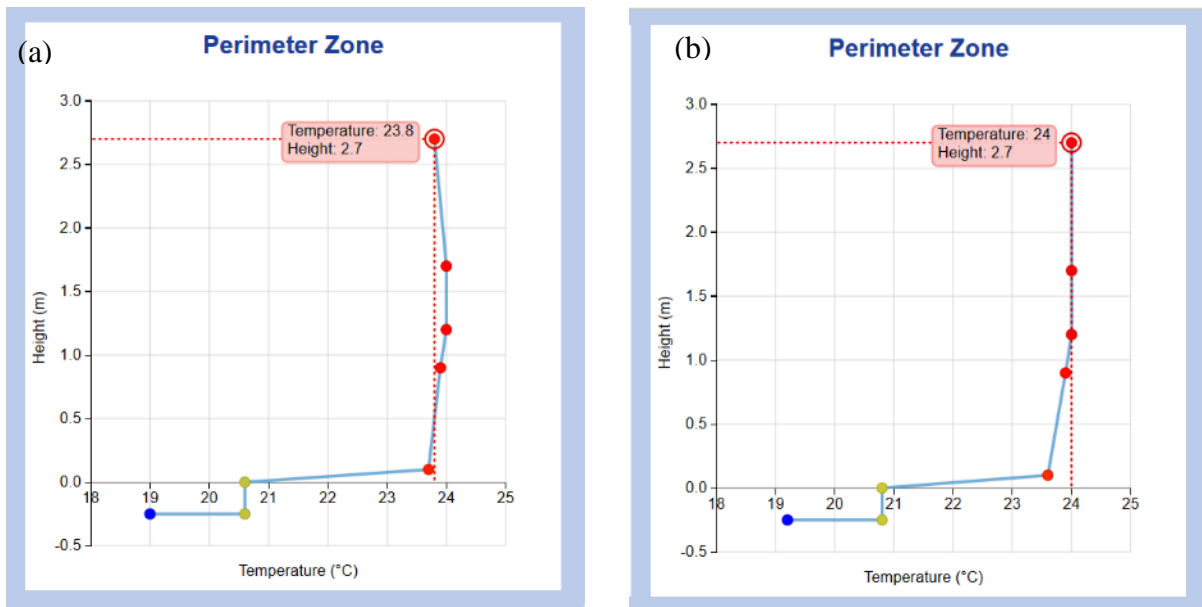


Figure 48 Screenshot of the thermal profile (a) before and (b) after reducing the cooling load

4.2.2. Adjusting the parameters in the interior zone to achieve acceptable stratification and thermal comfort

ASHRAE Standard 55 updated the maximum temperature difference between the air temperature at the head level and the ankle level to be less than 3 °C (5.4 °F) for seated occupants and 4°C (7.2 °F) for standing occupants. This will be added to next release of ASRHAE standard 55. In order to make the most use of the thermal stratification without impacting occupants' thermal comfort, users are able to use the updated CBE UFAD Cooling Load Design Tool to test how many diffusers they should use to achieve that goal.

For the interior zone, 13 swirl diffusers are used as a starting point and the predicted thermal profile is shown in Figure 49a. The temperature difference between the head and the ankle is 1.2 °C (2.2 °F), however the supply airflow rate per diffuser is 49 L/s (103 cfm), which is higher than the design airflow rate 35 L/s (75 cfm) for a swirl diffuser. In order to lower the airflow rate of each diffuser, four more diffusers are added. As is shown in Table 17 and Figure 49b, the airflow rate per diffuser is decreased to the design value and there's 0.6 °C (1 °F) more stratification than case 1. As for the optimal number of diffusers, there's not only one answer. It is recommended for designers to have more stratification and lower airflow rate per diffuser. In this case, each diffuser will be supplied with the airflow rate below its design value. Once there are higher loads on certain days, users simply need to increase the supply airflow rate to meet the load requirements without worrying about exceeding the design airflow rate per diffuser. Besides, more diffusers will increase the stratification, as case 3 and Figure 49 shows, and users could have personal control of each diffuser to increase their comfort level.

Table 17 Results of the temperature stratification and calculated airflow rate per diffuser from updated CBE UFAD Cooling Load Design Tool

| | No. of Diffuser | ΔT_{oc} °C (°F) | Airflow rate per diffuser L/s (cfm) |
|--------|-----------------|-------------------------|--|
| Case 1 | 13 | 1.1 (2.0) | 50 (106) |
| Case 2 | 17 | 1.7 (3.0) | 36 (76) |
| Case 3 | 20 | 2.0 (3.6) | 30 (64) |

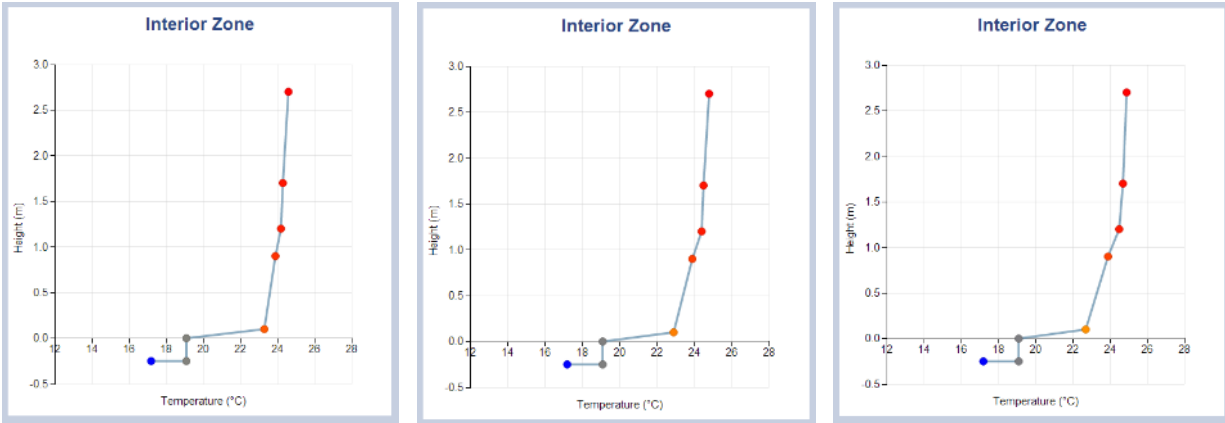


Figure 49 Screenshot of thermal stratification profile with (a) 13 swirl diffusers (b) with 17 swirl diffusers (c) with 20 swirl diffusers

The reason why more stratification should be created within the stratification limit from ASHRAE Standard 55 is that increased stratification reduces airflow requirements and allows cooling set point to be higher. Lower airflow rate will drive down the energy use from fans, thereby reducing building HVAC energy use. In addition, UFAD systems promote thermal stratification in the space, which may have a higher ventilation effectiveness in the breathing zone than overhead systems (ASHRAE, 2013b). Therefore, more stratification will increase the air distribution effectiveness and have better indoor air quality.

4.3. Conclusions

The CBE UFAD Cooling Load Design Tool has implemented two important additions - updated $\Gamma-\Phi$ equations designed for VAV directional diffusers in the interior zone, as well as new features that improve the usability of the design tool. Highlights of these new features include:

- An alert function is now able to provide notification to the users for preventing reverse stratification in perimeter zones where linear bar grilles are installed.
- A new type of linear bar grille (called linear bar grille #2, found in the RP-1522 database) is added.
- The ability to calculate the air distribution effectiveness is provided for swirl diffusers in interior zones.
- An in-floor cooling unit can be selected in the perimeter zone if desired.

The additional consideration of a dual-unit system, as well as, the use of new data visualization of the predicted stratification profile will further improve the user experience with the design tool.

The main functionality of the updated CBE UFAD Cooling Load Design Tool is to predict UFAD cooling load, temperature stratification, and calculate the supply air flow rate for UFAD systems. The examples shown in paragraph 4.2 illustrate how users could interact with the design tool and make their design decisions based on the feedback from the design tool. This will likely result in the desired maximization of energy performance and thermal comfort provided by the UFAD system.

5. Conclusions

The aim of this thesis is to comprehensively compare two UFAD design tools (CBE and RP-1522) and update the CBE UFAD Cooling Load Design Tool with the new stratification model and capabilities. The study included a comparison of features, as well as numeric comparisons to assess the accuracy of thermal stratification prediction. New Γ - Φ models were developed from the combined UFAD database and compared with the old ones to show the difference in stratification prediction and airflow rate calculation.

The results of the features comparison show that both tools have practical advantages and limitations. CBE UFAD tool has the key advantage of being able to predict the UFAD cooling load, calculate heat gain in the supply plenum, model different plenum configurations and zone types. It has the limitation of primarily being used in office buildings and not able to calculate air distribution effectiveness. RP-1522 tool covers more buildings types (classrooms, offices, workshops, restaurants, retail shops, conference rooms and auditoriums), and is able to calculate the air distribution effectiveness. However it requires users to input the zone cooling load, supply plenum factor and the supply airflow rate of each diffuser, which is difficult to get during the design stage for UFAD system.

There are slight differences in terms of the accuracy to predict the thermal stratification of the two tools. From the comparison of CVRMSD, the RP-1522 tool predicts thermal stratification slightly more accurately than the CBE model in cases using swirl diffusers (0.03 vs. 0.05), VAV directional diffusers in interior zones (0.03 vs. 0.05), and VAV directional diffusers in the perimeter zones (0.01 vs. 0.03). CBE model is slightly more accurate than RP-1522 model in cases using linear bar grille (0.03 vs. 0.04). However, given that the MMRE of both models in four cases are far less than 25%, both are acceptably accurate prediction models for design purposes.

The results of RP-1522 database and the CBE database agree very well. This is a good validation of both air distribution models for thermal stratification prediction, which were developed independently. The combined database with larger data samples does not make a significant difference in terms of increasing the accuracy of the Γ - Φ model, except for the VAV directional diffusers in the interior zone. .

For swirl diffusers, there's slight improvement from the updated Γ - Φ equation in terms of the decrease in CVRMSD and MMRE. However, the difference can be negligible in practical cases. For VAV directional diffusers and linear bar grilles in the perimeter zone, there is no difference between the old and updated Γ - Φ model. For VAV directional diffusers in the interior zone the improvement is significant (CVRMSD improved from 0.05 to 0.04 and MMRE improved from 4.4% to 3.0%). The old Γ - Φ equation for VAV directional diffusers in the interior zone tends to underestimate the cooling supply airflow rate, which might lead to warmer spaces and discomfort to occupants.

Two important additions have been implemented in the CBE UFAD Cooling Load Design Tool - updated $\Gamma-\Phi$ equations designed for VAV directional diffusers in the interior zone, as well as new features that improve the usability of the design tool. Highlights of these new features include: 1) An alert function is now able to provide notification to the users for preventing reverse stratification in perimeter zones where linear bar grilles are installed; 2) A new type of linear bar grille (called linear bar grille #2, found in the RP-1522 database) is added; 3) The ability to calculate the air distribution effectiveness is provided for swirl diffusers in interior zones; and 4) An in-floor cooling unit can be selected in the perimeter zone if desired. The additional consideration of a dual-unit system, as well as, the use of new data visualization of the predicted stratification profiles will further improve the user experience with the design tool.

The main functionality of the updated CBE UFAD Cooling Load Design Tool is to predict UFAD cooling load, temperature stratification, and calculate the supply air flow rate for UFAD systems. The design examples were provided to illustrate how users could interact with the design tool and make their design decisions based on the feedback from the design tool. This will likely result in the desired maximization of energy performance and thermal comfort provided by the UFAD system, which would also be beneficial for green building development and to reduce buildings' impact on the total U.S. energy consumption.

6. Reference

Alajmi A and El-Amer W (2010) Saving energy by using underfloor-air-distribution (UFAD) system in commercial buildings. *Energy Conversion and Management*, 51, 8, 1637-1642.

ANSI/ASHRAE (2013a) ANSI/ASHRAE 55-2013: Thermal environmental conditions for human occupancy. *American Society of Heating, Refrigerating and Air-Conditioning Engineers, Atlanta, GA, US*.

ANSI/ASHRAE (2013b) ANSI/ASHRAE 62.1-2013: Ventilation for acceptable indoor air quality. *American Society of Heating, Refrigerating and Air-Conditioning Engineers, Atlanta, GA, US*.

ANSI/ASHRAE (2010a) ANSI/ASHRAE 55-2010: Thermal environmental conditions for human occupancy. *American Society of Heating, Refrigerating and Air-Conditioning Engineers, Atlanta, GA, US*.

ANSI/ASHRAE (2010b) ANSI/ASHRAE 62.1-2010: Ventilation for acceptable indoor air quality. *American Society of Heating, Refrigerating and Air-Conditioning Engineers, Atlanta, GA, US*.

ASHRAE (2013a) 2013 ASHRAE Handbook-Fundamentals. *American Society of Heating, Air-Conditioning and Refrigeration Engineers, Atlanta, GA*.

ASHRAE (2013b) UFAD Guide: Design, construction and operation of underfloor air distribution systems. *American Society of Heating, Refrigerating and Air-Conditioning Engineers, Atlanta, GA*.

ASHRAE (2005) ASHRAE Handbook of Fundamentals. *American Society of Heating, Refrigerating and Air-Conditioning Engineers, Atlanta, GA*.

ASHRAE (2002) ASHRAE GUIDELINE: Measurement of energy and demand savings. *American Society of Heating, Refrigerating and Air-Conditioning Engineers, Atlanta, GA*.

Athens L (2007) Design for social sustainability at Seattle's central library. *Journal of Greenbuilding*, 2, 1-21.

Bauman FS (2003) Underfloor air distribution (UFAD) design guide. *American Society of Heating, Refrigerating and Air-Conditioning Engineers, Atlanta*.

Bauman FS, Carter TG, Baughman AV et al (1998) Field study of the impact of a desktop task/ambient conditioning system in office buildings. *ASHRAE Transactions*, 104, 1.

Bauman FS, Webster T, Jin H et al (2007a) Energy performance of underfloor air distribution systems. *California Energy Commission, PIER Building End-Use Energy Efficiency Program, Sacramento*.

Bauman FS, Jin H, Webster T (2006) Heat transfer pathways in underfloor air distribution (UFAD) systems. *ASHRAE Transaction*, 112, Part 2, 567-580.

- Bauman FS, Schiavon S, Webster T et al (2010) Cooling load design tool for UFAD systems. *ASHRAE Journal*, September, 62-71.
- Bauman F, Pecora P, Webster T (1999) How low can you go? Airflow performance of low-height underfloor plenums. Summary report, *Center for the Built Environment (CBE)*.
- Bauman F and Webster T (2001) Outlook for underfloor air distribution. *ASHRAE Journal*, 43(6), 18-27.
- Bauman F, Webster T, Benedek C (2007b) Cooling airflow design calculations for UFAD. *ASHRAE Journal*, 49, 10, 36-44.
- Bauman FS, Arens EA, Tanabe S et al (1995) Testing and optimizing the performance of a floor-based task conditioning system. *Energy and Buildings*, 22, 3, 173-186.
- Bos MA and Love JA (2013) A field study of thermal comfort with underfloor air distribution. *Building and Environment*, 69, 233-240.
- Briand LC and Wieczorek I Resource modeling in software engineering. (Ed. J. Marciniak) Wiley, in press, *Encyclopedia of Software Engineering*, second edition.
- Brown GZ and Dekay M (2000) *Sun, Wind & Light: Architectural Design Strategies*, 2nd Edition.
- Chen Q and Glicksman LR (2003) System performance evaluation and design guidelines for displacement ventilation. *ASHRAE, Atlanta, GA, US*.
- Chou PC, Chang KF, Chiang CM (2004) Performances on indoor air quality and energy consumption in the working spaces using under-floor air distribution (UFAD) system. *9th international conference in University of Coimbra - Portugal*, 4.
- Conte SD, Dunsmore HE, Shen VY (1986) *Software Engineering Metrics and Models*. Menlo Park, CA.
- Crawley DB, Hand JW, Kummert M et al (2008) Contrasting the capabilities of building energy performance simulation programs. *Building and Environment*, 43, 4, 661-673.
- Della Barba M, P. (2005) The dollar value of commissioning. *National Conference on Building Commissioning*.
- EIA (2012) Annual energy review 2011.
- EPA (2012a) Basic Information, Green Building. Available at: <http://www.epa.gov/greenbuilding/pubs/about.htm> 2014.
- EPA (2012b) ENERGY STAR portfolio manager. *U.S. Environmental Protection Agency, Washing, DC*.
- Fisk WJ, Faulkner D, Sullivan DP et al (2006) Performance of underfloor air distribution in a field setting. *International Journal of Ventilation*, 5, 291-300.

- Ho SH, Rosario L, Rahman MM (2011) Comparison of underfloor and overhead air distribution systems in an office environment. *Building and Environment*, 46, 7, 1415-1427.
- Jung A and Zeller M (1994) Analysis and testing of methods to determine indoor air quality and air change effectiveness. *Rheinisch-Westfälische Technical University of Aachen, Germany*.
- Kim G, Schaefer L, Lim TS et al (2013) Thermal comfort prediction of an underfloor air distribution system in a large indoor environment. *Energy and Buildings*, 64, 323-331.
- Kong Q and Yu B (2008) Numerical study on temperature stratification in a room with underfloor air distribution system. *Energy and Buildings*, 40, 4, 495-502.
- Lee K, Xue G, Jiang Z et al (2011) Thermal stratification in building interior zones with under-floor air-distribution systems. *Proceedings of the 12th International Conference on Indoor Air Quality and Climate*.
- Lee K, Jiang Z, Chen Q (2009a) Air distribution effectiveness with stratified air distribution systems. *ASHRAE Transaction*, 115(2).
- Lee K, Xue G, Jiang Z et al (2012a) Thermal environment in indoor spaces with under-floor air distribution systems: Part I. Impact of design parameters (1522-RP). *HVAC&R Research*, 18, 6, 1182-1191.
- Lee K, Zhang T, Jiang Z et al (2009b) Comparison of airflow and contaminant distributions in rooms with traditional displacement ventilation and under-floor air distribution systems. *ASHRAE Transactions*, 115(2).
- Lee KH, Schiavon S, Bauman FS et al (2012b) Thermal decay in underfloor air distribution (UFAD) systems: Fundamentals and influence on system performance. *Applied Energy*, 91, 1, 197-207.
- Lee K, Zhang T, Jiang Z et al (2009c) Comparison of airflow and contaminant distributions in rooms with traditional displacement ventilation and under-floor air distribution systems. *ASHRAE Transactions*, 115, 2, 306-321.
- Lim TS, Schaefer L, Kim JT et al (2012) Energy benefit of the underfloor air distribution system for reducing air-conditioning and heating loads in buildings. *Indoor and Built Environment*, 21, 62-70.
- Lin YJP and Linden PF (2005) A model for an under floor air distribution system. *Energy and Buildings*, 37, 4, 399-409.
- Lin Z, Chow TT, Fong KF et al (2005) Comparison of performances of displacement and mixing ventilations. Part II: Indoor air quality. *International Journal of Refrigeration*, 28, 2, 288-305.
- Liu QA and Linden PF (2008) The EnergyPlus UFAD module. In: Proceedings of the Third National Conference of IBPSA-USA, Berkeley, CA, USA, pp.23-28.

- Liu QA and Linden PF (2006) The fluid dynamics of an underfloor air distribution system. *Journal of Fluid Mechanics*, 554, 323-341.
- McGregor A, Roberts C, Cousins F (2013) *Two Degrees: The Built Environment and our Changing Climate*. Routledge.
- Montanya EC, Keith D, Love J (2009) Integrated design & UFAD. *ASHRAE Journal*, 30-40.
- Montgomery D, C., Peck E, C., Vining GG (2012) *Introduction to Linear Regression Analysis*, 5th Edition. Wiley.
- Mundt E (1996) The performance of displacement ventilation systems: experimental and theoretical studies. *Kungliga Tekniska Högskolan, Stockholm, Sweden*.
- Nielsen PV (1993) *Displacement Ventilation: Theory and Practice*. Aalborg University, Aalborg, Denmark.
- Pasut W. (2011) Using ductwork to improve supply plenum temperature distribution in underfloor air distribution (UFAD) system. PhD thesis. Università degli Studi di Padova, Italy.
- R Development Core Team (2013) R: A Language and Environment for Statistical Computing. R version 3.0.2.
- Rim D and Novoselac A (2010) Occupational exposure to hazardous airborne pollutants: Effects of air mixing and source location. *Journal of Occupational and Environmental Hygiene*, 7, 12, 683-692.
- Rim D and Novoselac A (2009) Transport of particulate and gaseous pollutants in the vicinity of a human body. *Building and Environment*, 44, 9, 1840-1849.
- Rock BA. and Zhu D (2002) *Designer's Guide to Ceiling-Based Air Diffusion*. ASHRAE.
- Saiz A, Urchueguía JF, Martos J (2010) A cellular automaton based model simulating HVAC fluid and heat transport in a building. Modeling approach and comparison with experimental results. *Energy and Buildings*, 42, 9, 1536-1542.
- Schiavon S, Lee KH, Bauman FS et al (2011) Simplified calculation method for design cooling loads in underfloor air distribution (UFAD) systems. *Energy and Buildings*, 43, 2-3, 517-528.
- Schiavon S, Lee KH, Bauman FS et al (2010a) Influence of raised floor on zone design cooling load in commercial buildings. *Energy and Buildings*, 42, 8, 1182-1191.
- Schiavon S, Lee KH, Bauman SF et al (2010b) Development of a simplified cooling load design tool for underfloor air distribution (UFAD) systems. *Final Report to CEC PIER Program*.
- Shah R, Melati S, Yusof M et al (2005) The effectiveness of underfloor air distribution (UFAD) system in controlling thermal comfort and indoor air quality. *National Seminar on Energy in Buildings (NSEB2005)*.

- Shao J (1992) Linear model selection by cross-validation. *Journal of the American Statistical Association*, 88, 486.
- Skistad H, Mundt E, Nielsen P,V. et al (2011) REHVA Guidebook no 1: Displacement ventilation in non-industrial premises. *Federation of European Heating and Air-conditioning Associations, Belgium*.
- Skistad H, Mundt E, Nielsen PV et al (2002) Displacement ventilation in non-industrial premises. Guidebook n. 1, *REHVA*.
- Sodec F and Craig R (1990) The underfloor air supply system-the European experience. *ASHRAE Transactions*, 96, **No. Part 2**.
- Tate Access Floor I (2012) EcoCore-phase change technology for energy efficiency.
- Tate Access Floor I (2011) In-floor active chilled beams.
- Thais Aya H, Inatomi, Viviane A, Brenda CCL (2006) Energy consumption of underfloor air distribution systems: A literature overview. *The 23rd Conference on Passive and Low Energy Architecture*.
- US Department of Energy *EnergyPlus*. Available at: <http://apps1.eere.energy.gov/buildings/energyplus/> (Accessed 11/03/2011).
- Versteeg HK and Malalasekera W (1995) An Introduction to Computational Fluid Dynamics. Longman Group Ltd, New York.
- Wan MP and Chao CY (2005) Numerical and experimental study of velocity and temperature characteristics in a ventilated enclosure with underfloor ventilation systems. *Indoor air*, 15, **5**, 342-355.
- Webster T, Bauman F, Dickerhoff D et al (2013) A post-occupancy monitored evaluation of the dimmable lighting, automated shading, and underfloor air distribution system in the New York times building.
- Webster T, Hoyt T, Lee E et al (2012) Influence of designing and operating conditions on underfloor air distribution (UFAD) system performance. *In: SimBuild2012 Fifth National Conference of IBPSA-USA*.
- Webster T, Bauman F, Reese J (2002a) Underfloor air distribution: thermal stratification. *ASHRAE Journal*.
- Webster T, Bauman F, Dickerhoff D et al (2008a) Case study of environmental protection agency (EPA) region 8 headquarters building. *Center for the Built Environment, University of California, Berkeley, California. US*.
- Webster T, Bauman F, Shi M et al (2002b) Thermal stratification performance of underfloor air distribution (UFAD) systems. *Proceedings, Indoor Air 2002, Monterey, CA, June 30 - July 5*.

Webster T, Lukaschek W, Dickerhoff D et al (2007) Energy performance of UFAD systems. Part II: Room air stratification full scale testing. *Center for the Built Environment, University of California, Berkeley, California. US.*

Webster T, Bauman F, Buhl F et al (2008b) Modeling of underfloor air distribution (UFAD) systems. *In: Proceedings of the Third National Conference of IBPSA-USA, Berkeley, California, USA.*

Wyon DP and Sandberg M (1996) Discomfort due to vertical thermal gradients. *Indoor Air*, 6, 1, 48-54.

Xing H, Hatton A, Awbi HB (2001) A study of the air quality in the breathing zone in a room with displacement ventilation. *Building and Environment*, 36, 7, 809-820.

Xue G, Lee K, Jiang Z et al (2012a) Thermal environment in indoor spaces with under-floor air distribution systems: 2. determination of design parameters (1522-RP). *HVAC&R Research*, 18, 6, 1192-1201.

Xue G, Lee K, Jiang Z et al (2012b) Thermal environment in indoor spaces with under-floor air distribution systems: Part 2. Determination of design parameters (1522-RP). *HVAC&R Research*, 18, 6, 1192-1201.

YORK (2006) Underfloor-air distribution for today's sustainable, energy-efficient buildings.

Zheng J, Chen Q, Lee K et al (2012) Establishment of design procedures to predict room airflow requirements in partially mixed room air distribution systems. *ASHRAE Research Project (RP-1522) Final Report.*

Zhou L and Haghghat F (2009) Optimization of ventilation systems in office environment, part II: Results and discussions. *Building and Environment*, 44, 4, 657-665.

Zucchini W (2000) An introduction to model selection. *Journal of mathematical psychology*, 44, 1, 41-61.

7. Appendix

7.1. CBE full-scale experimental database

7.1.1. Experimental input parameters

| Test | Diff-user Type | Zone Type | No. of diff-user | No. of plumes | Window Blinds | Work-station (W) | Lighting (W) | Solar (W) | Q (m ³ /s) | W _L (kW/m) |
|----------|----------------|-----------|------------------|---------------|---------------|------------------|--------------|-----------|-----------------------|-----------------------|
| INT_8-2 | Swirl | Interior | 6 | 6 | - | 1491 | 591 | 0 | 0.183 | - |
| INT_8-3 | Swirl | Interior | 8 | 6 | - | 1497 | 594 | 0 | 0.194 | - |
| INT_8-4 | Swirl | Interior | 10 | 6 | - | 1492 | . | 0 | 0.182 | - |
| INT_8-5 | Swirl | Interior | 12 | 6 | - | 1466 | 580 | 0 | 0.178 | - |
| INT_8-6 | Swirl | Interior | 14 | 6 | - | 1465 | 582 | 0 | 0.189 | - |
| INT_8-7 | Swirl | Interior | 4 | 6 | - | 1475 | 585 | 0 | 0.181 | - |
| INT_8-8 | Swirl | Interior | 6 | 4 | - | 1051 | 587 | 0 | 0.148 | - |
| INT_8-9 | Swirl | Interior | 6 | 2 | - | 578 | 586 | 0 | 0.110 | - |
| INT_8-10 | Swirl | Interior | 6 | 6 | - | 1466 | 583 | 0 | 0.112 | - |
| INT_8-12 | Swirl | Interior | 12 | 6 | - | 1479 | 589 | 0 | 0.133 | - |
| INT_6-3 | Swirl | Interior | 2 | 6 | - | 1587 | 598 | 0 | 0.156 | - |
| INT_6-4 | Swirl | Interior | 2 | 2 | - | 589 | 593 | 0 | 0.096 | - |
| INT_6-6 | Swirl | Interior | 4 | 6 | - | 1568 | 587 | 0 | 0.179 | - |
| INT_6-7 | Swirl | Interior | 4 | 6 | - | 1567 | 588 | 0 | 0.149 | - |
| INT_6-8 | Swirl | Interior | 10 | 6 | - | 1572 | 586 | 0 | 0.224 | - |
| INT_6-9 | Swirl | Interior | 6 | 2 | - | 578 | 574 | 0 | 0.143 | - |
| INT_6-10 | Swirl | Interior | 2 | 2 | - | 581 | 577 | 0 | 0.128 | - |
| INT_6-11 | VAV | Interior | 4 | 6 | - | 1500 | 578 | 0 | 0.215 | - |
| INT_6-13 | VAV | Interior | 6 | 6 | - | 1517 | 584 | 0 | 0.248 | - |
| INT_6-14 | VAV | Interior | 4 | 6 | - | 1510 | 578 | 0 | 0.262 | - |
| INT_6-15 | VAV | Interior | 4 | 6 | - | 584 | 582 | 0 | 0.123 | - |
| INT_6-16 | VAV | Interior | 2 | 6 | - | 584 | 580 | 0 | 0.161 | - |

| | | | | | | | | | | |
|----------|-----|-----------|---|---|------|------|-----|------|-------|-------|
| INT_6-17 | VAV | Interior | 2 | 6 | - | 575 | 581 | 0 | 0.087 | - |
| INT_6-18 | VAV | Interior | 4 | 6 | - | 572 | 578 | 0 | 0.097 | - |
| INT_6-19 | VAV | Interior | 6 | 6 | - | 1514 | 593 | 0 | 0.187 | - |
| INT_6-20 | VAV | Interior | 4 | 6 | - | 1527 | 597 | 0 | 0.188 | - |
| VAVDA-1 | VAV | Perimeter | 2 | 3 | Up | 439 | 228 | 2169 | 0.189 | 0.422 |
| VAVDA-2 | VAV | Perimeter | 1 | 3 | Up | 163 | 0 | 1978 | 0.142 | 0.319 |
| VAVDA-3 | VAV | Perimeter | 3 | 3 | Up | 161 | 0 | 2219 | 0.141 | 0.353 |
| VAVDA-4 | VAV | Perimeter | 1 | 3 | Up | 305 | 228 | 852 | 0.099 | 0.210 |
| VAVDA-5 | VAV | Perimeter | 2 | 3 | Up | 439 | 228 | 1107 | 0.123 | 0.264 |
| VAVDA-6 | VAV | Perimeter | 3 | 3 | Up | 303 | 0 | 808 | 0.071 | 0.150 |
| VAVDA-7 | VAV | Perimeter | 2 | 3 | Up | 438 | 228 | 2369 | 0.259 | 0.462 |
| VAVDA-8 | VAV | Perimeter | 3 | 3 | Up | 438 | 228 | 2435 | 0.212 | 0.496 |
| VAVDA-9 | VAV | Perimeter | 2 | 3 | Up | 438 | 228 | 2333 | 0.189 | 0.464 |
| VAVDA-10 | VAV | Perimeter | 3 | 3 | Up | 438 | 229 | 1965 | 0.208 | 0.392 |
| VAVDA-11 | VAV | Perimeter | 2 | 3 | Up | 442 | 229 | 1869 | 0.186 | 0.369 |
| VAVDA-12 | VAV | Perimeter | 1 | 3 | Up | 165 | 0 | 1742 | 0.140 | 0.267 |
| VAVDA-13 | VAV | Perimeter | 2 | 3 | Up | 166 | 229 | 756 | 0.074 | 0.150 |
| VAVDA-14 | VAV | Perimeter | 2 | 3 | Down | 442 | 229 | 1316 | 0.190 | 0.316 |
| VAVDA-15 | VAV | Perimeter | 3 | 3 | Down | 438 | 230 | 1324 | 0.212 | 0.337 |
| VAVDA-16 | VAV | Perimeter | 1 | 3 | Down | 165 | 0 | 1232 | 0.136 | 0.215 |
| VAVDA-17 | VAV | Perimeter | 2 | 3 | Down | 444 | 230 | 1185 | 0.255 | 0.314 |
| VAVDA-18 | VAV | Perimeter | 2 | 3 | Up | 447 | 230 | 1828 | 0.254 | 0.377 |
| VAVDA-19 | VAV | Perimeter | 3 | 3 | Up | 300 | 0 | 711 | 0.072 | 0.139 |
| VAVDA-20 | VAV | Perimeter | 3 | 3 | Down | 292 | 0 | 656 | 0.072 | 0.140 |
| VAVDB-1 | VAV | Perimeter | 1 | 3 | Up | 165 | 0 | 1849 | 0.139 | 0.287 |
| VAVDB-2 | VAV | Perimeter | 2 | 3 | Up | 441 | 229 | 1929 | 0.183 | 0.388 |
| VAVDB-3 | VAV | Perimeter | 2 | 3 | Up | 167 | 229 | 733 | 0.074 | 0.151 |
| VAVDB-4 | VAV | Perimeter | 2 | 3 | Up | 444 | 229 | 767 | 0.122 | 0.212 |

| | | | | | | | | | | |
|---------|--------|-----------|------|---|----|-----|-----|------|-------|-------|
| LBGA-1 | Linear | Perimeter | 1 | 3 | Up | 437 | 228 | 2148 | 0.260 | 0.410 |
| LBGA-2 | Linear | Perimeter | 0.5 | 3 | Up | 435 | 228 | 2651 | 0.270 | 0.459 |
| LBGA-3 | Linear | Perimeter | 1 | 3 | Up | 160 | 0 | 2237 | 0.165 | 0.348 |
| LBGA-4 | Linear | Perimeter | 1 | 3 | Up | 304 | 228 | 895 | 0.106 | 0.209 |
| LBGA-5 | Linear | Perimeter | 1 | 3 | Up | 160 | 0 | 750 | 0.066 | 0.114 |
| LBGA-6 | Linear | Perimeter | 1.61 | 3 | Up | 162 | 0 | 805 | 0.066 | 0.121 |
| LBGA-7 | Linear | Perimeter | 1 | 3 | Up | 444 | 228 | 2357 | 0.212 | 0.471 |
| LBGA-8 | Linear | Perimeter | 0.5 | 3 | Up | 301 | 0 | 1993 | 0.179 | 0.295 |
| LBGA-9 | Linear | Perimeter | 1 | 3 | Up | 443 | 228 | 2155 | 0.283 | 0.416 |
| LBGA-10 | Linear | Perimeter | 1 | 3 | Up | 437 | 228 | 2444 | 0.236 | 0.483 |
| LBGA-11 | Linear | Perimeter | 1 | 3 | Up | 440 | 228 | 2447 | 0.213 | 0.484 |
| LBGB-1 | Linear | Perimeter | 1 | 3 | Up | 159 | 0 | 2091 | 0.166 | 0.338 |
| LBGB-2 | Linear | Perimeter | 1 | 3 | Up | 437 | 230 | 1499 | 0.257 | 0.305 |
| LBGB-3 | Linear | Perimeter | 0.5 | 3 | Up | 439 | 230 | 1733 | 0.266 | 0.356 |
| LBGB-4 | Linear | Perimeter | 0.5 | 3 | Up | 305 | 0 | 1646 | 0.177 | 0.262 |
| LBGB-5 | Linear | Perimeter | 1 | 3 | Up | 304 | 229 | 804 | 0.105 | 0.194 |
| LBGB-6 | Linear | Perimeter | 1 | 3 | Up | 160 | 0 | 697 | 0.066 | 0.112 |
| LBGB-7 | Linear | Perimeter | 1 | 3 | Up | 159 | 0 | 762 | 0.057 | 0.110 |
| LBGB-8 | Linear | Perimeter | 1 | 3 | Up | 446 | 116 | 1808 | 0.211 | 0.358 |
| LBGB-9 | Linear | Perimeter | 0.5 | 3 | Up | 300 | 0 | 1585 | 0.178 | 0.257 |
| LBGB-10 | Linear | Perimeter | 1 | 3 | Up | 440 | 230 | 1561 | 0.286 | 0.315 |
| LBGB-11 | Linear | Perimeter | 1 | 3 | Up | 437 | 229 | 1739 | 0.240 | 0.363 |
| LBGB-12 | Linear | Perimeter | 1 | 3 | Up | 438 | 229 | 1709 | 0.227 | 0.349 |

7.1.2. Experimental results

| Test | T _s | T _{0.1} | T _{OZ} | T _{1.7} | T _R | Gamma | Phi _{0.1} | Phi _{1.7} |
|----------|----------------|------------------|-----------------|------------------|----------------|-------|--------------------|--------------------|
| | °C | °C | °C | °C | °C | Γ | Φ _{0.1} | Φ _{1.7} |
| INT_8-2 | 18.7 | 22.1 | 23.1 | 23.9 | 24.2 | 25.8 | 0.6032 | 0.9377 |
| INT_8-3 | 18.4 | 21.6 | 22.8 | 23.9 | 24.2 | 18.8 | 0.5424 | 0.9504 |
| INT_8-4 | 18.5 | 21.2 | 22.8 | 24.0 | 24.3 | 13.3 | 0.4736 | 0.9506 |
| INT_8-5 | 18.5 | 21.1 | 22.8 | 24.1 | 24.4 | 10.4 | 0.4326 | 0.9498 |
| INT_8-6 | 18.4 | 20.8 | 22.6 | 24.0 | 24.3 | 9.1 | 0.4240 | 0.9526 |
| INT_8-7 | 18.6 | 22.4 | 23.3 | 23.6 | 23.8 | 43.2 | 0.7253 | 0.9555 |
| INT_8-8 | 19.3 | 22.0 | 22.9 | 23.8 | 24.1 | 20.2 | 0.5549 | 0.9162 |
| INT_8-9 | 19.4 | 21.8 | 23.0 | 24.0 | 24.1 | 12.8 | 0.6054 | 0.9593 |
| INT_8-10 | 16.0 | 20.0 | 22.4 | 24.1 | 24.5 | 12.8 | 0.4802 | 0.9558 |
| INT_8-12 | 18.3 | 21.4 | 23.7 | 25.2 | 25.5 | 7.0 | 0.4291 | 0.9538 |
| INT_6-3 | 18.6 | 23.8 | 24.2 | 24.3 | 24.6 | 78.5 | 0.8752 | 0.9533 |
| INT_6-4 | 19.9 | 23.6 | 24.1 | 24.4 | 24.7 | 42.3 | 0.7541 | 0.9333 |
| INT_6-6 | 19.0 | 23.5 | 24.2 | 24.5 | 24.8 | 40.6 | 0.7730 | 0.9516 |
| INT_6-7 | 17.9 | 22.9 | 23.8 | 24.5 | 25.0 | 30.7 | 0.7044 | 0.9170 |
| INT_6-8 | 18.0 | 21.2 | 22.1 | 23.1 | 23.6 | 16.8 | 0.5626 | 0.8812 |
| INT_6-9 | 18.5 | 21.2 | 21.9 | 22.5 | 22.8 | 17.5 | 0.6292 | 0.9329 |
| INT_6-10 | 18.6 | 21.8 | 22.3 | 22.5 | 22.6 | 60.2 | 0.8008 | 0.9709 |
| INT_6-11 | 17.8 | 21.4 | 22.0 | 22.3 | 22.3 | 54.4 | 0.7757 | 0.9620 |
| INT_6-13 | 18.0 | 22.1 | 21.9 | 23.1 | 22.3 | 7.8 | 0.7491 | 0.9576 |
| INT_6-14 | 18.1 | 22.0 | 21.8 | 22.9 | 22.1 | 8.0 | 0.7753 | 0.9763 |
| INT_6-15 | 18.9 | 22.3 | 22.1 | 23.1 | 22.6 | 7.4 | 0.7456 | 0.9487 |
| INT_6-16 | 18.4 | 22.1 | 21.9 | 22.7 | 22.0 | 7.1 | 0.8437 | 1.0000 |
| INT_6-17 | 20.1 | 24.2 | 24.0 | 25.4 | 24.5 | 7.4 | 0.7191 | 0.9526 |
| INT_6-18 | 20.6 | 24.2 | 23.9 | 25.5 | 24.5 | 7.4 | 0.6782 | 0.9476 |
| INT_6-19 | 19.5 | 24.1 | 23.8 | 25.4 | 24.8 | 7.4 | 0.6984 | 0.9107 |

| | | | | | | | | |
|----------|------|------|------|------|------|------|--------|--------|
| INT_6-20 | 19.4 | 24.2 | 23.8 | 25.3 | 24.4 | 7.7 | 0.7470 | 0.9573 |
| VAVDA-1 | 17.8 | 24.2 | 24.8 | 25.4 | 26.6 | 8.3 | 0.7222 | 0.8568 |
| VAVDA-2 | 17.8 | 25.2 | 26.0 | 26.7 | 26.7 | 13.7 | 0.8330 | 0.9978 |
| VAVDA-3 | 18.2 | 24.8 | 25.3 | 25.9 | 28.2 | 4.4 | 0.6585 | 0.7704 |
| VAVDA-4 | 18.8 | 24.8 | 25.3 | 25.8 | 27.2 | 10.9 | 0.7124 | 0.8321 |
| VAVDA-5 | 18.8 | 23.9 | 24.5 | 25.1 | 27.3 | 6.3 | 0.6024 | 0.7459 |
| VAVDA-6 | 19.9 | 24.7 | 26.0 | 27.4 | 28.3 | 2.9 | 0.5652 | 0.8844 |
| VAVDA-7 | 18.0 | 24.4 | 24.7 | 24.9 | 25.1 | 11.1 | 0.9103 | 0.9809 |
| VAVDA-8 | 18.2 | 23.9 | 24.5 | 25.0 | 27.5 | 5.9 | 0.6162 | 0.7380 |
| VAVDA-9 | 17.6 | 24.3 | 24.9 | 25.6 | 27.4 | 8.0 | 0.6831 | 0.8171 |
| VAVDA-10 | 18.4 | 23.9 | 24.5 | 25.1 | 25.9 | 6.2 | 0.7312 | 0.8961 |
| VAVDA-11 | 17.7 | 23.9 | 24.7 | 25.4 | 25.6 | 8.5 | 0.7877 | 0.9812 |
| VAVDA-12 | 18.0 | 25.2 | 25.5 | 25.8 | 25.6 | 14.3 | 0.9487 | 1.0264 |
| VAVDA-13 | 19.1 | 24.1 | 25.0 | 26.0 | 27.1 | 4.6 | 0.6256 | 0.8542 |
| VAVDA-14 | 16.3 | 21.0 | 21.4 | 21.9 | 22.9 | 9.2 | 0.7000 | 0.8000 |
| VAVDA-15 | 16.9 | 20.8 | 21.5 | 22.1 | 23.2 | 6.7 | 0.6000 | 0.8000 |
| VAVDA-16 | 16.5 | 21.7 | 22.3 | 22.9 | 22.8 | 15.0 | 0.8000 | 1.0000 |
| VAVDA-17 | 16.6 | 20.7 | 21.1 | 21.4 | 21.5 | 12.4 | 0.8000 | 1.0000 |
| VAVDA-18 | 17.7 | 23.3 | 23.6 | 24.0 | 23.6 | 11.6 | 0.9553 | 1.0692 |
| VAVDA-19 | 19.4 | 23.3 | 24.5 | 25.7 | 27.0 | 3.1 | 0.5128 | 0.8240 |
| VAVDA-20 | 18.7 | 22.0 | 23.2 | 24.4 | 26.4 | 3.0 | 0.4000 | 0.7000 |
| VAVDB-1 | 18.1 | 24.6 | 25.3 | 26.0 | 26.3 | 20.7 | 0.7876 | 0.9651 |
| VAVDB-2 | 17.6 | 23.9 | 24.6 | 25.2 | 26.0 | 12.4 | 0.7527 | 0.9020 |
| VAVDB-3 | 18.9 | 24.2 | 25.1 | 25.9 | 27.0 | 6.8 | 0.6574 | 0.8579 |
| VAVDB-4 | 18.2 | 22.8 | 23.4 | 24.0 | 25.1 | 10.1 | 0.6577 | 0.8415 |
| LBGA-1 | 19.2 | 24.9 | 25.1 | 25.3 | 25.5 | 11.5 | 0.9126 | 0.9741 |
| LBGA-2 | 19.9 | 26.7 | 26.7 | 26.8 | 26.7 | 22.9 | 0.9984 | 1.0175 |
| LBGA-3 | 19.0 | 24.7 | 25.4 | 26.0 | 27.3 | 7.7 | 0.6875 | 0.8412 |

| | | | | | | | | |
|---------|------|------|------|------|------|------|--------|--------|
| LBGA-4 | 19.8 | 23.9 | 24.9 | 25.8 | 27.7 | 5.9 | 0.5223 | 0.7605 |
| LBGA-5 | 20.8 | 24.4 | 25.8 | 27.2 | 27.6 | 4.5 | 0.5362 | 0.9386 |
| LBGA-6 | 20.5 | 24.1 | 25.7 | 27.4 | 27.8 | 2.7 | 0.4954 | 0.9462 |
| LBGA-7 | 18.9 | 24.8 | 25.4 | 26.0 | 27.7 | 8.9 | 0.6723 | 0.8095 |
| LBGA-8 | 19.4 | 26.7 | 26.6 | 26.5 | 26.0 | 17.7 | 1.1125 | 1.0780 |
| LBGA-9 | 19.0 | 24.5 | 24.8 | 25.2 | 24.8 | 12.4 | 0.9468 | 1.0708 |
| LBGA-10 | 19.3 | 24.7 | 25.2 | 25.7 | 27.4 | 9.8 | 0.6709 | 0.7889 |
| LBGA-11 | 18.4 | 24.3 | 25.0 | 25.6 | 27.5 | 8.9 | 0.6513 | 0.7928 |
| LBGB-1 | 18.5 | 23.2 | 24.0 | 24.9 | 26.6 | 7.3 | 0.5770 | 0.7869 |
| LBGB-2 | 18.8 | 23.9 | 24.4 | 24.8 | 23.5 | 11.7 | 1.0841 | 1.2785 |
| LBGB-3 | 18.7 | 24.5 | 24.8 | 25.2 | 24.0 | 23.0 | 1.0965 | 1.2119 |
| LBGB-4 | 18.6 | 25.4 | 25.7 | 26.1 | 24.5 | 16.9 | 1.1405 | 1.2675 |
| LBGB-5 | 19.7 | 23.3 | 24.7 | 26.0 | 27.1 | 5.5 | 0.4933 | 0.8573 |
| LBGB-6 | 20.6 | 23.9 | 25.4 | 26.9 | 27.3 | 4.2 | 0.4822 | 0.9366 |
| LBGB-7 | 20.0 | 23.8 | 25.6 | 27.3 | 27.8 | 3.6 | 0.4925 | 0.9407 |
| LBGB-8 | 18.5 | 23.4 | 24.0 | 24.6 | 25.2 | 9.1 | 0.7326 | 0.9029 |
| LBGB-9 | 18.5 | 25.1 | 25.5 | 25.8 | 24.2 | 17.1 | 1.1657 | 1.2871 |
| LBGB-10 | 18.7 | 23.7 | 24.2 | 24.8 | 23.0 | 12.9 | 1.1438 | 1.3983 |
| LBGB-11 | 18.8 | 23.9 | 24.4 | 24.9 | 24.8 | 10.3 | 0.8376 | 1.0156 |
| LBGB-12 | 18.5 | 23.5 | 24.0 | 24.6 | 24.6 | 9.9 | 0.8098 | 1.0009 |

7.2. RP-1522 CFD simulation database

7.2.1. Experimental input parameters

| Test | Diffuser Type | Zone Type | No. of diffusers | No. of plumes | Window Blinds | Total heat Gain (W) | Q (m ³ /s) | W _L (kW/m) |
|------|---------------|-----------|------------------|---------------|---------------|---------------------|-----------------------|-----------------------|
| OF1 | Swirl | Interior | 3 | 2 | - | 1528 | 0.108 | - |
| OF2 | Swirl | Interior | 2 | 2 | - | 1528 | 0.108 | - |
| OF3 | Swirl | Interior | 4 | 2 | - | 1528 | 0.108 | - |
| OF4 | Swirl | Interior | 3 | 2 | - | 1528 | 0.081 | - |
| OF5 | Swirl | Interior | 3 | 2 | - | 1528 | 0.134 | - |
| OF6 | Swirl | Interior | 3 | 2 | - | 1528 | 0.108 | - |
| OF7 | Swirl | Interior | 3 | 2 | - | 1528 | 0.108 | - |
| OF8 | Swirl | Interior | 2 | 2 | - | 651 | 0.126 | - |
| OF9 | Swirl | Interior | 2 | 2 | - | 658 | 0.097 | - |
| OF10 | Swirl | Interior | 2 | 2 | - | 661 | 0.079 | - |
| OF11 | Swirl | Interior | 4 | 2 | - | 649 | 0.126 | - |
| OF12 | Swirl | Interior | 4 | 2 | - | 650 | 0.097 | - |
| OF13 | Swirl | Interior | 4 | 2 | - | 656 | 0.079 | - |
| OF14 | VAV | Interior | 2 | 2 | - | 643 | 0.097 | - |
| OF15 | VAV | Interior | 2 | 2 | - | 657 | 0.075 | - |
| OF16 | VAV | Interior | 2 | 2 | - | 655 | 0.060 | - |
| OF17 | VAV | Interior | 4 | 2 | - | 683 | 0.097 | - |
| OF18 | VAV | Interior | 4 | 2 | - | 666 | 0.075 | - |
| OF19 | VAV | Interior | 4 | 2 | - | 681 | 0.060 | - |
| OF32 | VAV | Perimeter | 2 | 2 | Up | 887 | 0.133 | 0.049 |
| OF33 | VAV | Perimeter | 2 | 2 | Up | 913 | 0.109 | 0.051 |
| OF34 | VAV | Perimeter | 2 | 2 | Up | 943 | 0.094 | 0.052 |
| OF35 | VAV | Perimeter | 3 | 2 | Up | 914 | 0.132 | 0.051 |
| OF36 | VAV | Perimeter | 3 | 2 | Up | 949 | 0.109 | 0.053 |

| | | | | | | | | |
|------|--------|-----------|---|---|----|-----|-------|-------|
| OF37 | VAV | Perimeter | 3 | 2 | Up | 966 | 0.095 | 0.054 |
| OF38 | Linear | Perimeter | 2 | 2 | Up | 909 | 0.132 | 0.050 |
| OF39 | Linear | Perimeter | 2 | 2 | Up | 956 | 0.109 | 0.053 |
| OF40 | Linear | Perimeter | 2 | 2 | Up | 949 | 0.093 | 0.053 |
| OF41 | Linear | Perimeter | 3 | 2 | Up | 953 | 0.134 | 0.053 |
| OF42 | Linear | Perimeter | 3 | 2 | Up | 954 | 0.110 | 0.053 |
| OF43 | Linear | Perimeter | 3 | 2 | Up | 933 | 0.093 | 0.052 |

7.2.2. Experimental results

| Test | T _s | T _{0.1} | T _{0z} | T _{1.7} | T _R | Gamma Γ | Phi _{0.1} Φ _{0.1} | Phi _{1.7} Φ _{1.7} |
|------|----------------|------------------|-----------------|------------------|----------------|------------|--|--|
| | °C | °C | °C | °C | °C | | | |
| OF1 | 16.5 | 22 | 22.7 | 24.5 | 28.3 | 19.3 | 0.5679 | 0.9510 |
| OF2 | 16.5 | 23 | 23 | 23.2 | 28.3 | 32.0 | 0.6747 | 0.9510 |
| OF3 | 16.5 | 21.5 | 22.5 | 24.4 | 28.3 | 13.4 | 0.5024 | 0.9510 |
| OF4 | 12.7 | 20.4 | 22.5 | 24.8 | 28.5 | 12.5 | 0.4903 | 0.9510 |
| OF5 | 18.8 | 22.2 | 22.5 | 23.5 | 28.2 | 26.9 | 0.6364 | 0.9510 |
| OF6 | 16.5 | 21.2 | 22.3 | 24.3 | 28.3 | 19.3 | 0.5679 | 0.9510 |
| OF7 | 16.5 | 21.7 | 22.4 | 24.1 | 28.3 | 19.3 | 0.5679 | 0.9510 |
| OF8 | 19.1 | 23.1 | 23.8 | 24.4 | 24.7 | 62.4 | 0.8370 | 0.9510 |
| OF9 | 17.6 | 22.5 | 23.6 | 24.5 | 24.9 | 41.6 | 0.7379 | 0.9510 |
| OF10 | 16.1 | 21.9 | 23.5 | 24.6 | 25 | 30.8 | 0.6661 | 0.9510 |
| OF11 | 19.1 | 22.5 | 23.4 | 24.1 | 24.7 | 26.3 | 0.6311 | 0.9510 |
| OF12 | 17.6 | 21.8 | 23 | 24.2 | 24.8 | 17.6 | 0.5507 | 0.9510 |
| OF13 | 16.1 | 21.2 | 23 | 24.4 | 25 | 13.0 | 0.4966 | 0.9510 |
| OF14 | 19.5 | 23.5 | 23.8 | 24.3 | 24.9 | 4.8 | 0.7450 | 0.9560 |
| OF15 | 18.1 | 22.8 | 23.8 | 24.9 | 25.1 | 3.3 | 0.7450 | 0.9560 |
| OF16 | 16.5 | 21.9 | 23.4 | 24.6 | 25.1 | 2.4 | 0.7450 | 0.9560 |
| OF17 | 19.5 | 22.8 | 23.7 | 24.7 | 25.2 | 2.0 | 0.7450 | 0.9560 |

| | | | | | | | | |
|------|------|------|------|------|------|------|--------|--------|
| OF18 | 18.1 | 21.6 | 23.4 | 24.6 | 25.2 | 1.4 | 0.7450 | 0.9560 |
| OF19 | 16.5 | 20.7 | 23.6 | 25 | 25.5 | 1.0 | 0.7450 | 0.9560 |
| OF32 | 18 | 22.9 | 23.1 | 23.1 | 23.4 | 13.0 | 0.8396 | 0.9635 |
| OF33 | 16.6 | 22 | 23 | 23.5 | 23.6 | 10.5 | 0.7677 | 0.9167 |
| OF34 | 15.3 | 21.4 | 22.9 | 23.5 | 23.7 | 9.0 | 0.7231 | 0.8877 |
| OF35 | 17.8 | 22.4 | 23 | 23.3 | 23.7 | 8.5 | 0.7082 | 0.8780 |
| OF36 | 16.4 | 21.8 | 22.9 | 23.6 | 23.7 | 6.9 | 0.6627 | 0.8484 |
| OF37 | 15.2 | 21.2 | 22.8 | 24.3 | 24 | 6.0 | 0.6367 | 0.8315 |
| OF38 | 17.6 | 22.8 | 22.9 | 23.3 | 23.3 | 20.5 | 1.1071 | 1.2009 |
| OF39 | 16.2 | 22.1 | 22.8 | 23.5 | 23.5 | 16.7 | 1.0583 | 1.1210 |
| OF40 | 15.2 | 21.9 | 22.8 | 24 | 23.5 | 14.2 | 0.9952 | 1.0703 |
| OF41 | 17.5 | 22.4 | 22.8 | 23.2 | 23.6 | 13.7 | 0.9791 | 1.0599 |
| OF42 | 16.1 | 21.7 | 22.8 | 23.4 | 23.7 | 11.3 | 0.8843 | 1.0084 |
| OF43 | 15.3 | 22 | 22.8 | 24.1 | 23.8 | 9.5 | 0.8036 | 0.9728 |

7.3. Numeric comparison results

| Test | Diffuser Type | Zone Type | T _{0.1} | | | | T _{1.7} | | | |
|----------|---------------|-----------|------------------|---------|------|------|------------------|---------|------|------|
| | | | Data base | RP-1522 | CBE | New | Data base | RP-1522 | CBE | New |
| | | | °C | °C | °C | °C | °C | °C | °C | °C |
| OF1 | Swirl | Interior | 22.0 | 22.1 | 23.2 | 22.8 | 24.5 | 23.4 | 27.7 | 27.7 |
| OF2 | Swirl | Interior | 23.0 | 22.4 | 24.5 | 24.0 | 23.2 | 23.7 | 27.7 | 27.7 |
| OF3 | Swirl | Interior | 21.5 | 21.9 | 22.4 | 22.2 | 24.4 | 23.2 | 27.7 | 27.7 |
| OF4 | Swirl | Interior | 20.4 | 21.4 | 20.4 | 20.2 | 24.8 | 23.7 | 27.7 | 27.7 |
| OF5 | Swirl | Interior | 22.2 | 22.2 | 24.8 | 24.4 | 23.5 | 22.9 | 27.7 | 27.7 |
| OF6 | Swirl | Interior | 21.2 | 21.7 | 23.2 | 22.8 | 24.3 | 22.9 | 27.7 | 27.7 |
| OF7 | Swirl | Interior | 21.7 | 21.8 | 23.2 | 22.8 | 24.1 | 23.0 | 27.7 | 27.7 |
| OF8 | Swirl | Interior | 23.1 | 23.4 | 23.8 | 23.6 | 24.4 | 24.3 | 24.4 | 24.4 |
| OF9 | Swirl | Interior | 22.5 | 23.0 | 23.0 | 22.7 | 24.5 | 24.2 | 24.5 | 24.5 |
| OF10 | Swirl | Interior | 21.9 | 22.8 | 22.0 | 21.7 | 24.6 | 24.3 | 24.6 | 24.5 |
| OF11 | Swirl | Interior | 22.5 | 23.0 | 22.6 | 22.4 | 24.1 | 23.9 | 24.4 | 24.4 |
| OF12 | Swirl | Interior | 21.8 | 22.4 | 21.6 | 21.3 | 24.2 | 23.6 | 24.4 | 24.4 |
| OF13 | Swirl | Interior | 21.2 | 22.2 | 20.5 | 20.3 | 24.4 | 23.9 | 24.6 | 24.5 |
| INT_8-2 | Swirl | Interior | 22.1 | 22.6 | 22.1 | 21.9 | 23.9 | 23.5 | 23.9 | 23.9 |
| INT_8-3 | Swirl | Interior | 21.6 | 22.4 | 21.7 | 21.5 | 23.9 | 23.3 | 23.9 | 23.9 |
| INT_8-4 | Swirl | Interior | 21.2 | 22.3 | 21.4 | 21.3 | 24.0 | 23.3 | 24.0 | 24.0 |
| INT_8-5 | Swirl | Interior | 21.1 | 22.2 | 21.2 | 21.2 | 24.1 | 23.3 | 24.1 | 24.1 |
| INT_8-6 | Swirl | Interior | 20.8 | 22.0 | 21.0 | 21.0 | 24.0 | 23.1 | 24.0 | 23.9 |
| INT_8-7 | Swirl | Interior | 22.4 | 22.9 | 22.5 | 22.3 | 23.6 | 23.8 | 23.6 | 23.5 |
| INT_8-8 | Swirl | Interior | 22.0 | 22.6 | 22.1 | 21.9 | 23.8 | 23.3 | 23.9 | 23.9 |
| INT_8-9 | Swirl | Interior | 21.8 | 22.6 | 21.7 | 21.6 | 24.0 | 23.4 | 23.9 | 23.9 |
| INT_8-10 | Swirl | Interior | 20.0 | 21.6 | 20.2 | 20.0 | 24.1 | 23.2 | 24.1 | 24.0 |
| INT_8-12 | Swirl | Interior | 21.4 | 22.8 | 21.2 | 21.3 | 25.2 | 24.5 | 25.2 | 25.1 |
| INT_6-3 | Swirl | Interior | 23.8 | 23.6 | 24.1 | 23.8 | 24.3 | 24.7 | 24.3 | 24.3 |

| | | | | | | | | | | |
|----------|-------|-----------|------|------|------|------|------|------|------|------|
| INT_6-4 | Swirl | Interior | 23.6 | 23.7 | 23.4 | 23.3 | 24.4 | 24.5 | 24.4 | 24.4 |
| INT_6-6 | Swirl | Interior | 23.5 | 23.7 | 23.2 | 23.0 | 24.5 | 24.7 | 24.5 | 24.5 |
| INT_6-7 | Swirl | Interior | 22.9 | 23.2 | 22.6 | 22.3 | 24.5 | 24.4 | 24.6 | 24.6 |
| INT_6-8 | Swirl | Interior | 21.2 | 21.7 | 21.0 | 20.8 | 23.1 | 22.6 | 23.3 | 23.3 |
| INT_6-9 | Swirl | Interior | 21.2 | 21.5 | 20.8 | 20.7 | 22.5 | 22.2 | 22.6 | 22.6 |
| INT_6-10 | Swirl | Interior | 21.8 | 22.0 | 22.0 | 21.8 | 22.5 | 22.7 | 22.4 | 22.4 |
| INT_6-11 | Swirl | Interior | 21.4 | 21.6 | 21.5 | 21.3 | 22.3 | 22.4 | 22.1 | 22.1 |
| OF14 | VAV | Interior | 23.5 | 23.5 | 23.5 | 23.6 | 24.3 | 24.1 | 24.7 | 25.6 |
| OF15 | VAV | Interior | 22.8 | 23.2 | 23.3 | 23.0 | 24.9 | 24.5 | 24.8 | 25.7 |
| OF16 | VAV | Interior | 21.9 | 22.2 | 22.9 | 22.1 | 24.6 | 24.6 | 24.7 | 25.6 |
| OF17 | VAV | Interior | 22.8 | 23.0 | 23.7 | 23.0 | 24.7 | 24.4 | 24.9 | 25.4 |
| OF18 | VAV | Interior | 21.6 | 22.1 | 23.4 | 22.1 | 24.6 | 24.7 | 24.9 | 25.2 |
| OF19 | VAV | Interior | 20.7 | 21.4 | 23.2 | 21.1 | 25.0 | 25.8 | 25.1 | 25.2 |
| OF32 | VAV | Perimeter | 22.9 | 22.8 | 22.5 | 22.5 | 23.1 | 23.4 | 23.2 | 23.2 |
| OF33 | VAV | Perimeter | 22.0 | 22.5 | 22.0 | 22.1 | 23.5 | 23.5 | 23.0 | 23.1 |
| OF34 | VAV | Perimeter | 21.4 | 22.1 | 21.4 | 21.6 | 23.5 | 23.7 | 22.8 | 22.9 |
| OF35 | VAV | Perimeter | 22.4 | 22.6 | 22.0 | 22.2 | 23.3 | 23.5 | 23.0 | 23.1 |
| OF36 | VAV | Perimeter | 21.8 | 22.1 | 21.2 | 21.4 | 23.6 | 23.8 | 22.6 | 22.8 |
| OF37 | VAV | Perimeter | 21.2 | 21.5 | 20.8 | 20.9 | 24.3 | 24.1 | 22.5 | 22.8 |
| VAVDA-1 | VAV | Perimeter | 24.2 | 24.4 | 24.0 | 24.3 | 25.4 | 25.2 | 25.5 | 25.7 |
| VAVDA-2 | VAV | Perimeter | 25.2 | 25.6 | 25.5 | 25.3 | 26.7 | 26.4 | 26.5 | 26.4 |
| VAVDA-3 | VAV | Perimeter | 24.8 | 24.5 | 24.1 | 24.0 | 25.9 | 26.1 | 26.2 | 26.6 |
| VAVDA-4 | VAV | Perimeter | 24.8 | 25.0 | 25.4 | 25.6 | 25.8 | 25.7 | 26.6 | 26.7 |
| VAVDA-5 | VAV | Perimeter | 23.9 | 24.1 | 24.3 | 24.4 | 25.1 | 24.9 | 25.9 | 26.2 |
| VAVDA-6 | VAV | Perimeter | 24.7 | 24.6 | 24.5 | 24.2 | 27.4 | 27.4 | 26.4 | 26.8 |
| VAVDA-7 | VAV | Perimeter | 24.4 | 24.4 | 23.6 | 23.7 | 24.9 | 25.0 | 24.6 | 24.6 |
| VAVDA-8 | VAV | Perimeter | 23.9 | 24.1 | 24.0 | 24.2 | 25.0 | 24.9 | 25.9 | 26.2 |
| VAVDA-9 | VAV | Perimeter | 24.3 | 24.5 | 24.4 | 24.7 | 25.6 | 25.3 | 26.1 | 26.3 |

| | | | | | | | | | | |
|----------|--------|-----------|------|------|------|------|------|------|------|------|
| VAVDA-10 | VAV | Perimeter | 23.9 | 24.1 | 23.2 | 23.3 | 25.1 | 24.9 | 24.6 | 24.9 |
| VAVDA-11 | VAV | Perimeter | 23.9 | 24.3 | 23.3 | 23.5 | 25.4 | 25.1 | 24.6 | 24.8 |
| VAVDA-12 | VAV | Perimeter | 25.2 | 25.1 | 24.6 | 24.4 | 25.8 | 25.8 | 25.5 | 25.4 |
| VAVDA-13 | VAV | Perimeter | 24.1 | 24.2 | 23.9 | 23.8 | 26.0 | 25.8 | 25.6 | 25.9 |
| VAVDA-14 | VAV | Perimeter | 21.0 | 21.2 | 20.3 | 20.5 | 21.9 | 21.7 | 22.2 | 22.3 |
| VAVDA-15 | VAV | Perimeter | 20.8 | 21.3 | 20.2 | 20.3 | 22.1 | 21.8 | 22.2 | 22.4 |
| VAVDA-16 | VAV | Perimeter | 21.7 | 22.1 | 21.3 | 21.0 | 22.9 | 22.6 | 22.8 | 22.7 |
| VAVDA-17 | VAV | Perimeter | 20.7 | 20.9 | 20.0 | 20.0 | 21.4 | 21.3 | 21.3 | 21.2 |
| VAVDA-18 | VAV | Perimeter | 23.3 | 23.3 | 22.4 | 22.5 | 24.0 | 23.9 | 23.2 | 23.2 |
| VAVDA-19 | VAV | Perimeter | 23.3 | 23.5 | 23.6 | 23.3 | 25.7 | 25.6 | 25.3 | 25.7 |
| VAVDA-20 | VAV | Perimeter | 22.0 | 22.3 | 21.9 | 21.6 | 24.4 | 24.1 | 24.7 | 25.0 |
| VAVDB-1 | VAV | Perimeter | 24.6 | 25.0 | 25.5 | 24.7 | 26.0 | 25.6 | 26.3 | 26.8 |
| VAVDB-2 | VAV | Perimeter | 23.9 | 24.2 | 24.5 | 24.5 | 25.2 | 24.9 | 25.6 | 25.6 |
| VAVDB-3 | VAV | Perimeter | 24.2 | 24.4 | 24.3 | 24.4 | 25.9 | 25.7 | 25.8 | 26.0 |
| VAVDB-4 | VAV | Perimeter | 22.8 | 23.1 | 23.5 | 23.6 | 24.0 | 23.7 | 24.5 | 24.6 |
| INT_6-13 | VAV | Interior | 22.1 | 21.5 | 21.2 | 21.1 | 23.1 | 22.2 | 22.1 | 22.7 |
| INT_6-14 | VAV | Interior | 22.0 | 21.6 | 21.0 | 21.3 | 22.9 | 22.0 | 21.9 | 22.6 |
| INT_6-15 | VAV | Interior | 22.3 | 21.7 | 21.6 | 21.3 | 23.1 | 22.4 | 22.4 | 22.8 |
| INT_6-16 | VAV | Interior | 22.1 | 21.7 | 21.1 | 21.6 | 22.7 | 22.1 | 21.9 | 22.7 |
| INT_6-17 | VAV | Interior | 24.2 | 23.6 | 23.4 | 23.3 | 25.4 | 24.3 | 24.3 | 24.9 |
| INT_6-18 | VAV | Interior | 24.2 | 23.3 | 23.5 | 23.0 | 25.5 | 24.4 | 24.4 | 24.6 |
| INT_6-19 | VAV | Interior | 24.1 | 23.2 | 23.5 | 22.9 | 25.4 | 24.4 | 24.6 | 25.1 |
| INT_6-20 | VAV | Interior | 24.2 | 23.5 | 23.1 | 23.0 | 25.3 | 24.2 | 24.2 | 24.9 |
| OF38 | Linear | Perimeter | 22.8 | 22.7 | 23.9 | 22.8 | 23.3 | 23.1 | 24.4 | 23.3 |
| OF39 | Linear | Perimeter | 22.1 | 22.4 | 23.9 | 22.2 | 23.5 | 23.3 | 24.4 | 23.5 |
| OF40 | Linear | Perimeter | 21.9 | 22.0 | 23.5 | 21.8 | 24.0 | 23.6 | 24.1 | 23.5 |
| OF41 | Linear | Perimeter | 22.4 | 22.4 | 23.5 | 22.3 | 23.2 | 23.3 | 24.0 | 23.6 |
| OF42 | Linear | Perimeter | 21.7 | 21.9 | 22.8 | 22.0 | 23.4 | 23.8 | 23.8 | 23.7 |

| | | | | | | | | | | |
|---------|--------|-----------|------|------|------|------|------|------|------|------|
| OF43 | Linear | Perimeter | 22.0 | 21.4 | 22.1 | 21.9 | 24.1 | 24.2 | 23.6 | 23.8 |
| LBGA-1 | Linear | Perimeter | 24.9 | 24.9 | 24.8 | 24.8 | 25.3 | 25.3 | 25.6 | 25.6 |
| LBGA-2 | Linear | Perimeter | 26.7 | 26.6 | 27.4 | 26.8 | 26.8 | 26.8 | 28.4 | 27.2 |
| LBGA-3 | Linear | Perimeter | 24.7 | 24.8 | 24.9 | 24.4 | 26.0 | 25.9 | 26.8 | 26.2 |
| LBGA-4 | Linear | Perimeter | 23.9 | 24.1 | 24.4 | 24.1 | 25.8 | 25.6 | 26.8 | 26.4 |
| LBGA-5 | Linear | Perimeter | 24.4 | 24.6 | 24.1 | 24.2 | 27.2 | 27.1 | 26.7 | 26.7 |
| LBGA-6 | Linear | Perimeter | 24.1 | 25.7 | 23.1 | 23.9 | 27.4 | 25.8 | 26.5 | 27.5 |
| LBGA-7 | Linear | Perimeter | 24.8 | 25.1 | 25.7 | 25.3 | 26.0 | 25.8 | 27.4 | 26.9 |
| LBGA-8 | Linear | Perimeter | 26.7 | 26.4 | 26.5 | 27.2 | 26.5 | 26.7 | 26.9 | 27.9 |
| LBGA-9 | Linear | Perimeter | 24.5 | 24.7 | 24.4 | 24.5 | 25.2 | 25.0 | 25.0 | 25.2 |
| LBGA-10 | Linear | Perimeter | 24.7 | 25.0 | 25.9 | 25.6 | 25.7 | 25.5 | 27.2 | 26.9 |
| LBGA-11 | Linear | Perimeter | 24.3 | 24.6 | 25.4 | 24.9 | 25.6 | 25.4 | 27.1 | 26.6 |
| LBGB-1 | Linear | Perimeter | 23.2 | 23.5 | 24.0 | 23.5 | 24.9 | 24.5 | 26.0 | 25.4 |
| LBGB-2 | Linear | Perimeter | 23.9 | 24.2 | 23.1 | 23.1 | 24.8 | 24.6 | 23.6 | 23.7 |
| LBGB-3 | Linear | Perimeter | 24.5 | 24.7 | 24.6 | 24.1 | 25.2 | 24.9 | 25.4 | 24.4 |
| LBGB-4 | Linear | Perimeter | 25.4 | 25.5 | 24.9 | 25.6 | 26.1 | 25.9 | 25.3 | 26.2 |
| LBGB-5 | Linear | Perimeter | 23.3 | 23.8 | 23.9 | 23.6 | 26.0 | 25.5 | 26.3 | 25.9 |
| LBGB-6 | Linear | Perimeter | 23.9 | 24.2 | 23.8 | 23.9 | 26.9 | 26.6 | 26.4 | 26.5 |
| LBGB-7 | Linear | Perimeter | 23.8 | 27.7 | 23.3 | 23.7 | 27.3 | 23.5 | 26.6 | 27.0 |
| LBGB-8 | Linear | Perimeter | 23.4 | 23.7 | 23.8 | 23.4 | 24.6 | 24.3 | 25.0 | 24.6 |
| LBGB-9 | Linear | Perimeter | 25.1 | 25.3 | 24.6 | 25.2 | 25.8 | 25.7 | 24.9 | 25.8 |
| LBGB-10 | Linear | Perimeter | 23.7 | 24.1 | 22.8 | 22.9 | 24.8 | 24.4 | 23.2 | 23.5 |
| LBGB-11 | Linear | Perimeter | 23.9 | 24.1 | 23.9 | 23.7 | 24.9 | 24.6 | 24.8 | 24.6 |
| LBGB-12 | Linear | Perimeter | 23.5 | 23.8 | 23.5 | 23.3 | 24.6 | 24.3 | 24.5 | 24.3 |

7.4. R package example

The cross validation analysis in paragraph 3.2.2 is performed with the package DAAG and cvTools in R. DAAG is the package standing for “Data Analysis and Graphics Using R”. CVlm is the function in DAAG that is used to perform the cross-validation analysis. This function gives internal and cross-validation measures of predictive accuracy for multiple linear regression. The data are randomly assigned to a number of ‘folds’. Each fold is removed, in turn, while the remaining data is used to re-fit the regression model and to predict at the deleted observations (R documentation). cvTools is another package standing for “Cross-validation tools for regression models”. Two main functions were used to perform the cross validation analysis, including cvFolds and repCV. cvFolds split n observations into K groups to be used for (repeated) K-fold cross-validation. K should thereby be chosen such that all groups are of approximately equal size. repCV estimates that prediction error of a linear model via (repeated) K-fold cross-validation.

Here’s is an example of performing the cross validation of $\Gamma-\Phi_{0.1}$ for swirl diffuser (R code):

```
##Load data
CB <- read.csv("F:/Research/Research with Stefano/New Gamma-Phi/CBnew.csv")
attach(CB)

##Swirl
x.1.7=PHI1.7[Diff.type=="Swirl"]; gamma=Gamma[Diff.type=="Swirl"]
x.0.1=PHI0.1[Diff.type=="Swirl"];db=data.frame(gamma,x.0.1)
x.oz=PHIoz[Diff.type=="Swirl"]

##Regression equation
##Linear
lm.li<-lm(x.0.1 ~ gamma)
##Logarithmic
lm.lo<-lm(x.0.1 ~ log(gamma))
##Polynomial second order
lm.p2<-lm(x.0.1~ gamma + I(gamma^2))
##Polynomial third order
lm.p3<-lm(x.0.1~ gamma + I(gamma^2)+I(gamma^3))
##Power
lm.po<-lm(log(x.0.1)~log(gamma))

#Analysis-Cross validation
CVlm(df=db, lm.li, m=3, plotit="Residual")
CVlm(df=db, lm.p2,m=3, plotit=" Residual ")
CVlm(df=db, lm.p3,m=3, plotit=" Residual ")
## For logarithm and power model, cvTools is used.
##First pre-process that data. For logarithmic model, get the logarithm of gamma, create a new
csv file, containing x as phi0.1, y as logarithm of gamma.
```

```

test1<- read.csv("F:/Research/Research with Stefano/New Gamma-Phi/test1.csv")
# set up folds for cross-validation
folds <- cvFolds(nrow(test1), K = 3, type = "random" )
# perform cross-validation for an linear regression model
fitLm <- lm( test1$y ~ test1$x, data = test1)
repCV(fitLm, cost = rtmspe, folds = folds, trim = 0.1)

```

##Here taking linear model as an example to show the results from cross validation analysis:

Analysis of Variance Table

Response: x.0.1

| | Df | Sum Sq | Mean Sq | F value | Pr(>F) |
|-----------|----|--------|---------|---------|-------------|
| gamma | 1 | 0.417 | 0.417 | 70.2 | 3.1e-09 *** |
| Residuals | 29 | 0.172 | 0.006 | | |

Signif. codes: 0 '***' 0.001 '**' 0.01 '*' 0.05 '.' 0.1 ' ' 1

fold 1

Observations in test set: 6

| | 4 | 8 | 12 | 20 | 21 | 29 |
|------------------|---------|---------|---------|---------|---------|---------|
| gamma | 10.4000 | 12.8000 | 42.2000 | 32.0000 | 13.4000 | 26.3000 |
| cvpred | 0.4755 | 0.4908 | 0.6780 | 0.6131 | 0.4946 | 0.5768 |
| x.0.1 | 0.4282 | 0.5029 | 0.7676 | 0.5508 | 0.4237 | 0.6071 |
| CV residual | -0.0473 | 0.0121 | 0.0896 | -0.0623 | -0.0709 | 0.0303 |
| Sum of squares = | 0.02 | | | | | |
| Mean square = | 0 | | | | | |
| n = | 6 | | | | | |

fold 2

Observations in test set: 7

| | 5 | 7 | 9 | 10 | 24 | 28 | 30 |
|------------------|---------|---------|---------|---------|---------|---------|---------|
| gamma | 9.1000 | 20.1000 | 12.7000 | 7.0000 | 19.3000 | 30.8000 | 17.6000 |
| cvpred | 0.4686 | 0.5390 | 0.4916 | 0.4551 | 0.534 | 0.6075 | 0.5230 |
| x.0.1 | 0.4152 | 0.5621 | 0.4713 | 0.4284 | 0.398 | 0.6517 | 0.5833 |
| CV residual | -0.0534 | 0.0231 | -0.0203 | -0.0267 | -0.136 | 0.0442 | 0.0603 |
| Sum of squares = | 0.03 | | | | | | |
| Mean square = | 0 | | | | | | |
| n = | 7 | | | | | | |

fold 3

Observations in test set: 6

| | 13 | 14 | 22 | 26 | 27 | 31 |
|------------------|---------|---------|---------|---------|----------|---------|
| gamma | 40.6000 | 30.7000 | 12.5000 | 62.4000 | 41.60000 | 13.0000 |
| cvpred | 0.667 | 0.598 | 0.4699 | 0.820 | 0.67422 | 0.4734 |
| x.0.1 | 0.780 | 0.716 | 0.4873 | 0.714 | 0.67120 | 0.5730 |
| CV residual | 0.113 | 0.118 | 0.0174 | -0.106 | -0.00302 | 0.0996 |
| Sum of squares = | 0.05 | | | | | |
| Mean square = | 0.01 | | | | | |
| n = | 6 | | | | | |

fold 4

Observations in test set: 6

| | 2 | 3 | 15 | 17 | 19 | 25 |
|-----------------------|-----------------|---------|---------|----------|---------|---------|
| gamma | 18.800 | 13.3000 | 16.8000 | 60.20000 | 19.3000 | 19.3000 |
| cvpred | 0.529 | 0.4933 | 0.5162 | 0.80017 | 0.5326 | 0.5326 |
| x.0.1 | 0.540 | 0.4691 | 0.5801 | 0.80380 | 0.4661 | 0.4407 |
| CV residual | 0.011 | -0.0242 | 0.0639 | 0.00363 | -0.0665 | -0.0919 |
| Sum of squares = 0.02 | Mean square = 0 | | | | | n = 6 |

fold 5

Observations in test set: 6

| | 1 | 6 | 11 | 16 | 18 | 23 |
|-----------------------|--------------------|---------|--------|--------|---------|--------|
| gamma | 25.8000 | 43.2000 | 78.400 | 17.500 | 54.4000 | 26.900 |
| cvpred | 0.5733 | 0.6947 | 0.940 | 0.515 | 0.7729 | 0.581 |
| x.0.1 | 0.6137 | 0.7366 | 0.870 | 0.625 | 0.8034 | 0.362 |
| CV residual | 0.0404 | 0.0419 | -0.071 | 0.109 | 0.0305 | -0.219 |
| Sum of squares = 0.07 | Mean square = 0.01 | | | | | n = 6 |

Overall (Sum over all 6 folds)

ms

0.00593

“ms” is the cross validation average error, which is used as an indicator of the predictive ability of the models.

7.1. Code for updated CBE UFAD online design tool

7.1.1. Gamma Phi equations

```
## HTML(add window blinds option)

<tr>
  <td>Window Blinds</td>
  <td align=right><input disabled="disabled" /></td>
  <td align=right><select name="blinds">
    <option></option>
    <option value="up">Up</option>
    <option value="down">Down</option>
  </select></td>
  <td class="unit">-</td>
  <td class="symbol">-</td>
</tr>

##Javascript

function get_int_phi(intGamma, intDiffType) {
  if(intDiffType === 'Swirl'){
    intPhi67 = 0.951;
    if(intGamma > 78.4){
      intPhi4 = 0.9155;
    } else if(intGamma > 7.0){
      intPhi4 = 0.2075 * Math.pow(intGamma,0.3403);
    } else {
      intPhi4 = 0.4024;
    }
  } else if (intDiffType === 'VAV Directional Int.'){
    if(intGamma > 9.1){
      intPhi4 = 0.8700;
      intPhi67 = 0.9896;
    } else if (intGamma > 1.0){
      intPhi4 = 0.1645 * Math.log(intGamma) + 0.5076;
      intPhi67 = 0.0078*intGamma + 0.9186;
    } else {
      intPhi4 = 0.5076;
      intPhi67 = 0.9264;
    }
  }
}

function get_per_phi(perGamma, perDiffType) {
```

```

if(perDiffType == 'VAV Directional Per.'){
  if(perGamma > 15){
    if(blinds == 'down'){
      perPhi4 = 0.8987 - 0.13;
    }else {
      perPhi4 = 0.8987;
    }
    perPhi67 = 1.0018;
  }else if (perGamma > 2.9){
    if(blinds == 'down'){
      perPhi4 = 0.4605+0.0292 * perGamma - 0.13;
    }else{
      perPhi4 = 0.4605+0.0292 * perGamma;
    }
    perPhi67 = 0.7168 + 0.0190 * perGamma;
  }else{
    if(blinds == 'down'){
      perPhi4 = 0.5452 - 0.13;
    }else{
      perPhi4 = 0.5452;
    }
    perPhi67 = 0.7719;
  }
}else if(perDiffType == 'Linear Bar Grille CBE' || perDiffType ==
'Linear Bar Grille RP'){
  if(perGamma > 23){
    if(blinds == 'down'){
      perPhi4=1.1074-0.13;
    }else{
      perPhi4=1.1074;
    }
    perPhi67 = 1.2535;
  }else if(perGamma >2.7){
    if(blinds == 'down'){
      perPhi4 = 0.1282 + 0.0908 * perGamma -
0.0021 * Math.pow(perGamma,2) - 0.13;
    }else{
      perPhi4 = 0.1282 + 0.0908 * perGamma -
0.0021 * Math.pow(perGamma,2);
    }
    perPhi67 = 0.7742+0.0208 * perGamma;
  }else{

```

```

        if(blinds == 'down'){
            perPhi4 = 0.3582 - 0.13 ;
        }else{
            perPhi4 = 0.3582;
        }
        perPhi67 = 0.8305;
    }
}
}
}

```

7.1.2. Interior air distribution effectiveness

##HTML

```

<tr>
  <td>Air Distribution Effectiveness</td>
  <td title="The value is only valid for the interior zone swirl diffusers when airflow rate
per diffuser is around its design value" class = "result"><span id="intdisteff">-</span></td>
  <td title="Note that the empiracal equation to calculate Ez is not applicable to the
perimeter zone" class = "result"><span id="perdisteff">-</span></td>
  <td class="unit">-</td>
  <td class="symbol">E<sub>z</sub></td>
</tr>

```

##Javascript

```

if(intDiffType === 'Swirl' && intAirflowPerDiff < 90 ){
    $("#intdisteff").html(intdisteff.toFixed(2));
} else {
    $("#intdisteff").html('-');
};
function intDistEff(){
    console.log("start to calculate the intdisseff");

    Vr = intDesAirflowRate * 0.000472;
    Qrm = intZCoolingLoad;
    Af = intFloorArea * 0.0929;
    Ts = Util.FtoC(intDiffT);
    H = intRoomHeight * 0.3048;
    n = intNumDiffs;

```

```

    intdisteff = 1.9 + 0.9252 * Vr * Qrm / (Af * Af) + 37.8 * Vr * Ts / (Af * H) + 103.68 *
    Vr * Vr * Ts / (Af * H * n) - 1288.8 * Vr / (Af * H) - 3240 * Vr * Vr / (Af * H * n) + 0.00591 *
    Qrm / Af;
    console.log("intdisseff =" +intdisteff);
}

```

7.1.3. Infloor unit

```
##HTML
```

```

<tr id="test1" class="offstate-a">
  <td title="The cooling capacity of the in-floor cooling unit">In-floor Cooling Unit
  Capacity</td>
  <td align=right><input disabled="disabled" /></td>
  <td align=right><input name="infloorCap" onchange="test()"/></td>
  <td class="loadunit" id="DiffL1">kBtu/hr</td>
  <td class="symbol">W<sub>unit</sub></td>
</tr>

```

```
##Javascript
```

```

function calc_per_zoneT_indep(perAirflowRate) {
  perDesAirflowRate = perAirflowRate + perFloorArea * perLeakage;
  perSupplyPlenumT = perAhuT;
  perDiffT = perSupplyPlenumT + (3.412 * (perSPCoolingLoad-infloorCap)) / (1.08 *
perDesAirflowRate);
  perReturnT = perDiffT + (3.412 * perZCoolingLoad) / (1.08 * perDesAirflowRate);
  perReturnPlenumT = perReturnT + (3.412 * perRPCoolingLoad) / (1.08 *
perDesAirflowRate);

  return perAvgOZT_calc(perAirflowRate);
}

```

```

function calc_per_zoneT_reverse(perAirflowRate) {
  perDesAirflowRate = perAirflowRate + perFloorArea * perLeakage;
  totDesAirflowRate = intDesAirflowRate + perDesAirflowRate;
  perSupplyPlenumT = perAhuT;
  perDiffT = perSupplyPlenumT + (3.412 * (perSPCoolingLoad-infloorCap)) / (1.08 *
totDesAirflowRate);
  perReturnT = perDiffT + (3.412 * perZCoolingLoad) / (1.08 * perDesAirflowRate);
  perReturnPlenumT = perReturnT + (3.412 * perRPCoolingLoad) / (1.08 *
perDesAirflowRate);

  return perAvgOZT_calc(perAirflowRate);
}

```

```

}

function calc_per_zoneT_series(perAirflowRate) {
  intDesAirflowRate = intAirflowRate + intFloorArea * intLeakage;
  perDesAirflowRate = perAirflowRate + perFloorArea * perLeakage;
  totDesAirflowRate = intDesAirflowRate + perDesAirflowRate;
  intSupplyPlenumT = intAhuT;
  intDiffT = intSupplyPlenumT + (3.412 * intSPCoolingLoad) / (1.08 * totDesAirflowRate);
  perDiffT = intDiffT + (3.412 * (perSPCoolingLoad - infloorCap)) / (1.08 *
perDesAirflowRate);
  perReturnT = perDiffT + (3.412 * perZCoolingLoad) / (1.08 * perDesAirflowRate);
  perReturnPlenumT = perReturnT + (3.412 * perRPCoolingLoad) / (1.08 *
perDesAirflowRate);

  return perAvgOZT_calc(perAirflowRate);
}

```

```

function calc_per_zoneT_common(perAirflowRate) {
  intDesAirflowRate = intAirflowRate + intFloorArea * intLeakage;
  perDesAirflowRate = perAirflowRate + perFloorArea * perLeakage;
  totDesAirflowRate = intDesAirflowRate + perDesAirflowRate;
  intSupplyPlenumT = intAhuT;
  perDiffT = intSupplyPlenumT + (3.412 * (intSPCoolingLoad + perSPCoolingLoad -
infloorCap)) / (1.08 * totDesAirflowRate);
  perReturnT = perDiffT + (3.412 * perZCoolingLoad) / (1.08 * perDesAirflowRate);
  perReturnPlenumT = perReturnT + (3.412 * perRPCoolingLoad) / (1.08 *
perDesAirflowRate);

  return perAvgOZT_calc(perAirflowRate);
}

```